No. SOC-182

A UNIFIED TREATMENT OF YIELD ANALYSIS,

WORST-CASE DESIGN AND YIELD OPTIMIZATION

H.L. Abdel-Malek

November 1977

YIELD ANALYSIS, WORST-CASE DESIGN

AND

YIELD OPTIMIZATION

A UNIFIED TREATMENT

OF

YIELD ANALYSIS, WORST-CASE DESIGN AND YIELD OPTIMIZATION

By

HANY L. ABDEL-MALEK

A Thesis

Submitted to the Faculty of Graduate Studies

in Partial Fulfilment of the Requirements

for the Degree

Doctor of Philosophy

McMaster University

September 1977

DOCTOR OF PHILOSOPHY (1977)   McMASTER UNIVERSITY
(Electrical Engineering)   Hamilton, Ontario

TITLE: A UNIFIED TREATMENT OF YIELD ANALYSIS, WORST-CASE DESIGN

              AND YIELD OPTIMIZATION

AUTHOR: Hany Lamei Abdel-Malek, B.Sc. (E.E.) (Cairo University)

                                      B.Sc. (Math.) (Cairo University)

SUPERVISOR: J.W. Bandler, Professor of Electrical Engineering

                        B.Sc. (Eng.), Ph.D., D.Sc. (Eng.)

                        (University of London)

                        D.I.C. (Imperial College)

                        P.Eng. (Province of Ontario)

                        C.Eng., M.I.E.E. (United Kingdom)

NUMBER OF PAGES: xv, 190

SCOPE AND CONTENTS

This thesis addresses itself to what is considered to be one of
the most general theoretical problems associated with the art of
engineering design. A unified treatment is presented of production
yield evaluation, worst-case design and yield optimization. The
formulation is suited to nonlinear programming methods of solution.

Viewed in its entirety the approach integrates the following
concepts: design centering, assignment of component tolerances,
post-production tuning, yield estimation for realistic distributions and
modeling of response functions. Many of the ideas can also be used
separately depending on the type of design evaluation required, the
number of degrees of freedom involved and the availability and
properties of suitable simulation programs.

The thesis presents an analytical approach to yield and yield
sensitivity evaluation. Basic to the approach is the discretization of
the distributions by use of orthotopic cells to which suitable uniform
distributions are applied. Multidimensional polynomials provide
approximations to actual functions, which may be expensive to compute.
Algorithms for updating and evaluating these polynomials are developed
to permit efficient use of gradient optimization methods.

Industrially oriented design examples are furnished to justify
the theory. A telephone channel (lossy) bandpass filter is considered
with relative insertion loss specifications to illustrate the analysis

of yield. The cascade connection of nonideal, inhomogeneous sections of rectangular waveguides is considered from the worst-case design point of view. A current switch emitter follower involving transistors, a diode and a transmission line provides a challenging example for yield optimization including parameter correlations.

ACKNOWLEDGEMENTS

TABLE OF CONTENTS

TABLE OF CONTENTS (continued)

LIST OF FIGURES

LIST OF FIGURES (continued)

LIST OF TABLES

xiv

CHAPTER 1

INTRODUCTION

The practical problem of optimally designing circuits in the face
of statistical uncertainty on the parameters is the subject of this
thesis. The estimation of the percentage of manufactured circuits which
meet specifications, called _production yield_, has always been important
but, increasingly mandatory for modern circuit design, is the associated
optimization problem called _design centering_. This is the process of
defining a set of nominal parameter values to optimize the economics of
the circuit in terms of maximum _tolerances_, or yield, or minimum cost.
Particularly, for mass-produced designs (such as integrated circuits,
telephone channel filters, etc.), large savings are possible if
permissible tolerances can be relatively large.

Many variations of the problem may occur. Given the circuit
specifications find, for example, a design that (1) maximizes the
worst-case tolerances, or (2) maximizes the production yield w.r.t. an
assumed probability distribution function of the parameters around
nominal values, or (3) minimizes the overall production cost given
relations between cost of the components and their tolerances. In
general, tight tolerances imply high production cost but high yield,
while large tolerances lower the production cost at the expense of low
yield.

The practical question of _tuning_ is closely related to design

centering. A design may require tuning as a post-manufacturing process in order to meet specifications.

Unlike conventional minimax or constrained optimization where interest is in a single point in the parameter space, due to parameter spreads in the tolerance problem we have certain regions of interest. These are typically the regions where possible worst cases can occur or where constraints may even be violated. Detection of these critical regions is a difficult problem. See Tromp (1977). For high yield, however, a worst-case design (a design which meets the specifications in the worst case) should provide a good indication of these regions and is, therefore, felt to be worthwhile investigating as a preliminary exercise to statistical design. Fig. 1.1 shows a possible sequence of problems in computer-aided design which fall into the present context (Bandler and Abdel-Malek 1977b). The problems increase in complexity as one proceeds down the graph.

The nominal approximation is the most well-known and widely used design technique. By least squares or any other suitable measure a best nominal (single design) may be obtained. If the specificatons cannot be met by this single solution, it is impossible to seek better or more realistic designs. An improved approximation, e.g., a minimax or a Chebyshev solution can be found if tolerances are not involved. If explicit assignment of tolerances is not required one could carry out a sensitivity minimization. This involves an objective function which usually includes first-order sensitivities at the nominal design.

Many complications may arise if one jumps straight into a cost minimization without having sufficient information about the problem.

3
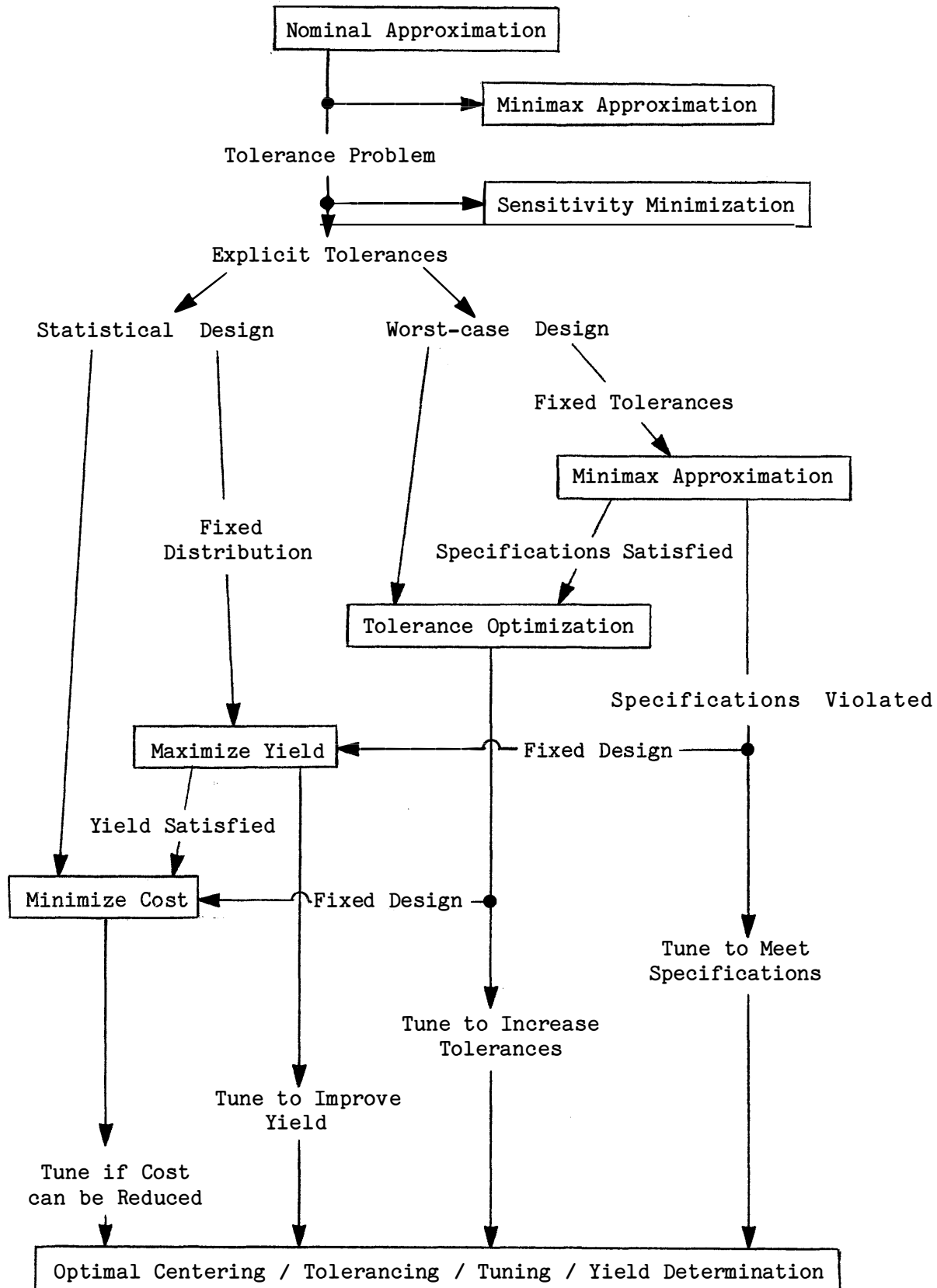
Fig. 1.1   Typical sequence of problems in modern computer-aided design
shown in approximate order of increasing complexity.

Thus, it is felt that proceeding down the graph shown in Fig. 1.1 is safer if the increase in problem complexity per step is not too great.

Due to the mass of calculations involved in statistical and worst-case evaluations, the use of <u>multidimensional approximations</u> appears as an economical necessity. Approximation of design constraints using truncated Taylor series expansions (Pinel and Roberts 1972, Karafin 1974) or <u>quadratic interpolation</u> (Bandler, Abdel-Malek, Johns and Rizk 1976) or by <u>simplicial approximation</u>(Director and Hachtel 1976) to the constraint region boundary are described in the literature. As a result, estimation of production yield, tolerance assignment, design centering and other uncertainties can be handled at low computational cost.

The work presented in this thesis provides a new approach for design centering, optimal tolerancing, post-production tuning and yield determination as part of modern computer-aided design. <u>Nonlinear programming</u>, which has proved to be successful (Bandler, Liu and Tromp 1976), is the approach used. Low-order multidimensional approximations of responses, as functions of design parameters, are employed. They facilitate cheap function evaluations required for solving the nonlinear program, the use of any available simulation program, whether it provides sensitivity information or not, as well as the development of a new analytical technique for evaluating production yield.

To provide insight into the tolerance-tuning problem, Chapter 2 presents a brief review of some different approaches to the problem. Definitions and concepts as well as geometric interpretations are given. Production yield is introduced into the original nonlinear programming

formulation of Bandler and Liu (1974b).

A tolerance problem equivalent to the tolerance-tuning problem is constructed in Chapter 3. This equivalence allows us to treat only tolerances in the ensuing chapters. Geometric interpretation and a simple example are given.

Chapter 4 presents a new analytical approach which not only provides a value of yield but also facilitates the evaluation of yield sensitivities. The approach is general enough to be applied in conjunction with any statistical distribution and not necessarily for electrical circuits (Abdel-Malek and Bandler 1977). The availability of yield sensitivities permits the use of efficient gradient techniques in solving the nonlinear program (Bandler and Abdel-Malek 1977a).

Chapter 5 deals with a multidimensional approximation procedure suitable for the tolerance problem. Quadratic polynomials are used since they are simple functions which have curvature and being polynomials are cheaply evaluated along with their derivatives. It is shown how to obtain the approximations with minimal effort and to evaluate them efficiently. Theorems dealing with preserving certain properties of the original functions in the approximation are stated and proved.

The ideas presented in Chapters 4 and 5 are implemented in the algorithms given in Chapter 6. Algorithms for worst-case design as well as design for yield less than 100% are described (Bandler and Abdel-Malek 1977a). Simple lumped and distributed circuit examples illustrating the algorithms are given.

Chapter 7 is devoted to practical implementation of the approach

and the algorithms presented. Yield determination for a telephone channel bandpass filter (Butler 1971, Karafin 1971 and 1974, Pinel and Roberts 1972, Bandler and Liu 1974a) applying different statistical distributions is described. The worst-case designs of two-section and three-section nonideal inhomogeneous waveguide transformers (Bandler 1969) are given. A nonlinear current switch emitter follower (CSEF) circuit containing a transmission line (Ho 1971) is considered for worst-case design as well as design for yield less than 100%.

The formulation of the state equations required for the analysis of the CSEF is given in Appendix A.

Original contributions claimed for this thesis are:

(1)   A formulation of the design problem embodying centering, tolerancing, tuning and yield.

(2)   The construction of the tolerance problem equivalent to the tolerance-tuning problem.

(3)   An approach for updated multidimensional approximations suitable for the tolerance problem.

(4)   Based upon the approximations, analytical expressions for yield and yield sensitivities.

(5)   Sufficient conditions for preserving one-dimensional convexity and parameter symmetry in the quadratic polynomial approximation.

(6)   An efficient algorithm for evaluating the quadratic approximation at the vertices of the tolerance orthotope.

(7)   Algorithms, which employ the approximations, for worst-case design as well as designs for yield less than 100%.

CHAPTER 2

DESIGN CENTERING AND STATISTICAL ANALYSIS:

A REVIEW

2.1   Introduction

Several approaches for design centering and for statistical circuit analysis have been suggested in the literature. Emphasis will be placed here on some of the more ingenious methods. Relevant definitions of concepts such as constraint region, tolerance region, tuning region and manufacturing yield are given. The idea of one-dimensional convexity is presented.

A method dealing with pairwise parameter interaction (Butler 1971) is described. The simplicial approximation of Director and Hachtel (1976) and the nonlinear programming approach (Bandler 1972, Pinel and Roberts 1972) are given.

Techniques for statistical analysis using Monte Carlo methods, space regionalization and analytical evaluation are described.

2.2   Fundamental Concepts and Definitions

A design is described by a nominal parameter vector ϕ^0, a tolerance vector ϵ and a tuning vector t, where

$$
\underset{\sim}{\phi}^0 \triangleq
\begin{bmatrix}
\phi_1^0 \\
\phi_2^0 \\
\cdot \\
\cdot \\
\cdot \\
\phi_k^0
\end{bmatrix}, \quad
\underset{\sim}{\varepsilon} \triangleq
\begin{bmatrix}
\varepsilon_1 \\
\varepsilon_2 \\
\cdot \\
\cdot \\
\cdot \\
\varepsilon_k
\end{bmatrix}, \quad
\underset{\sim}{t} \triangleq
\begin{bmatrix}
t_1 \\
t_2 \\
\cdot \\
\cdot \\
\cdot \\
t_k
\end{bmatrix}
\tag{2.1}
$$

and k is the number of designable parameters. The tolerance vector $\underset{\sim}{\varepsilon}$ may be used to define the extremes of the tolerance region or the standard deviation, etc. The tuning vector $\underset{\sim}{t}$, defines the size of the tuning range. See Bandler, Liu and Tromp (1976). It is assumed that the parameters can be varied continuously. Some of these vector elements may be set to zero or held constant.

An _outcome_ $\{\underset{\sim}{\phi}^0, \underset{\sim}{\varepsilon}, \underset{\sim}{\mu}\}$ of a design $\{\underset{\sim}{\phi}^0, \underset{\sim}{\varepsilon}, \underset{\sim}{t}\}$ implies a point in the parameter space given by

$$
\underset{\sim}{\phi} = \underset{\sim}{\phi}^0 + \underset{\sim}{E}\,\underset{\sim}{\mu},
\tag{2.2}
$$

where

$$
\underset{\sim}{E} \triangleq
\begin{bmatrix}
\varepsilon_1 & & & & \\
& \varepsilon_2 & & & \\
& & \cdot & & \\
& & & \cdot & \\
& & & & \varepsilon_k
\end{bmatrix}, \quad
\underset{\sim}{\mu} \triangleq
\begin{bmatrix}
\mu_1 \\
\mu_2 \\
\cdot \\
\cdot \\
\cdot \\
\mu_k
\end{bmatrix}
\tag{2.3}
$$

and where $\underset{\sim}{\mu}$ is a _random vector_ distributed according to a _joint probability distribution function_ (PDF). The PDF might extend as far as $(-\infty, \infty)$, however, for all practical cases it is possible to consider a _tolerance region_ R_ε such that

$$\int_{R_\epsilon} F(\underset{\sim}{\phi}) \, d\phi_1 \, d\phi_2 \, \dots \, d\phi_k \simeq 1 \, , \qquad (2.4)$$

where $F(\underset{\sim}{\phi})$ is the PDF.

For the sake of simplicity as well as the implications of independent design parameters, there is no loss of generality to consider R_ϵ to be an <u>orthotope</u> defined by

$$R_\epsilon \triangleq \{ \underset{\sim}{\phi} \mid \underset{\sim}{\phi} = \underset{\sim}{\phi}^0 + \underset{\sim}{E} \underset{\sim}{\mu} , \ \underset{\sim}{\mu} \in R_\mu \} \, , \qquad (2.5)$$

where

$$R_\mu \triangleq \{ \underset{\sim}{\mu} \mid -1 \leq \mu_i \leq 1, \ i = 1, 2, \dots, k \} \, . \qquad (2.6)$$

This orthotope is centered at $\underset{\sim}{\phi}^0$ and has edges of length $2\epsilon_i$, $i = 1, 2,$ $\dots, k$. The extreme points of R_ϵ are called <u>vertices</u> and the set of vertices is defined by (Bandler, Liu and Tromp 1976)

$$R_V \triangleq \{ \underset{\sim}{\phi} \mid \phi_i = \phi_i^0 + \epsilon_i \mu_i, \ \mu_i \in \{-1,1\}, \ i = 1, 2, \dots, k \} \, . \qquad (2.7)$$

The number of these vertices is 2^k and the following enumeration scheme used by Bandler (1974) will be considered. For a vertex

$$\underset{\sim}{\phi}^r = \underset{\sim}{\phi}^0 + \underset{\sim}{E} \underset{\sim}{\mu}^r, \ \mu_i^r \in \{-1,1\} \qquad (2.8)$$

we have

$$r = 1 + \sum_{i=1}^{k} \left(\frac{\mu_i^r + 1}{2} \right) 2^{i-1} . \qquad (2.9)$$

The <u>tuning region</u> is defined by (Bandler and Liu 1974b)

$$R_t(\underset{\sim}{\mu}) \triangleq \{\underset{\sim}{\phi} \mid \underset{\sim}{\phi} = \underset{\sim}{\phi}^0 + \underset{\sim}{E} \underset{\sim}{\mu} + \underset{\sim}{T} \underset{\sim}{\rho}, \underset{\sim}{\rho} \in R_\rho\} , \qquad (2.10)$$

where

$$\underset{\sim}{T} \triangleq \begin{bmatrix} t_1 & & & & \\ & t_2 & & & \\ & & \cdot & & \\ & & & \cdot & \\ & & & & t_k \end{bmatrix} , \qquad \underset{\sim}{\rho} \triangleq \begin{bmatrix} \rho_1 \\ \rho_2 \\ \cdot \\ \cdot \\ \cdot \\ \rho_k \end{bmatrix} \qquad (2.11)$$

and R_ρ may be defined, for example, by

$$R_\rho \triangleq \{\underset{\sim}{\rho} \mid -1 \leq \rho_i \leq 1, \ i = 1, 2, \ldots, k\} \qquad (2.12)$$

or in the case of <u>one-way tuning</u> or <u>irreversible trimming,</u>

$$R_\rho \triangleq \{\underset{\sim}{\rho} \mid -1 \leq \rho_i \leq 0, \ i = 1, 2, \ldots, k\} \qquad (2.13)$$

or

$$R_\rho \triangleq \{\underset{\sim}{\rho} \mid 0 \leq \rho_i \leq 1, \ i = 1, 2, \ldots, k\} . \qquad (2.14)$$

The <u>constraint region</u> (or <u>feasible region</u>) itself is given by

$$R_c \triangleq \{\underset{\sim}{\phi} \mid g_i(\underset{\sim}{\phi}) \geq 0, \ i = 1, 2, \ldots, m_c\} , \qquad (2.15)$$

where m_c is the number of constraints g_i. The tolerance, tuning and

constraint regions are illustrated in Fig. 2.1.

2.3   Production Yield

The production or manufacturing yield is simply defined by

$$Y \triangleq N/M \; , \tag{2.16}$$

where M is the total number of outcomes and N is the number of outcomes which satisfy the specifications.   Similarly we define the _potential yield_ by

$$Y_p \triangleq N_p/M \; , \tag{2.17}$$

where N_p is the number of outcomes which meet the specification, after tuning if necessary.   Hence, the relative frequency of outcomes which require tuning is

$$Y_t = Y_p - Y \; . \tag{2.18}$$

2.4   One-dimensional Convexity

A region R is said to be _one-dimensionally convex_ (Bandler 1972) if for any direction defined by the unit vector $\underset{\sim}{e}_j$, j = 1, 2, ..., k, and for any two points $\underset{\sim}{\phi}^a$, $\underset{\sim}{\phi}^b \in R$, where

$$\underset{\sim}{\phi}^b = \underset{\sim}{\phi}^a + c \, \underset{\sim}{e}_j \; , \quad c \text{ is a scalar,} \tag{2.19}$$

then
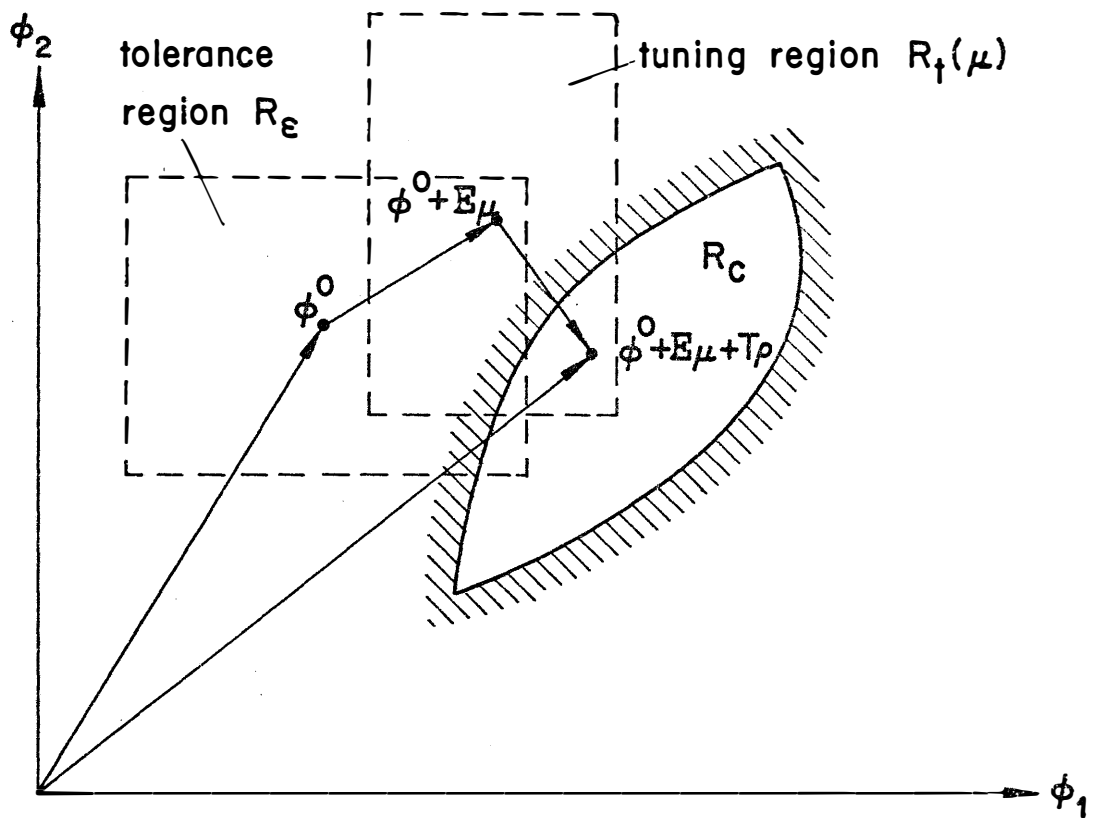
Fig. 2.1   Illustration of regions R_c, R_ε and R_t (Bandler, Liu and Tromp 1976).

$$\phi = \phi^a + \lambda(\phi^b - \phi^a) \in R \text{ for all } 0 \le \lambda \le 1. \tag{2.20}$$

One-dimensional convexity is illustrated in Fig. 2.2.

The region R is said to be convex if (2.19) is not assumed. See Mangasarian (1969).

If all vertices of the tolerance orthotope are within a one-dimensionally convex constraint region, then the whole tolerance orthotope lies inside the constraint region. For a proof, see Bandler (1972).

2.5   Design Centering

2.5.1 Centering via Large-change Sensitivities and Performance Contours

Large-change sensitivities together with performance contours were used by Butler (1971). A scalar continuous function of design parameters which reflects the goodness of a design is chosen as a performance criterion. A nominal design which satisfies this performance criterion is assumed to exist. The concept of large-change sensitivities is that of finding changes in function values due to significant deviations in designable parameters. This concept is used to draw contours of the performance criterion changing parameters in a pairwise manner for each contour. The design center is obtained by inspection, i.e., by choosing a nominal value which is well centered for all contours. As an example of a performance criterion, we might use
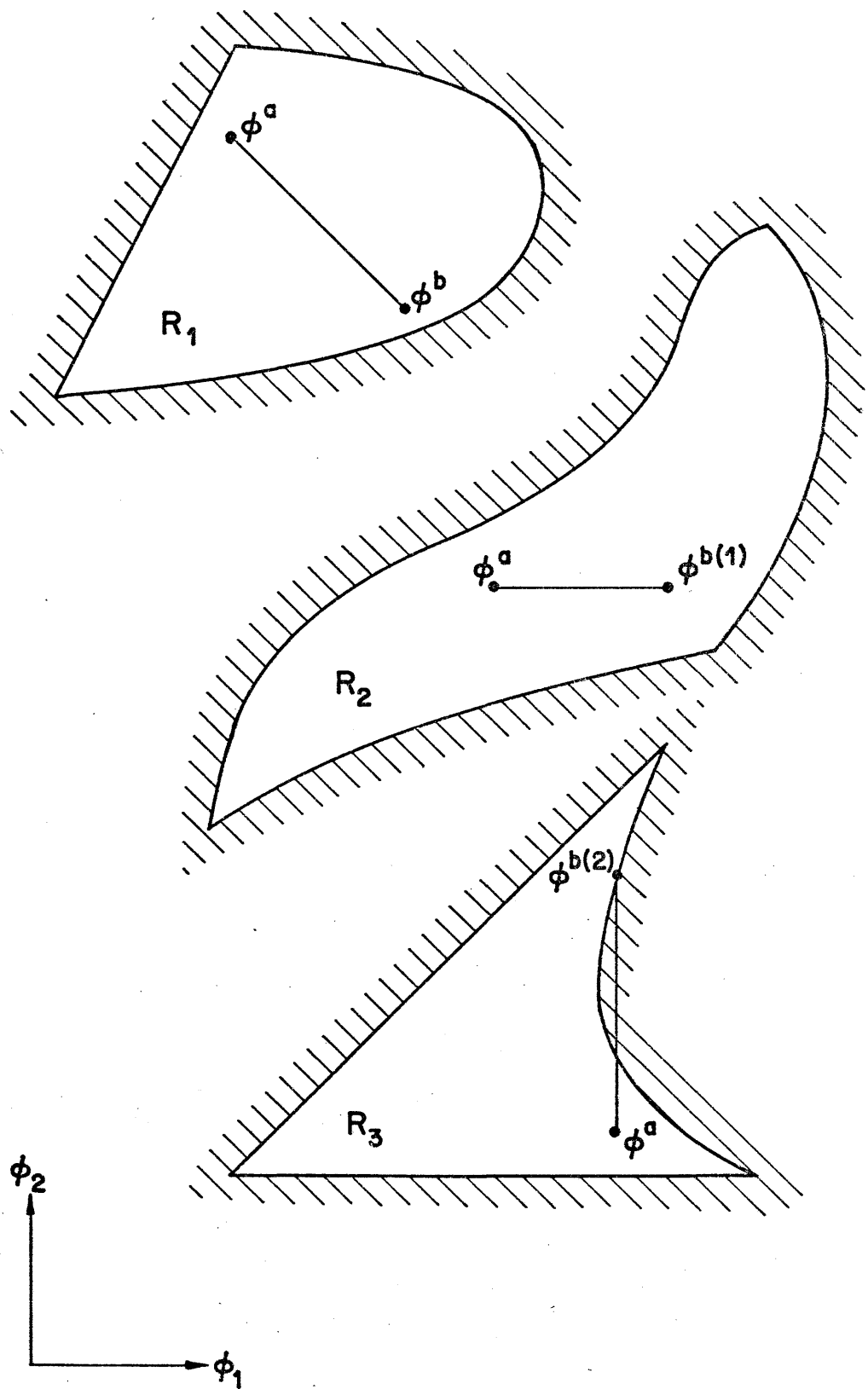
Fig. 2.2   Illustrations of convex, one-dimensionally convex

and nonconvex regions (Liu 1975).

$$ J = \min_{1 \le i \le m_c} g_i(\underset{\sim}{\phi}) \ , \qquad\qquad (2.21) $$

where g_i, $i = 1, 2, \ldots, m_c$, are the m_c design constraints defining the feasible region. The method is illustrated in Fig. 2.3 for the case of three parameters.

2.5.2 Simplicial Approximation

The simplicial approximation approach of Director and Hachtel (1976) involves <u>linear programming</u> as well as <u>one-dimensional search</u> techniques. Their approach is to inscribe a hypersphere inside the constraint region. During the process of enlarging this hypersphere a polytope which approximates the boundary of the constraint region is constructed.

The procedure is illustrated in Fig. 2.4. The algorithm initially searches for points on the constraint boundary in both positive and negative directions for each parameter from a feasible point (a point within the constraint region). The convex hull described by these boundary points provides the initial polytope approximating the boundary of the constrant region. This polytope will be an interior approximation only if the constraint region is convex. Using linear programming a hypersphere is to be inflated inside this polytope in a k-dimensional space. The tangent hyperplanes are determined. These hyperplanes, faces of the polytope, are simplices (Coxeter 1963) in a space of k-1 dimensions. The largest simplex, i.e., the one which contains the largest hypersphere, is to be broken and replaced by k simplices. This is performed by adding a new vertex to the polytope
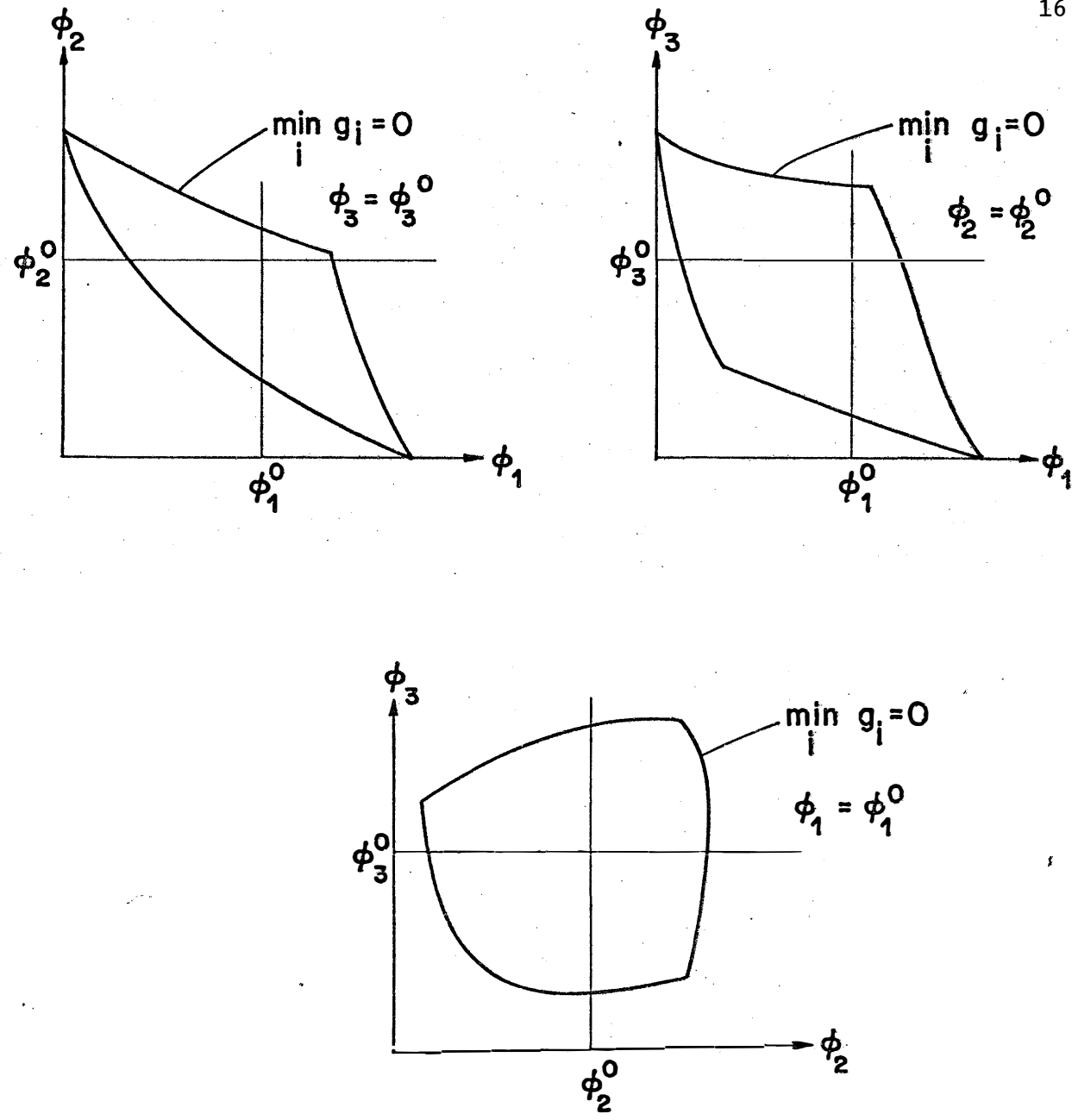
Fig. 2.3   Performance contours for pairwise changes in parameters. Reducing ϕ_1^0 will result in a better centered nominal design.
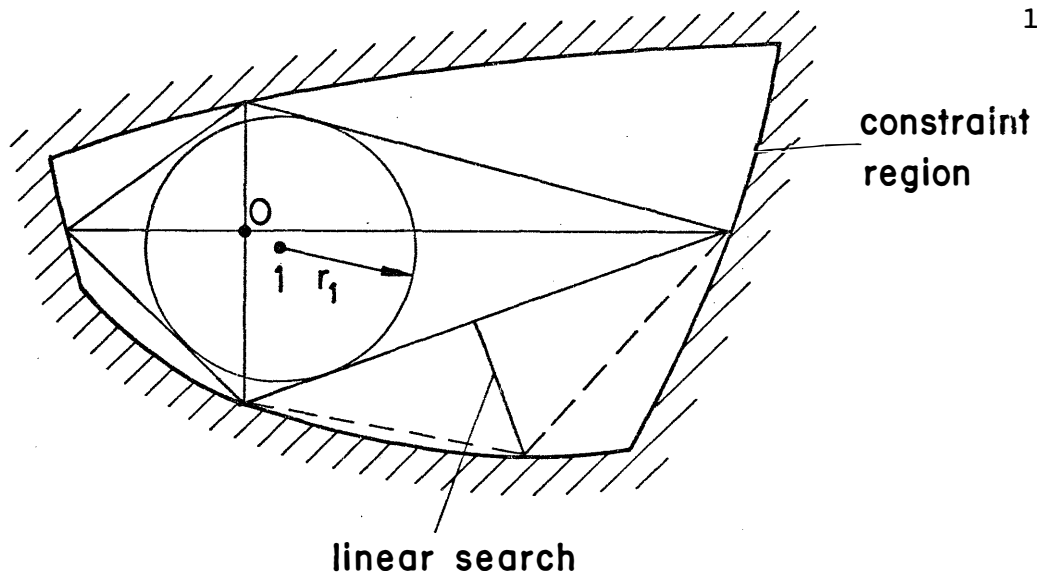
(a) Initial search for boundary points.
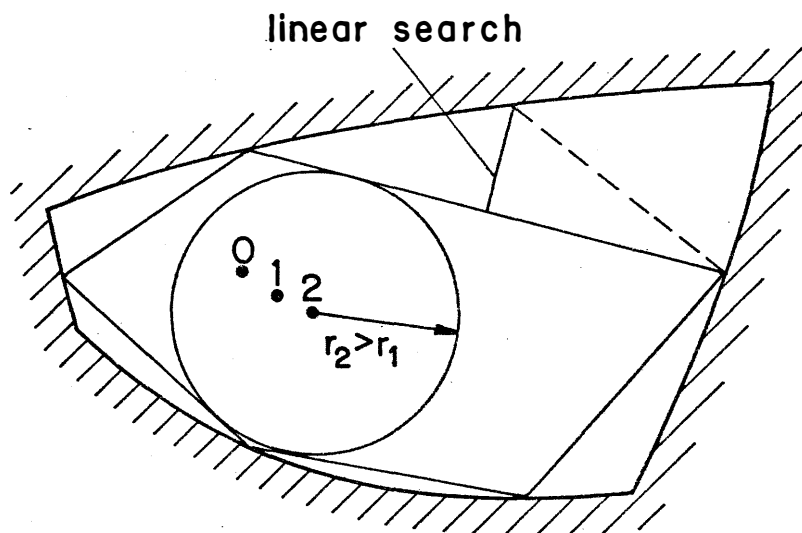
(b) The polytope approximating the boundary of

the constraint region after two iterations.

Fig. 2.4 Illustration of the simplicial approximation

approach (Director and Hachtel 1976).

obtained by searching for a boundary point along the normal direction to the largest simplex from the center of the corresponding hypersphere. The computational effort per iteration can be expressed as

$$CE = LP_k + (k+1) \ LP_{k-1} + LS \ , \qquad (2.22)$$

where LP_j is the computational effort to solve a j-dimensional linear program and LS is the computational effort in a one-dimensional search.

It is to be noted that the number of constraints for the linear programming problem increases with the number of faces of the polytope. For the k-dimensional linear program and at the nth iteration we have 2^k + (n-1)k constraints, while for the k-1 dimensional linear program the number of constraints is fixed and is equal to k. The sequence of approximations is regarded to have converged when

$$r_{n+1} - r_n \leq \delta_1 \ r_n + \delta_2 \ , \qquad (2.23)$$

where r_n is the radius of the hypersphere obtained in the nth iteration, δ_1 and δ_2 are given relative and absolute convergence parameters.

2.5.3 The Nonlinear Programming Approach

The two methods described before do not explicitly optimize values for parameter tolerances, in other words there is no optimal tolerance assignment.

Pinel and Roberts (1972) used nonlinear programming to assign parameter tolerances. The nominal parameter values are fixed and the

constraints are approximated by truncated Taylor series expansions.
Bandler (1972, 1974) and Bandler and Liu (1974a) treated centering and
tolerancing simultaneously for the benefit of increased tolerances by
permitting the nominal point to move.

A nonlinear programming formulation of the optimal centering,
tolerancing and tuning problem is

$$\underset{\phi^0,\ \varepsilon,\ t\ \geq\ 0}{\text{minimize}}\quad C(\phi^0,\ \varepsilon,\ \mu,\ t)\ , \tag{2.24}$$

subject, for example, to a constraint on yield

$$Y(\phi^0,\ \varepsilon,\ \mu,\ t)\ \geq\ Y_L\ , \tag{2.25}$$

where C is a suitable cost function, sometimes called objective
function, and Y_L is a lower yield specification.

The objective function C should reflect a realistic cost-
tolerance and tuning relation. Reasonable properties of the objective
function are (Bandler, Liu and Tromp 1976)

$$C(\phi^0,\ \varepsilon,\ \mu,\ t) \to \text{constant} \qquad \text{as } \varepsilon \to \infty$$

$$C(\phi^0,\ \varepsilon,\ \mu,\ t) \to \infty \qquad \text{for any } \varepsilon_i \to 0 \tag{2.26}$$

$$C(\phi^0,\ \varepsilon,\ \mu,\ t) \to C(\phi^0,\ \varepsilon,\ \mu) \qquad \text{as } t \to 0$$

$$C(\phi^0,\ \varepsilon,\ \mu,\ t) \to \infty \qquad \text{for any } t_i \to \infty\ .$$

An appropriate objective function, for example, is

$$C = \sum_{i=1}^{k} \frac{c_i}{x_i} + \sum_{i=1}^{k} c_i' \, y_i \qquad (2.27)$$

where x_i and y_i may indicate either the absolute tolerances and tuning ranges, respectively, or the relative values w.r.t. nominals. If tuning is not allowed or is fixed for some parameters, their corresponding c_i' should be set to zero. Similarly, c_i may be set to zero if the corresponding tolerance is fixed.

In the case of no tuning, Pinel and Roberts (1972) suggested an objective function of the form

$$C = \sum_{i=1}^{k} (\alpha_i + \frac{c_i}{\varepsilon_i}) , \qquad (2.28)$$

where α_i and c_i are constants. This objective is essentially the same as (2.27), since the α_i will contribute only a constant value to the optimum cost. A unit cost function (Karafin 1974) can be expressed as

$$C_u = C(\phi^0, \, \varepsilon, \, t)/Y . \qquad (2.29)$$

An orthotope describing the tolerance region is to be inflated by minimizing the cost function. The center of the orthotope provides the nominal parameter values and the lengths of the orthotope edges are twice the absolute tolerances.

2.5.4   Sensitivity Minimization

Some <u>sensitivity measures</u> such as the measure of Lee and Su (1977) and that of Styblinski (1977), can be considered as objective functions also.   The constraints are implicitly expressed in the objective, hence an unconstrained optimization problem results.

2.6   Statistical Circuit Analysis

2.6.1   The Monte Carlo Method

Statistical circuit analysis, providing an estimate of manufacturing yield, has usually been treated through the Monte Carlo method.   A set of random parameter values is generated according to the anticipated distribution of outcomes and corresponding analyses are performed.

Elias (1975) presented an approach which applies the Monte Carlo analysis directly to the nonlinear constraints.   In an effort to reduce computational cost, Director and Hachtel (1976) suggested applying the Monte Carlo method in conjunction with an approximation to the boundary of the constraint region.   The approximation is the polytope obtained in the simplicial method described in Subsection 2.5.2.

The Director and Hachtel polytope might be described by quite a large number of hyperplanes, for example, if the algorithm converges in n iterations, the number of these hyperplanes is $2^k + nk$.   The yield estimate obtained by this approximation is not accurate enough (Director 1977).   More recently, Director and Hachtel (1977) suggested updating the polytope according to the Monte Carlo points which fall within the

constraint boundary but not inside the polytope.

In order to reduce the number of Monte Carlo analyses, while keeping high confidence in the yield estimate, importance sampling (Hammersley and Handscomb 1964) was used by Pinel and Singhal (1977). The objective of importance sampling is to concentrate the distribution of sample points at critical regions instead of spreading them evenly. Compensation is done to correct for distorting the distribution. It is assumed that worst cases occur when one or more parameters assume extreme values, i.e., a one-dimensionally convex constraint region is implied.

2.6.2 Space Regionalization

Space regionalization was suggested by Scott and Walker (1976). Based upon the probability of having an outcome to fall within a region, a weight is assigned to this region and the center of the region is checked against the nonlinear constraints to determine whether this whole weight will contribute to the yield or not. See Fig. 2.5. The number of required analyses, however, increases exponentially with the number of variables subject to statistical variations, since the response at the center of each region is to be evaluated.

Regionalization was also used by Leung and Spence (1976, 1977) exploiting the technique of systematic exploration. The centers of the regions are scanned systematically by changing one parameter at a time. The circuit response is efficiently evaluated using matrix inverse modification methods. Hence, computational saving is only available for linear systems. Leung and Spence also suggested checking the worst
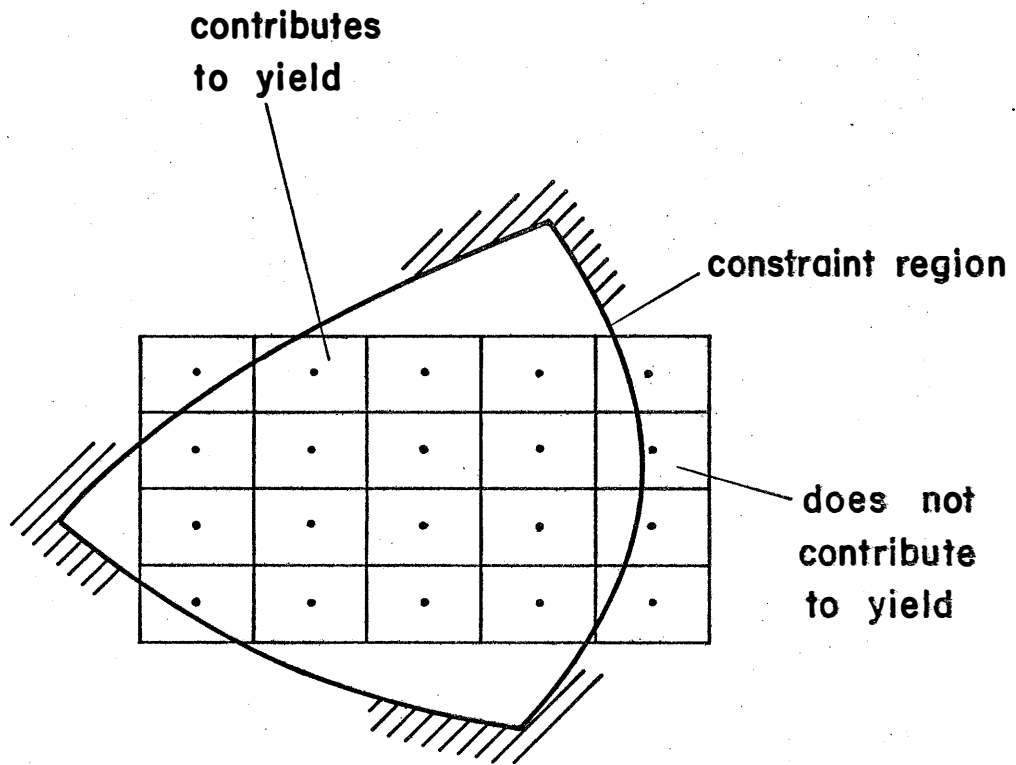
Fig. 2.5   Space regionalization for yield estimation.

outcome in each region, instead of the center of the region, if a lower bound on yield is required.

2.6.3 Analytical Methods

Karafin (1974) presented an approach using truncated Taylor series approximations to the constraints. The constraint function values are assumed to be normally distributed for all tolerance choices. The parameters are assumed to be statistically independent and each parameter is symmetrically distributed about its nominal value. According to these assumptions, Karafin was able to reduce the k-fold integration of the k-variate probability distribution function to at most 3-fold integration. The yield estimate is based upon the resulting distributions of the values of the constraints. Obviously, the method is computationally expensive.

CHAPTER 3

THE EQUIVALENT TOLERANCE PROBLEM

3.1   Introduction

A tolerance problem which is equivalent to the tolerance and tuning problem of Bandler and Liu (1974b) is presented. The generalized least pth function (Bandler and Charalambous 1972), required for constructing the equivalent problem, is given. Based on this equivalence, a mathematical definition of yield is developed.

The optimal worst-case design, in which all outcomes should meet the specifications, after tuning if necessary, is formulated as a nonlinear program. It is shown how to express the minimization of the maximum violations of the worst outcome, called worst-case centering, as a minimax problem.

3.2   The Generalized Least pth Function

Given a set of functions $f_j(\underset{\sim}{\phi})$, $j \in J$, we define (Bandler and Charalambous 1972)

$$U(f_j(\underset{\sim}{\phi}), J, p, \lambda) \overset{\Delta}{=} \begin{cases} 0 & , \quad M = 0 \quad , \\ \\ \lambda M \left[\displaystyle\sum_{j \in K} \left(\frac{\lambda f_j(\underset{\sim}{\phi})}{M} \right)^q \right]^{1/q} & , \quad M \neq 0 \ , \end{cases} \quad (3.1)$$

where

$$M = \max_{j \in K} (\lambda f_j) \quad , \quad q = p \text{ sign } (M) , \qquad (3.2)$$

$$K = \begin{cases} J, \ M < 0 , \\ \\ \{j \mid j \in J, \ \lambda f_j(\underset{\sim}{\phi}) > 0\} , \ M > 0 , \end{cases} \qquad (3.3)$$

$$\lambda = \begin{cases} 1 \text{ if U approximates } \max_{j \in J} f_j(\underset{\sim}{\phi}) , \\ \\ -1 \text{ if U approximates } \min_{j \in J} f_j(\underset{\sim}{\phi}) \end{cases} \qquad (3.4)$$

and where p is a scalar greater than one.

3.3   The Equivalent Tolerance Problem

It is possible to transform a tolerancing and tuning problem to an equivalent tolerance problem only. The following theorem confirms this observation.

3.3.1 Theorem 3.1

An outcome

$$\underset{\sim}{\phi} = \underset{\sim}{\phi}^0 + \underset{\sim}{E} \ \underset{\sim}{\mu} \qquad (3.5)$$

can be tuned to satisfy the constraints, i.e., there exists $\underset{\sim}{\rho} \in R_\rho$ such that

$$\underset{\sim}{\phi} + \underset{\sim}{T} \ \underset{\sim}{\rho} \in R_c , \qquad (3.6)$$

if and only if $\underset{\sim}{\phi} \in R_{ct}$, where R_{ct} is the <u>tunable constraint region</u> defined by

$$R_{ct} \overset{\Delta}{=} \{\underset{\sim}{\phi} \mid \max_{\underset{\sim}{\rho} \in R_\rho} U(g_i(\underset{\sim}{\phi} + \underset{\sim}{T}\underset{\sim}{\rho}), I, \infty, -1) \geq 0\}, \qquad (3.7)$$

where

$$I \overset{\Delta}{=} \{1, 2, \ldots, m_c\}. \qquad (3.8)$$

<u>Proof</u>

Assume that there exists $\underset{\sim}{\rho}^* \in R_\rho$ such that

$$\underset{\sim}{\phi} + \underset{\sim}{T} \underset{\sim}{\rho}^* \in R_c. \qquad (3.9)$$

Hence,

$$g_i(\underset{\sim}{\phi} + \underset{\sim}{T} \underset{\sim}{\rho}^*) \geq 0 \text{ for all } i \in I. \qquad (3.10)$$

Also,

$$\min_{i \in I} g_i(\underset{\sim}{\phi} + \underset{\sim}{T} \underset{\sim}{\rho}^*) \geq 0. \qquad (3.11)$$

But since

$$\max_{\underset{\sim}{\rho} \in R_\rho} U(g_i(\underset{\sim}{\phi}+\underset{\sim}{T}\underset{\sim}{\rho}), I, \infty, -1) \geq U(g_i(\underset{\sim}{\phi}+\underset{\sim}{T}\underset{\sim}{\rho}^*), I, \infty, -1), \qquad (3.12)$$

and

$$U(g_i(\underset{\sim}{\phi}+\underset{\sim}{T}\underset{\sim}{\rho}^*), I, \infty, -1) = \min_{i \in I} g_i(\underset{\sim}{\phi}+\underset{\sim}{T}\underset{\sim}{\rho}^*) \geq 0, \qquad (3.13)$$

then

$$\underset{\sim}{\phi} \in R_{ct}. \qquad (3.14)$$

Now, $\underset{\sim}{\phi} \in R_{ct}$ implies that there exists $\underset{\sim}{\rho}^* \in R_\rho$ such that (3.13) is satisfied. Consequently,

$$\phi + T \rho^* \in R_c .$$

<div align="right">Q.E.D.</div>

3.3.2 Example

To illustrate this idea, consider a two-dimensional example in which the constraint region is defined by the two constraints

$$g_1(\phi) = \phi_2 - \phi_1 \geq 0 ,$$

$$g_2(\phi) = 5\phi_1 - (\phi_2-5)^2 - 25 \geq 0 .$$

Let

$$\phi^0 = \begin{bmatrix} 4.5 \\ 8.0 \end{bmatrix} , \quad \varepsilon = \begin{bmatrix} 2.0 \\ 2.5 \end{bmatrix} \text{ and } \quad t = \begin{bmatrix} 0.5 \\ 1.0 \end{bmatrix} .$$

Fig. 3.1 shows the constraint region R_c and the tunable constraint region R_{ct}. In the figure R_ε and $R_t(\mu)$ are defined according to (2.5) and (2.10), respectively, where R_ρ is assumed as in (2.12).

3.4 Mathematical Definition of Yield

We are now ready to give a mathematical definition of production yield. An outcome ϕ is said to meet the design specifications either if $\phi \in R_c$ or there exists $\rho \in R_\rho$ such that

$$\phi + T \rho \in R_c , \tag{3.15}$$

i.e., this outcome is tunable. In other words

$$\phi \in R_{ct} . \tag{3.16}$$
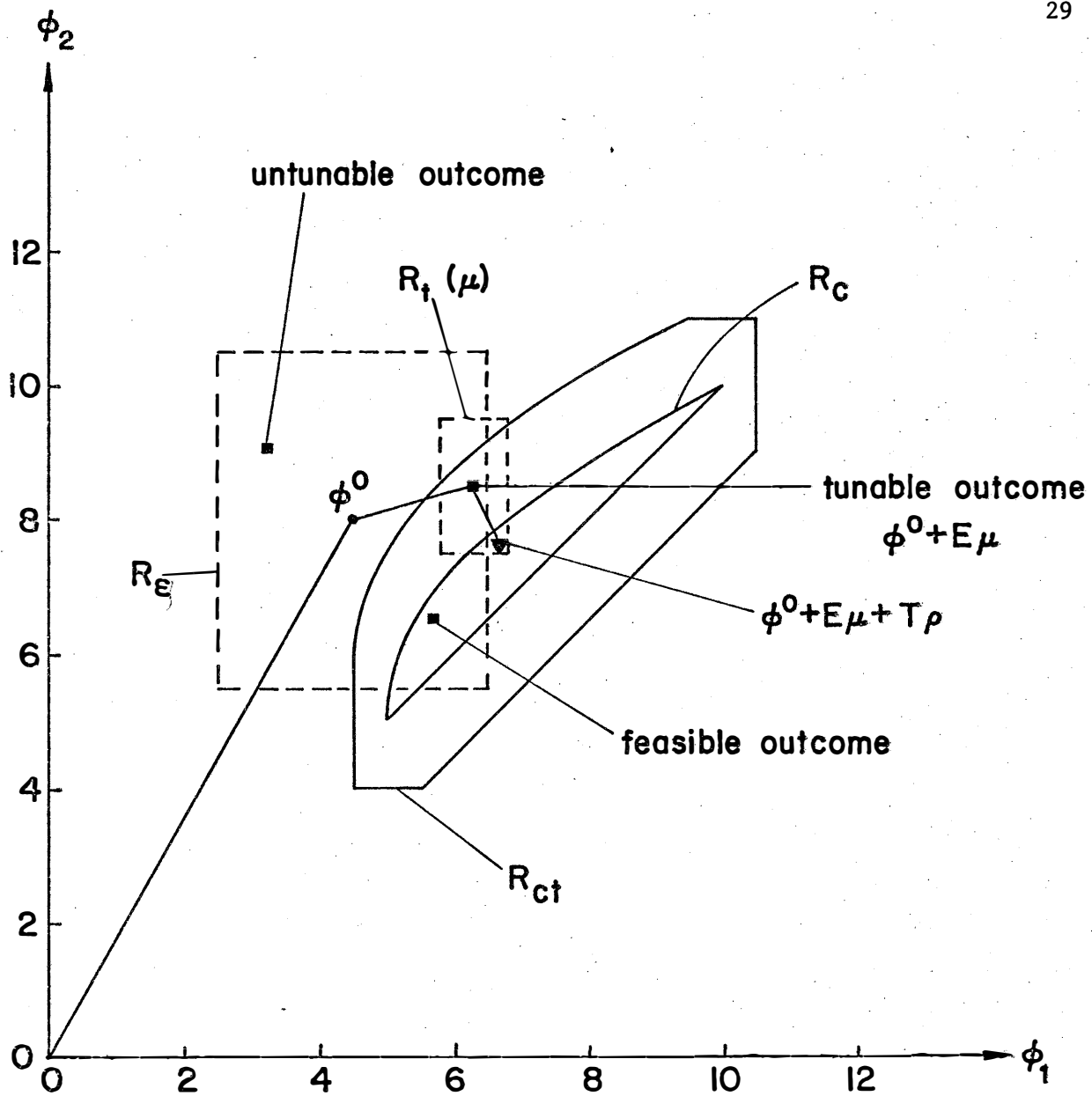
Fig. 3.1 Geometric interpretation of the tolerance problem equivalent to the tolerance-tuning problem.

In an abstract manner, the expected potential yield, i.e., the expected yield after tuning is given by

$$Y_p = \int_{R_{ct}} F(\phi)\, d\phi_1\, d\phi_2 \cdots d\phi_k \ , \qquad (3.17)$$

where $F(\phi)$ is the joint probability distribution function of the outcomes. The expected yield before tuning is

$$Y = \int_{R_c} F(\phi)\, d\phi_1\, d\phi_2 \cdots d\phi_k \ . \qquad (3.18)$$

If the outcomes are uniformly distributed between the tolerance extremes, i.e., inside the orthotope R_ε, the expected potential yield and the expected yield can be expressed as

$$Y_p = V(R_\varepsilon \cap R_{ct})/V(R_\varepsilon) \qquad (3.19)$$

and

$$Y = V(R_\varepsilon \cap R_c)/V(R_\varepsilon) \ , \qquad (3.20)$$

where $V(R)$ denotes the hypervolume of the region R. The expectation of having outcomes which require tuning as a post-manufacturing process is also given by (2.18).

3.5 Worst-case Design

The worst-case design problem arises when the worst outcome is supposed to meet the specifications. This implies a lower potential yield specification $Y_L = 100\%$. Thus, for the nonlinear program, the

constraint (2.25) reduces to

$$R_{\epsilon} \subset R_{ct} \ . \qquad\qquad (3.21)$$

For a one-dimensionally convex region R_{ct}, (3.21) can be replaced by

$$R_v \subset R_{ct} \ , \qquad\qquad (3.22)$$

where R_v is the set of vertices defined by (2.7).

At the worst-case optimum, the set of <u>active constraints</u> at a vertex $\underset{\sim}{\phi}^r \in R_v$ is defined by

$$I_{ac}^r = \{ i \mid g_i(\underset{\sim}{\phi}^r + \underset{\sim}{T} \ \underset{\sim}{\rho}^{r*}) = 0 \ , \ i \in \{ 1,2,\ldots,m_c \} \}, \qquad (3.23)$$

where $\underset{\sim}{\rho}^{r*}$ is the optimum setting for the tuning variable for the vertex

$$\underset{\sim}{\phi}^r = \underset{\sim}{\phi}^{0*} + \underset{\sim}{E}^{*} \ \underset{\sim}{\mu}^r \ , \qquad\qquad (3.24)$$

$\underset{\sim}{E}^{*}$ and $\underset{\sim}{\phi}^{0*}$ are the worst-case optimums of $\underset{\sim}{E}$ and $\underset{\sim}{\phi}^0$, respectively. The set of <u>active vertices</u> is consequently defined by

$$R_{av} = \{ \underset{\sim}{\phi}^r \mid \underset{\sim}{\phi}^r \in R_v, \ I_{ac}^r \neq \emptyset \} \ . \qquad (3.25)$$

The set of all active constraints is

$$I_{ac} = \bigcup_{r=1}^{2k} I_{ac}^r \ . \qquad\qquad (3.26)$$

An alternative approach is to define the set of active vertices for each constraint g_i, $i = 1, 2, \ldots, m_c$, given by

$$R_{av}^i = \{ \underset{\sim}{\phi}^r \mid g_i(\underset{\sim}{\phi}^r + \underset{\sim}{T} \underset{\sim}{\rho}^{r*}) = 0, \underset{\sim}{\phi}^r \in R_v \} , \tag{3.27}$$

where $\underset{\sim}{\phi}^r$ is given by (3.24) and $\underset{\sim}{\rho}^{r*}$ is the setting of the tuning variable for this vertex at the optimum. Thus, the set of active constraints is defined by

$$I_{ac} = \{ i \mid i \in \{1, 2, \ldots, m_c\}, R_{av}^i \neq \emptyset \} . \tag{3.28}$$

The set of all active vertices is

$$R_{av} = \bigcup_{i=1}^{m_c} R_{av}^i . \tag{3.29}$$

3.6   Worst-case Centering

Worst-case centering is a minimax problem in which the tolerance vector $\underset{\sim}{\varepsilon}$ is fixed either absolutely or relatively w.r.t. the nominal vector $\underset{\sim}{\phi}^0$ while $\underset{\sim}{\phi}^0$ and the tuning vector $\underset{\sim}{t}$ are variables. The problem can be expressed as

$$\underset{\substack{\underset{\sim}{\phi}^0 \geq 0, \ 0 \leq \underset{\sim}{t} \leq \underset{\sim}{t}_{max}}}{\text{minimize}} \quad U(-g_i(\underset{\sim}{\phi}^0 + \underset{\sim}{E} \underset{\sim}{\mu} + \underset{\sim}{T} \underset{\sim}{\rho}), I, \infty, 1) , \tag{3.30}$$

where $\underset{\sim}{t}_{max}$ is an upper bound on the tuning range, U is the least pth function defined by (3.1) and $\underset{\sim}{\mu}$ is chosen to give the worst outcome.

3.7   Conclusions

Having a tolerance problem which is equivalent to a tolerance-tuning problem allows us to deal solely with tolerance assignment. It permits the evaluation of yield to be based upon hypervolume computation as is shown in Chapter 4.

The one-dimensional convexity assumption implies that the vertices of the tolerance orthotope are the candidates for worst case. Hence, for a worst-case design, it reduces the infinite number of constraints for the nonlinear program to a finite number. Subsequently, a solution based on this, or any other assumption made to create a tractable problem, can be verified.

CHAPTER 4

YIELD DETERMINATION

THROUGH LINEAR CUTS

4.1   Introduction

An analytical approach to the evaluation of yield and yield sensitivities is presented. The availability of yield sensitivities allows the use of efficient gradient techniques for solving the nonlinear programming problem presented in Chapter 2.

In the case of a _uniform distribution_ of outcomes inside the tolerance orthotope, computation of _hypervolume_ plays the basic role in yield evaluation. Formulas for _nonfeasible hypervolumes_ (hypervolumes outside the constraint region but inside the tolerance orthotope) as well as their sensitivities are provided (Bandler and Abdel-Malek 1977a). An alternative approach to evaluating the nonfeasible hypervolumes based on feasible hypervolumes is also presented. Criteria for choosing a computationally efficient approach are given (Abdel-Malek and Bandler 1977).

The hypervolume formula is based upon _linear cuts_ of the tolerance orthotope. The linear cuts are functions of the nonlinear constraints defining the boundary of the constraint region. It is shown how to construct the cuts in the special cases of linear and quadratic constraints (linking this chapter with the next chapter).

For an arbitrary statistical distribution of outcomes, the

tolerance region is partitioned into a collection of orthotopic cells (orthocells). A weight is assigned to each orthocell and a uniform distribution is assumed inside it. This approach is suitable for circuits, since the distribution of outcomes is usually defined by a histogram rather than an expression for the probability distribution function. Formulas for evaluating the weighted hypervolume and its sensitivities are derived (Abdel-Malek and Bandler 1977). Some simple illustrative examples are given.

PART I

THE UNIFORM DISTRIBUTION

4.2   Evaluation of Hypervolume

Based upon either linearization or intersections of the hypersurface $g(\underset{\sim}{\phi}) = 0$ with the tolerance orthotope, we construct the linear cut

$$q^T_{\underset{\sim}{}} \underset{\sim}{\phi} - c \geq 0 , \qquad\qquad (4.1)$$

where q is a column vector of k components and c is a scalar. We will derive a general expression for the nonfeasible hypervolume defined by this linear cut and the tolerance region R_ε, denoted by $V(R)$, where

$$R = \{\underset{\sim}{\phi} \mid g(\underset{\sim}{\phi}) < 0\} \cap R_\varepsilon . \qquad\qquad (4.2)$$

Define a reference vertex

$$\underset{\sim}{\phi}^r = \underset{\sim}{\phi}^0 + \underset{\sim}{E} \underset{\sim}{\mu}^r , \qquad\qquad (4.3)$$

where

$$\mu^r_i = -\text{sign}(q_i) , \quad i = 1, 2, \ldots, k \qquad\qquad (4.4)$$

and $\underset{\sim}{E}$ is a $k \times k$ diagonal matrix with elements set to ε_i, $i = 1, 2, \ldots, k$, as in (2.3).

The general formula for the hypervolume* can be written as

*H. Tromp originally suggested such a formula (see Acknowlegements).

36

$$V = \left[\frac{1}{k!} \prod_{j=1}^{k} \alpha_j \right] \left[\sum_{s=1}^{2^k} (-1)^{\nu^s} (\delta^s)^k \right], \qquad (4.5)$$

where

$$\delta^s = \max \left(0, \; 1 - \sum_{j=1}^{k} \frac{\epsilon_j}{\alpha_j} \mid \mu_j^s - \mu_j^r \mid \right), \qquad (4.6)$$

$$\nu^s = \sum_{i=1}^{k} \mid \mu_i^s - \mu_i^r \mid / 2 \qquad (4.7)$$

and α_j is the distance between the intersections of the hyperplane $\underset{\sim}{q}^T \underset{\sim}{\phi} - c = 0$ and the reference vertex $\underset{\sim}{\phi}^r$ along an edge of R_ϵ in the jth direction. It is to be noted that δ^s is positive if and only if the vertex $\underset{\sim}{\phi}^s$ violates the linear cut (4.1).

4.2.1 Two Dimensional Examples

Consider the examples given in Fig. 4.1. The nonfeasible area in Fig. 4.1(a) is given by

$$V = \Delta \, \phi^r ab - \Delta \, \phi^4 ac - \Delta \, \phi^1 bd,$$

where Δ abc denotes the area of the triangle abc. Hence,

$$V = \frac{1}{2} \alpha_1 \alpha_2 - \frac{1}{2} \left[\alpha_1 (1 - \frac{2\epsilon_1}{\alpha_1}) \right] \left[\alpha_2 (1 - \frac{2\epsilon_1}{\alpha_1}) \right]$$

$$- \frac{1}{2} \left[\alpha_1 (1 - \frac{2\epsilon_2}{\alpha_2}) \right] \left[\alpha_2 (1 - \frac{2\epsilon_2}{\alpha_2}) \right]$$
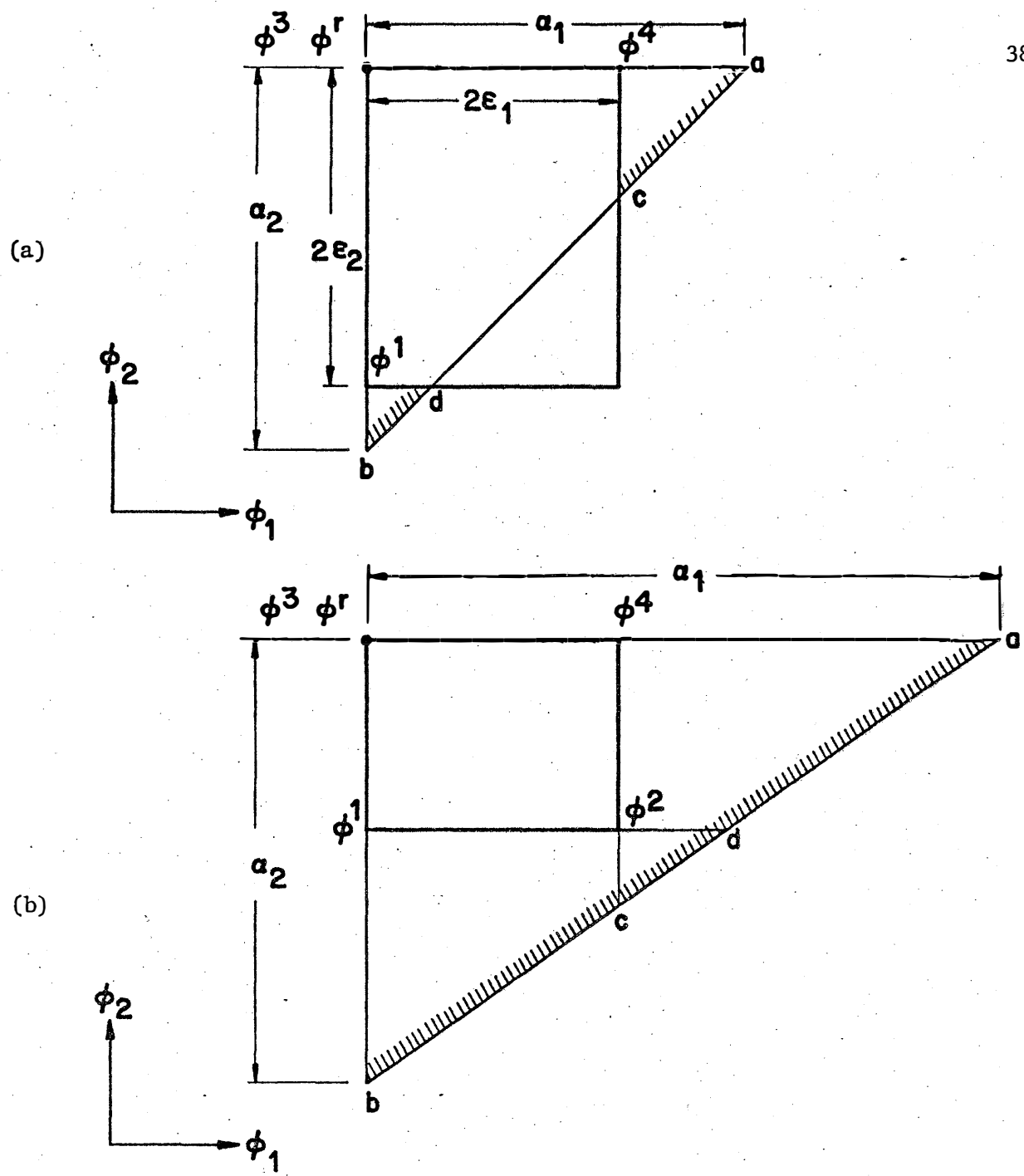
Fig. 4.1   Two-dimensional examples illustrating the calculation of
the nonfeasible hypervolumes, (a) partially feasible
tolerance region, (b) nonfeasible tolerance region.

$$= \frac{1}{2} \alpha_1 \alpha_2 \left[1- (1 - \frac{2\varepsilon_1}{\alpha_1})^2 - (1 - \frac{2\varepsilon_2}{\alpha_2})^2 \right].$$

Also, in Fig. 4.1(b), the nonfeasible area is given by

$$V = \Delta \phi^r \, ab - \Delta \phi^4 \, ac - \Delta \phi^1 \, bd + \Delta \phi^2 \, cd$$

$$= \frac{1}{2} \alpha_1 \alpha_2 \left[1- (1- \frac{2\varepsilon_1}{\alpha_1})^2 - (1- \frac{2\varepsilon_2}{\alpha_2})^2 + (1- \frac{2\varepsilon_1}{\alpha_1} - \frac{2\varepsilon_2}{\alpha_2})^2 \right].$$

4.2.2 Three Dimensional Example

In the example shown in Fig. 4.2, the intersections of the linear cut with the orthotope edges are defined by the polygon abcde. The nonfeasible volume is given by

$$V = \frac{1}{6} \alpha_1 \alpha_2 \alpha_3 \left[1- (1- \frac{2\varepsilon_1}{\alpha_1})^3 - (1- \frac{2\varepsilon_2}{\alpha_2})^3 - (1- \frac{2\varepsilon_3}{\alpha_3})^3 \right.$$

$$\left. + (1- \frac{2\varepsilon_1}{\alpha_1} - \frac{2\varepsilon_2}{\alpha_2})^3 \right].$$

4.3 Hypervolume Sensitivities

The hypervolume sensitivities can be expressed as

$$\frac{\partial V}{\partial \phi_i^0} = \frac{1}{k!} \left[\sum_{j=1}^{k} \frac{\partial \alpha_j}{\partial \phi_i^0} \prod_{\substack{p=1 \\ p \neq j}}^{k} \alpha_p \right] B + A \left[k \sum_{s=1}^{2k} (-1)^{\nu^s} (\delta^s)^{k-1} \frac{\partial \delta^s}{\partial \phi_i^0} \right], \quad (4.8)$$
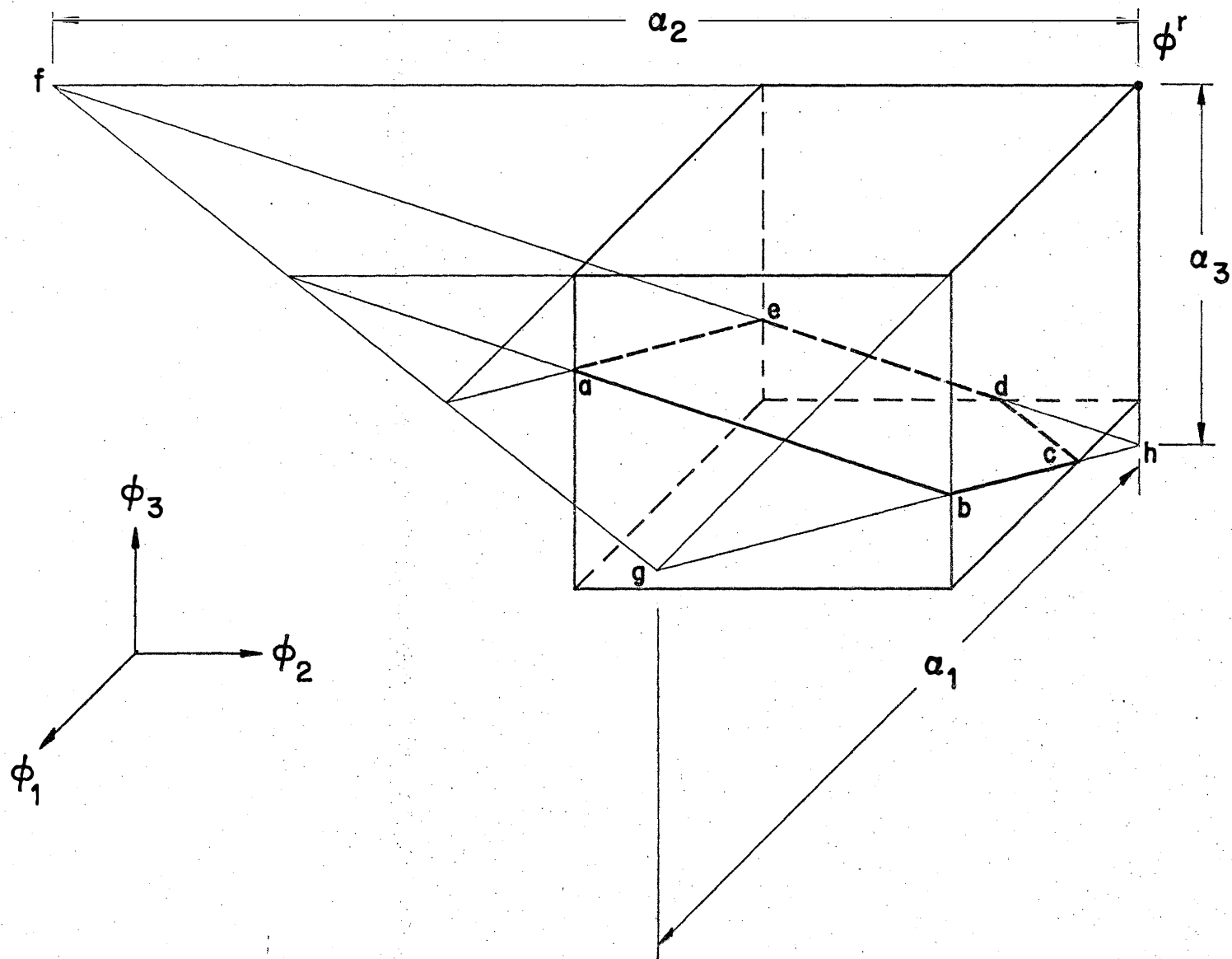
Fig. 4.2   Three-dimensional example illustrating the calculation of nonfeasible hypervolume for partially feasible tolerance region.

$$\frac{\partial V}{\partial \epsilon_i} = \mu_i^r \frac{\partial V}{\partial \phi_i^0} - A \left[\frac{k}{\alpha_i} \sum_{s=1}^{2^k} (-1)^{\nu^s} |\mu_i^s - \mu_i^r| (\delta^s)^{k-1} \right] , \qquad (4.9)$$

where

$$A = \frac{1}{k!} \prod_{j=1}^{k} \alpha_j , \qquad (4.10)$$

$$B = \sum_{s=1}^{2^k} (-1)^{\nu^s} (\delta^s)^k \qquad (4.11)$$

and

$$\frac{\partial \delta^s}{\partial \phi_i^0} = \begin{cases} 0 & \text{if } \delta^s = 0 , \\ \\ \sum_{j=1}^{k} \frac{\epsilon_i}{(\alpha_j)^2} |\mu_j^s - \mu_j^r| \frac{\partial \alpha_j}{\partial \phi_i^0} & \text{if } \delta^s > 0 . \end{cases} \qquad (4.12)$$

It is to be mentioned that the hypervolume and its sensitivities are defined when $\alpha_i \rightarrow \infty$ for any i, since the limit exists. But, the sensitivities are discontinuous whenever a vertex ϕ^s satisfies the equation

$$q^T \phi^s - c = 0 . \qquad (4.13)$$

4.4   An Alternative Approach

For an alternative approach to calculating the hypervolume V and its sensitivities we define a complementary vertex

$$\bar{\phi}^r = \phi^0 + E \bar{\mu}^r, \qquad (4.14)$$

where

$$\bar{\mu}_i^r = -\mu_i^r = \text{sign}(q_i), \quad i = 1, 2, \ldots, k . \qquad (4.15)$$

In a similar manner we define $\bar{\alpha}_j$ as the distance between the complementary vertex ϕ^r and the intersection of the hyperplane $q^T\phi - c = 0$ along an edge of R_ε in the jth direction. Hence, the nonfeasible hypervolume defined by the linear cut (4.1) is

$$V = 2^k \prod_{j=1}^k \varepsilon_j - \left[\frac{1}{k!} \prod_{j=1}^k \bar{\alpha}_j \right] \left[\sum_{s=1}^{2^k} (-1)^{\bar{\nu}^s} (\bar{\delta}^s)^k \right], \qquad (4.16)$$

where

$$\bar{\delta}^s = \max \left(0, 1 - \sum_{j=1}^k \frac{\varepsilon_j}{\bar{\alpha}_j} | \mu_j^s - \bar{\mu}_j^r | \right), \qquad (4.17)$$

$$\bar{\nu}^s = \sum_{i=1}^k | \mu_i^s - \bar{\mu}_i^r | / 2 . \qquad (4.18)$$

The hypervolume sensitivities can be expressed as

$$\frac{\partial V}{\partial \phi_i^0} = - \left(\frac{1}{k!} \sum_{j=1}^{k} \frac{\partial \overline{\alpha}_j}{\partial \phi_i^0} \prod_{\substack{p=1 \\ p \neq j}}^{k} \overline{\alpha}_p \right) \overline{B}$$

$$- \overline{A} \left(k \sum_{s=1}^{2k} (-1)^{\overline{\nu}^s} (\overline{\delta}^s)^{k-1} \frac{\partial \overline{\delta}^s}{\partial \phi_i^0} \right) , \qquad (4.19)$$

$$\frac{\partial V}{\partial \varepsilon_i} = 2^k \prod_{\substack{j=1 \\ j \neq i}}^{k} \varepsilon_j + \mu_i^{\overline{r}} \frac{\partial V}{\partial \phi_i^0}$$

$$+ \overline{A} \left(\frac{k}{\overline{\alpha}_i} \sum_{s=1}^{2k} (-1)^{\overline{\nu}^s} | \mu_i^s - \mu_i^{\overline{r}} | (\overline{\delta}^s)^{k-1} \right) , \qquad (4.20)$$

where

$$\overline{A} = \frac{1}{k!} \prod_{j=1}^{k} \overline{\alpha}_j , \qquad (4.21)$$

$$\overline{B} = \sum_{s=1}^{2k} (-1)^{\overline{\nu}^s} (\overline{\delta}^s)^k \qquad (4.22)$$

and

$$\frac{\partial \overline{\delta}^s}{\partial \phi_i^0} = \begin{cases} 0 & \text{if } \overline{\delta}^s = 0 , \\[3ex] \displaystyle\sum_{j=1}^{k} \frac{\varepsilon_j}{(\overline{\alpha}_j)^2} | \mu_j^s - \mu_j^{\overline{r}} | \frac{\partial \overline{\alpha}_j}{\partial \phi_i^0} & \text{if } \overline{\delta}^s > 0 . \end{cases} \qquad (4.23)$$

4.5   Efficient Computation

In order to evaluate the hypervolume and its sensitivities efficiently we use the following criteria:

(i)   If $q^T \phi^r - c \geq 0$, use the reference vertex approach.

(ii)   If $q^T \phi^{\overline{r}} - c \leq 0$, use the complementary vertex approach.

(iii)   If $q^T \phi^r - c < 0$ and $q^T \phi^{\overline{r}} - c > 0$, then

if $|q^T \phi^r - c| \leq |q^T \phi^{\overline{r}} - c|$, use reference vertex approach,

if $|q^T \phi^r - c| > |q^T \phi^{\overline{r}} - c|$, use complementary vertex approach,

where ϕ^r and $\phi^{\overline{r}}$ are the reference and complementary vertices, respectively. The cases (i) and (ii) are clear since the orthotope will be either completely feasible or completely nonfeasible, respectively. Case (iii) follows according to the following theorem.

4.5.1   Theorem 4.1

If $q^T \phi^r - c < 0$, $q^T \phi^{\overline{r}} - c > 0$ and $|q^T \phi^r - c| \leq |q^T \phi^{\overline{r}} - c|$, then

$$\text{Order } (S) \leq \text{Order } (\overline{S}), \tag{4.24}$$

where

$$S \triangleq \{s \mid s \in \{1, 2, \ldots, 2^k\}, q^T \phi^s - c < 0\}, \tag{4.25}$$

$$\overline{S} \triangleq \{s \mid s \in \{1, 2, \ldots, 2^k\}, q^T \phi^s - c > 0\}. \tag{4.26}$$

In other words

$$S \triangleq \{s \mid \delta^s > 0\} \,, \tag{4.27}$$

$$\overline{S} \triangleq \{s \mid \overline{\delta}^s > 0\} \,. \tag{4.28}$$

<u>Proof</u>

In the case under consideration the order of a set is simply the number of its elements. Assume that $s \in S$, then

$$\underset{\sim}{q}^T \underset{\sim}{\phi}^s - c < 0 \,, \tag{4.29}$$

$$\underset{\sim}{q}^T \underset{\sim}{\phi}^r - c + \underset{\sim}{q}^T(\underset{\sim}{\phi}^s - \underset{\sim}{\phi}^r) < 0 \,, \tag{4.30}$$

or

$$-(\underset{\sim}{q}^T \underset{\sim}{\phi}^r - c) + \sum_{i=1}^{k} q_i \varepsilon_i (-\mu_i^s + \mu_i^r) > 0 \,. \tag{4.31}$$

But, since

$$-(\underset{\sim}{q}^T \underset{\sim}{\phi}^r - c) \leq (\underset{\sim}{q}^T \overline{\underset{\sim}{\phi}^r} - c) \text{ and } \mu_i^r = -\overline{\mu}_i^r \,, \tag{4.32}$$

then

$$(\underset{\sim}{q}^T \overline{\underset{\sim}{\phi}^r} - c) + \sum_{i=1}^{k} q_i \varepsilon_i (-\mu_i^s - \overline{\mu}_i^r) > 0 \,, \tag{4.33}$$

i.e.,

$$\underset{\sim}{q}^T \overline{\underset{\sim}{\phi}}^s - c > 0 \,, \tag{4.34}$$

where

$$\bar{\phi}^s = \phi^0 - E \, \mu^s \, . \tag{4.35}$$

Hence,

$$\bar{s} \, \epsilon \, \bar{S} \, . \tag{4.36}$$

This means that for each vertex $s \, \epsilon \, S$ there exists a vertex $\bar{s} \, \epsilon \, \bar{S}$, thus

$$\text{Order } (S) \leq \text{Order } (\bar{S}) \, .$$

Q.E.D.

4.6   Example

Consider the following four-dimensional example, with a linear cut given by

$$\frac{\phi_1}{24} + \frac{\phi_2}{15} + \frac{\phi_3}{60} + \frac{\phi_4}{240} - 1 \geq 0 \, .$$

and where

$$\phi^0 = \begin{bmatrix} 9 \\ 7 \\ 9 \\ 26 \end{bmatrix} \, , \qquad \varepsilon = \begin{bmatrix} 5 \\ 2 \\ 4 \\ 6 \end{bmatrix} \, .$$

Hence,

$$\phi^r = \begin{bmatrix} 9 \\ 7 \\ 9 \\ 26 \end{bmatrix} + \begin{bmatrix} 5 & 0 & 0 & 0 \\ 0 & 2 & 0 & 0 \\ 0 & 0 & 4 & 0 \\ 0 & 0 & 0 & 6 \end{bmatrix} \begin{bmatrix} -1 \\ -1 \\ -1 \\ -1 \end{bmatrix} = \begin{bmatrix} 4 \\ 5 \\ 5 \\ 20 \end{bmatrix}$$

and

$$V = \left[\frac{1}{4!} \, 8 \times 5 \times 20 \times 80 \right] \left[1 - (1 - \frac{4}{5})^4 - (1 - \frac{8}{20})^4 - (1 - \frac{12}{80})^4 \right.$$

$$\left. + (1 - \frac{4}{5} - \frac{12}{80})^4 + (1 - \frac{8}{20} - \frac{12}{80})^4 \right]$$

$$= 1034.15$$

Table 4.1 shows the nonfeasible vertices. A check of the analytical formulas for the gradients and the numerical gradients obtained by central differences is shown in Table 4.2.

The alternative approach will lead to

$$\phi^r \begin{bmatrix} 9 \\ 7 \\ 9 \\ 26 \end{bmatrix} + \begin{bmatrix} 5 & 0 & 0 & 0 \\ 0 & 2 & 0 & 0 \\ 0 & 0 & 4 & 0 \\ 0 & 0 & 0 & 6 \end{bmatrix} \begin{bmatrix} 1 \\ 1 \\ 1 \\ 1 \end{bmatrix} = \begin{bmatrix} 14 \\ 9 \\ 13 \\ 32 \end{bmatrix},$$

$$V = 2^4 \times 5 \times 2 \times 4 \times 6 - \left[\frac{1}{4!} \, (8 \times 1.6)(5 \times 1.6)(20 \times 1.6)(80 \times 1.6) \right]$$

$$\cdot \left[1 - (1 - \frac{10}{8 \times 1.6})^4 - (1 - \frac{4}{5 \times 1.6})^4 - (1 - \frac{8}{20 \times 1.6})^4 \right.$$

$$+ (1 - \frac{4}{5 \times 1.6} - \frac{8}{20 \times 1.6})^4 - (1 - \frac{12}{80 \times 1.6})^4$$

$$+ (1 - \frac{10}{8 \times 1.6} - \frac{12}{80 \times 1.6})^4 + (1 - \frac{4}{5 \times 1.6} - \frac{12}{80 \times 1.6})^4$$

$$\left. + (1 - \frac{8}{20 \times 1.6} - \frac{12}{80 \times 1.6})^4 - (1 - \frac{4}{5 \times 1.6} - \frac{8}{20 \times 1.6} - \frac{12}{80 \times 1.6})^4 \right]$$

$$= 3840 - 2805.85 = 1034.15$$

TABLE 4.1

NONFEASIBLE VERTICES FOR THE EXAMPLE IN SECTION 4.6

Vertex	ϕ_1	ϕ_2	ϕ_3	ϕ_4	μ_1	μ_2	μ_3	μ_4	Nonfeasible vertices
1	4	5	5	20	-1	-1	-1	-1	X
2	14	5	5	20	1	-1	-1	-1	
3	4	9	5	20	-1	1	-1	-1	X
4	14	9	5	20	1	1	-1	-1	
5	4	5	13	20	-1	-1	1	-1	X
6	14	5	13	20	1	-1	1	-1	
7	4	9	13	20	-1	1	1	-1	
8	14	9	13	20	1	1	1	-1	
9	4	5	5	32	-1	-1	-1	1	X
10	14	5	5	32	1	-1	-1	1	
11	4	9	5	32	-1	1	-1	1	X
12	14	9	5	32	1	1	-1	1	
13	4	5	13	32	-1	-1	1	1	X
14	14	5	13	32	1	-1	1	1	
15	4	9	13	32	-1	1	1	1	
16	14	9	13	32	1	1	1	1	

TABLE 4.2

HYPERVOLUME GRADIENT CHECK

Parameters	Analytical gradients	Numerical gradients
ϕ_1^0	-337.50	-337.50
ϕ_2^0	-540.00	-540.00
ϕ_3^0	-135.00	-135.00
ϕ_4^0	- 33.75	- 33.75
ε_1	337.50	337.50
ε_2	573.60	573.60
ε_3	268.20	268.20
ε_4	173.18	173.18

4.7   The Linear Constraints Case

Let the constraint region be defined by the m linear constraints

$$g_\ell(\underset{\sim}{\phi}) = \underset{\sim}{\phi}^T \underset{\sim}{q}^\ell - c^\ell \geq 0, \quad \ell = 1, 2, \ldots, m. \tag{4.37}$$

Assuming <u>no overlapping</u> of nonfeasible regions defined by different constraints inside the orthotope R_ϵ, i.e.,

$$R_i \underset{i \neq j}{\cap} R_j = \emptyset \, , \tag{4.38}$$

where

$$R_\ell \overset{\Delta}{=} \{\underset{\sim}{\phi} \in R_\epsilon \mid g_\ell(\underset{\sim}{\phi}) < 0\} \, , \tag{4.39}$$

the yield can be expressed as

$$Y = 1 - \sum_{\ell=1}^{m} V(R_\ell)/V(R_\epsilon) \, . \tag{4.40}$$

Knowing that

$$V(R_\epsilon) = 2^k \prod_{j=1}^{k} \epsilon_j \, , \tag{4.41}$$

the yield sensitivities are given by

$$\frac{\partial Y}{\partial \phi_i^0} = - \sum_{\ell=1}^{m} \frac{\partial V^\ell}{\partial \phi_i^0} \Big/ \left(2^k \prod_{j=1}^{k} \epsilon_j \right) \, , \tag{4.42}$$

$$\frac{\partial Y}{\partial \epsilon_i} = \left(\frac{1}{\epsilon_i} \sum_{\ell=1}^{m} V^\ell - \sum_{\ell=1}^{m} \frac{\partial V^\ell}{\partial \epsilon_i} \right) \bigg/ \left((2^k \prod_{j=1}^{k} \epsilon_j) \right) , \qquad (4.43)$$

where V^ℓ denotes $V(R_\ell)$. The linear constraints can be used as linear cuts directly. Hence, the nonfeasible hypervolume V^ℓ and its sensitivities can be obtained using (4.5), (4.8) and (4.9) for each constraint and where

$$\alpha_j^\ell = \mu_j^r \, g_\ell(\phi^r) \big/ q_j^\ell \, ,$$

$$= \mu_j^r \left(\sum_{i=1}^{k} q_i^\ell \, (\phi_i^0 + \mu_i^r \, \epsilon_i) - c^\ell \right) \bigg/ q_j^\ell \, , \qquad (4.44)$$

$$\frac{\partial \alpha_j^\ell}{\partial \phi_i^0} = \mu_j^r \, q_i^\ell \big/ q_j^\ell \, , \qquad (4.45)$$

according to the reference vertex approach or using (4.16), (4.19) and (4.20), where

$$\overline{\alpha}_j^\ell = \overline{\mu}_j^r \, g_\ell(\overline{\phi}^r) / q_j^\ell$$

$$= \overline{\mu}_j^r \left(\sum_{i=1}^{k} q_i^\ell \, (\phi_i^0 + \overline{\mu}_i^r \, \epsilon_i) - c^\ell \right) \bigg/ q_j^\ell \, , \qquad (4.46)$$

$$\frac{\partial \overline{\alpha}_j^\ell}{\partial \phi_i^0} = \overline{\mu}_j^r \, q_i^\ell \big/ q_j^\ell \, , \qquad (4.47)$$

for the ℓth constraint using the complementary vertex approach.

4.8   The Quadratic Constraints Case

4.8.1 Method Based on Intersections

Consider a vertex $\underset{\sim}{\phi}^r$ detected to be active w.r.t. a quadratic constraint $g_\ell(\underset{\sim}{\phi}) \geq 0$ after the worst-case design process (see Section 3.5). If the tolerances are allowed to increase slightly beyond their worst-case values, intersections between the orthotope edges passing through $\underset{\sim}{\phi}^r$ and the hypersurface $g_\ell(\underset{\sim}{\phi}) = 0$ will arise. The number of these intersections is k, which is the number of edges passing through $\underset{\sim}{\phi}^r$, if

$$\partial g_\ell(\underset{\sim}{\phi}^r)/\partial \phi_j \neq 0 \ , \quad \text{for all } j \ . \tag{4.48}$$

In order to find the intersection point along the jth edge, or its extension in the direction $-\mu_j^r \underset{\sim}{e}_j$, where $\underset{\sim}{e}_j$ is a unit vector in the jth direction, we express $g_\ell(\underset{\sim}{\phi}) = 0$ as

$$(\phi_j)^2 + 2\phi_j \ \xi_\ell(\phi_1^r, \ \phi_2^r, \ \ldots, \ \phi_{j-1}^r, \ \phi_{j+1}^r, \ \ldots, \ \phi_k^r)$$

$$+ \ n_\ell(\phi_1^r, \ \phi_2^r, \ \ldots, \ \phi_{j-1}^r, \ \phi_{j+1}^r, \ \ldots, \ \phi_k^r) = 0 \ , \tag{4.49}$$

where ξ_ℓ and n_ℓ are constant functions and ϕ_j is the only variable. Hence, the point of intersection is $(\phi_1^r, \ \phi_2^r, \ \ldots, \ \lambda_j^\ell, \ \ldots, \ \phi_k^r)$, where

$$\lambda_j^\ell = -\ \xi_\ell \pm \sqrt{\xi_\ell^2 - n_\ell} \ , \quad \mu_j^r(\phi_j^r - \lambda_j^\ell) > 0 \ , \tag{4.50}$$

is a real root of (4.49). The condition imposed on the root insures that it is in the direction $-\mu_j^r e_j$ w.r.t. ϕ^r. If both roots lie to this direction, the one closer to ϕ^r is to be chosen.

The equation of the hyperplane, representing the linear cut, which passes through these k points of intersection is

$$
\det
\begin{bmatrix}
\phi_1 & \phi_2 & \cdots & \phi_k & 1 \\
\lambda_1^{\ell} & \phi_2^r & \cdots & \phi_k^r & 1 \\
\phi_1^r & \lambda_2^{\ell} & \cdots & \phi_k^r & 1 \\
\vdots & & & & \\
\phi_1^r & \phi_2^r & \cdots & \lambda_k^{\ell} & 1
\end{bmatrix}
= 0 ,
\qquad (4.51)
$$

and ϕ^r is a reference vertex for this cut.

The yield sensitivities are calculated according to the gradients of the k intersections.

$$
\frac{\partial \lambda_j^{\ell}}{\partial \phi_i} = - \frac{\partial \xi_{\ell}}{\partial \phi_i} \pm \frac{1}{2\sqrt{\xi_{\ell}^2 - \eta_{\ell}}} \left(2\xi_{\ell} \frac{\partial \xi_{\ell}}{\partial \phi_i} - \frac{\partial \eta_{\ell}}{\partial \phi_i} \right) , \quad i \neq j , \qquad (4.52)
$$

$$
\frac{\partial \lambda_i^{\ell}}{\partial \phi_i} = 0 . \qquad (4.53)
$$

Thus, if α_j^{ℓ} is the distance from the vertex ϕ^r to the point of intersection with the ℓth constraint along the orthotope edge in the jth direction, then

$$
\alpha_j^{\ell} = \mu_j^r (\phi_j^r - \lambda_j^{\ell}) , \qquad (4.54)
$$

$$
\frac{\partial \alpha_j^{\ell}}{\partial \phi_i^0} = - \mu_j^r \frac{\partial \lambda_j^{\ell}}{\partial \phi_i} , \quad i \neq j , \qquad (4.55)
$$

$$\frac{\partial \alpha_j^{\ell}}{\partial \phi_j^0} = \mu_j^r \quad .$$ (4.56)

4.8.2 Method Based on Linearization

An alternative method to obtain the cuts is to consider linearizing the quadratic constraints at a point $\phi^a_{\sim}$ which may be the nominal point $\phi^0_{\sim}$ or a vertex $\phi^r_{\sim}$. Hence, the linear cut based upon the ℓth constraint is given by

$$g_{\ell}(\phi^a_{\sim}) + (\phi_{\sim} - \phi^a_{\sim})^T \nabla_{\sim} g_{\ell}(\phi^a_{\sim}) \geq 0 \quad .$$ (4.57)

The reference vertex $\phi^r_{\sim}$ is identified by

$$\mu_j^r = -\text{sign}\left(\frac{\partial g_{\ell}(\phi^a_{\sim})}{\partial \phi_j}\right) \quad , \; j = 1, 2, \ldots, k \quad .$$ (4.58)

The distance from the reference vertex to the point of intersection with the ℓth cut along the orthotope edge in the jth direction is

$$\alpha_j^{\ell} = \mu_j^r \left[g_{\ell}(\phi^a_{\sim}) + (\phi^r_{\sim} - \phi^a_{\sim})^T \nabla g_{\ell}(\phi^a_{\sim})\right] \Big/ \left(\frac{\partial g_{\ell}(\phi^a_{\sim})}{\partial \phi_j}\right) .$$ (4.59)

Accordingly, we have

$$\frac{\partial \alpha_j^{\ell}}{\partial \phi_i^0} = \mu_j^r \left[\frac{\partial g_{\ell}(\phi^a_{\sim})}{\partial \phi_i} + (\phi^r_{\sim} - \phi^a_{\sim})^T H_{\sim i}\right] \Big/ \left(\frac{\partial g_{\ell}(\phi^a_{\sim})}{\partial \phi_j}\right)$$

$$- \mu_j^r \left[g_\ell(\phi^a) + (\phi^r - \phi^a)^T \nabla g_\ell(\phi^a) \right] H_{ji} \Big/ \left(\frac{\partial g_\ell(\phi^a)}{\partial \phi_j} \right)^2, \quad (4.60)$$

where

$$\underset{\sim}{H} = \begin{bmatrix} \frac{\partial^2 g_\ell(\phi)}{\partial \phi_1^2} & \frac{\partial^2 g_\ell(\phi)}{\partial \phi_1 \partial \phi_2} & \cdots & \frac{\partial^2 g_\ell(\phi)}{\partial \phi_1 \partial \phi_k} \\[2ex] \frac{\partial^2 g_\ell(\phi)}{\partial \phi_2 \partial \phi_1} & \frac{\partial^2 g_\ell(\phi)}{\partial \phi_2^2} & \cdots & \frac{\partial^2 g_\ell(\phi)}{\partial \phi_2 \partial \phi_k} \\[2ex] \vdots & & & \\[2ex] \frac{\partial^2 g_\ell(\phi)}{\partial \phi_k \partial \phi_1} & \frac{\partial^2 g_\ell(\phi)}{\partial \phi_k \partial \phi_2} & \cdots & \frac{\partial^2 g_\ell(\phi)}{\partial \phi_k^2} \end{bmatrix}, \quad (4.61)$$

is the <u>Hessian matrix</u> which is a constant matrix for a quadratic function $g_\ell(\phi)$, $\underset{\sim}{H}_i$ is the ith column of $\underset{\sim}{H}$ and H_{ji} is an element of $\underset{\sim}{H}$. In deriving (4.60) it is assumed that $(\phi^r - \phi^a)$ is independent of ϕ_i^0, $i = 1, 2, \ldots, k$.

PART II

ARBITRARY STATISTICAL DISTRIBUTIONS

4.9   The General Case

As described in Chapter 2, we can assume that all outcomes will lie within the tolerance orthotope R_ϵ. This orthotope is now partitioned into a set of orthocells $R(i_1, i_2, \ldots, i_k)$ as shown in Fig. 4.3, where $i_j = 1, 2, \ldots, n_j$, n_j is the number of intervals in the jth direction and $j = 1, 2, \ldots, k$. A _weighting factor_ $W(i_1, i_2, \ldots, i_k)$ is assigned to each orthocell and is given by

$$W(\underset{\sim}{i}) = w(\underset{\sim}{i})/V(R(\underset{\sim}{i})) \, , \tag{4.62}$$

where

$$\underset{\sim}{i} = (i_1, i_2, \ldots, i_k) \, , \tag{4.63}$$

$$w(\underset{\sim}{i}) = \int_{R(\underset{\sim}{i})} F(\underset{\sim}{\phi}) \, dv \, , \tag{4.64}$$

$$V(R(\underset{\sim}{i})) = \int_{R(\underset{\sim}{i})} dv = \prod_{j=1}^{k} \epsilon_{j,i_j} \, , \tag{4.65}$$

$$dv = d\phi_1 \, d\phi_2 \, \ldots \, d\phi_k \, , \tag{4.66}$$
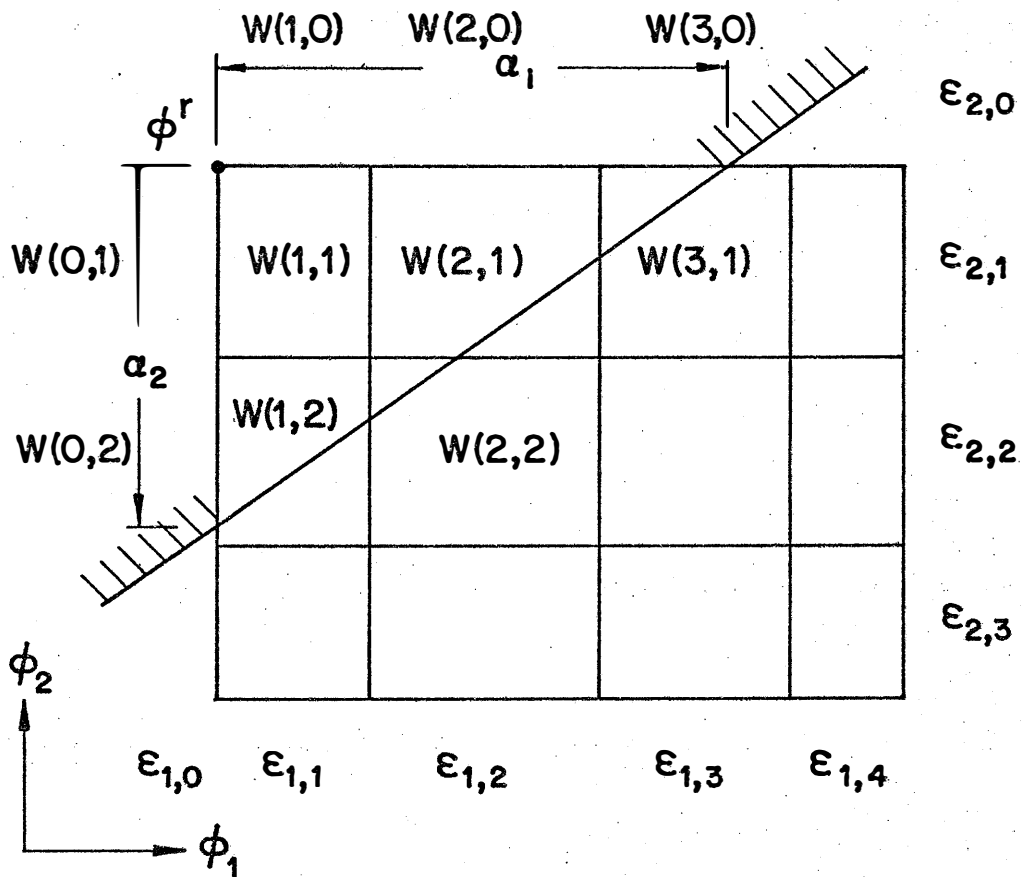
Fig. 4.3 Two-dimensional illustration of the partitioning
of the tolerance region into cells indicating the
dimensions and weighting of those cells relevant to
the calculation of the weighted nonfeasible hyper-
volume.

ε_{1,i_1}, ε_{2,i_2}, ..., ε_{k,i_k} are the dimensions of the orthocell and $F(\underset{\sim}{\phi})$ is the joint probability distribution function (PDF).

The weighting factors $W(\underset{\sim}{i})$ can also be obtained by sampling the parameters or from a histogram if the PDF is not available.

In principle, the problem of finding the yield is now reduced to finding the contribution to the yield given by all of these orthocells. Considering $\prod_{j=1}^{k} n_j$ orthocells independently, however, will be a tedious job. By exploiting how the hypervolume formula (4.5) is constructed, a formula for the __weighted nonfeasible hypervolume__ with respect to the ℓth constraint is constructed and is given by

$$V^\ell = \left(\frac{1}{k!} \prod_{j=1}^{k} \alpha_j^\ell \right) \left(\sum_{i_1=1}^{n_1+1} \sum_{i_2=1}^{n_2+1} \cdots \sum_{i_k=1}^{n_k+1} \Delta W(\underset{\sim}{i}) \left(\delta^\ell(\underset{\sim}{i}) \right)^k \right) , \qquad (4.67)$$

where, for indexing with respect to $\underset{\sim}{\phi}^r$, i.e., numbering starts at this vertex (see Fig. 4.3), α_j^ℓ is the distance from the reference vertex to the point of intersection of the ℓth linear cut with the orthotope edge in the jth direction,

$$\delta^\ell(\underset{\sim}{i}) = \max \left(0, 1 - \sum_{j=1}^{k} \frac{1}{\alpha_j^\ell} \sum_{p=1}^{i_j} \varepsilon_{j,p-1} \right) , \qquad (4.68)$$

$$\varepsilon_{j,0} = 0 , \quad j = 1, 2, \ldots, k , \qquad (4.69)$$

$$\Delta W(\underset{\sim}{i}) = W(\underset{\sim}{i}) - \sum_{j=1}^{k} W(\underset{\sim}{i}-e_j) + \sum_{j=1}^{k-1} \sum_{p=j+1}^{k} W(\underset{\sim}{i}- \underset{\sim}{e}_j - \underset{\sim}{e}_p) - \dots$$

$$+ (-1)^k W(\underset{\sim}{i} - \underset{\sim}{e}_1 - \underset{\sim}{e}_2 - \dots - \underset{\sim}{e}_k) , \qquad (4.70)$$

$$\underset{\sim j}{e} = (0, 0, \dots, 0, \underset{\underset{j}{\vdots}}{1}, 0, \dots, 0) \qquad (4.71)$$

and where

$$W(\underset{\sim}{i}) = 0 \text{ if } i_j = 0 \text{ or } i_j = n+1 \text{ for any } j. \qquad (4.72)$$

Again, assuming no overlapping of nonfeasible regions defined by different cuts inside the orthotope R_ε , the yield can be expressed as

$$Y = 1 - \sum_{\ell=1}^{m} V^\ell , \qquad (4.73)$$

where m is the number of linear cuts.

4.10   Independent Parameters

In the case of _independent parameters,_ (4.67) can be written as

$$V^\ell = \left(\frac{1}{k!} \prod_{j=1}^{k} \alpha_j^\ell \right) \left(\sum_{i_1=1}^{n_1+1} \Delta W_1(i_1) \sum_{i_2=1}^{n_2+1} \Delta W_2(i_2) \dots \right.$$

$$\left. \begin{array}{c} n_k+1 \\ \Sigma \\ i_k=1 \end{array} \Delta W_k(i_k) \ (\delta^\ell(\underset{\sim}{i}))^k \right] \ , \tag{4.74}$$

where $\underset{\sim}{i}$ and $\delta^\ell(\underset{\sim}{i})$ are as defined in (4.63) and (4.68), respectively, and where

$$\Delta W_j(i_j) = W_j(i_j) - W_j(i_j-1) \ , \ j = 1, 2, \ldots, k, \tag{4.75}$$

$$W_j(0) = W_j(n_j+1) = 0 \ , \qquad j = 1, 2, \ldots, k, \tag{4.76}$$

$$W_j(i_j) = w_j(i_j)/\epsilon_{j,i_j} \ , \qquad i_j = 1, 2, \ldots, n_j, \tag{4.77}$$

$$w_j(i_j) = \int_{R_j(i_j)} f_j(\phi_j) \ d\phi_j \ , \ i_j = 1, 2, \ldots, n_j, \tag{4.78}$$

$f_j(\phi_j)$ is the PDF of the jth parameter and $R_j(i_j)$ is the ith interval for that parameter. Similarly the yield will be given by (4.73).

4.11   Yield Sensitivities

Formulas for yield sensitivities can be derived assuming that the weighting factors $W(\underset{\sim}{i})$ are independent of $\underset{\sim}{\phi}^0$ as long as the ratios between ϵ_{j,i_j} , $i_j = 1, 2, \ldots, n_j$, are fixed for each parameter $j = 1, 2, \ldots, k$. This is true, for example, if the sizes of the orthocells are fixed.

Let

$$\kappa_{j,i_j} = \epsilon_{j,i_j}/\epsilon_j \ , \tag{4.79}$$

hence,

$$\sum_{i_j=1}^{n_j} \kappa_{j,i_j} = 2 \ , \ j = 1, 2, \ldots, k \ . \tag{4.80}$$

The yield sensitivities are now given by

$$\frac{\partial Y}{\partial \phi_i^0} = - \sum_{\ell=1}^{m} \frac{\partial V^\ell}{\partial \phi_i^0} \ , \tag{4.81}$$

$$\frac{\partial Y}{\partial \epsilon_i} = - \sum_{\ell=1}^{m} \frac{\partial V^\ell}{\partial \epsilon_i} \ , \tag{4.82}$$

where

$$\frac{\partial V^\ell}{\partial \phi_i^0} = \left[\frac{1}{k!} \sum_{j=1}^{k} \frac{\partial \alpha_j^\ell}{\partial \phi_i^0} \prod_{\substack{p=1 \\ p \neq j}}^{k} \alpha_p^\ell \right] B + A \left(k \sum_{i_1=1}^{n_1+1} \sum_{i_2=1}^{n_2+1} \cdots \sum_{i_k=1}^{n_k+1} \Delta W(\underset{\sim}{i}) \right.$$

$$\left. (\delta^\ell(\underset{\sim}{i}))^{k-1} \frac{\partial \delta^\ell(\underset{\sim}{i})}{\partial \phi_i^0} \right) \ , \tag{4.83}$$

$$\frac{\partial V^\ell}{\partial \epsilon_i} = \left[\frac{\mu_i^r}{k!} \sum_{j=1}^{k} \frac{\partial \alpha_j^\ell}{\partial \phi_i^0} \prod_{\substack{p=1 \\ p \neq j}}^{k} \alpha_p^\ell \right] B + A \left(k \sum_{i_1=1}^{n_1+1} \sum_{i_2=1}^{n_2+2} \cdots \sum_{i_k=1}^{n_k+1} \Delta W(\underset{\sim}{i}) \right.$$

$$\left. (\delta^\ell(\underset{\sim}{i}))^{k-1} \frac{\partial \delta^\ell(\underset{\sim}{i})}{\partial \epsilon_i} \right) \ , \tag{4.84}$$

$$A = \frac{1}{k!} \prod_{j=1}^{k} \alpha_j^{\ell} \, , \tag{4.85}$$

$$B = \sum_{i_1=1}^{n_1+1} \sum_{i_2=1}^{n_2+1} \ldots \sum_{i_k=1}^{n_k+1} \Delta W(\underset{\sim}{i}) \, (\delta^{\ell}(\underset{\sim}{i}))^k \tag{4.86}$$

and where

$$\frac{\partial \delta^{\ell}(\underset{\sim}{i})}{\partial \phi_i^0} = \begin{cases} 0 & \text{if } \delta^{\ell}(\underset{\sim}{i}) = 0, \\ \\ \\ \displaystyle\sum_{j=1}^{k} \frac{1}{(\alpha_j^{\ell})^2} \frac{\partial \alpha_j^{\ell}}{\partial \phi_i^0} \sum_{p=1}^{i_j} \varepsilon_{j,p-1} & \text{if } \delta^{\ell}(\underset{\sim}{i}) > 0 \, , \end{cases} \tag{4.87}$$

$$\frac{\partial \delta^{\ell}(\underset{\sim}{i})}{\partial \varepsilon_i} = \mu_i^r \frac{\partial \delta^{\ell}(\underset{\sim}{i})}{\partial \phi_i^0} - \sum_{j=1}^{k} \frac{1}{\alpha_j^{\ell}} \sum_{p=1}^{i_j} \kappa_{j,p-1} \, . \tag{4.88}$$

The formulas for $\partial \alpha_j^{\ell}/\partial \phi_i^0$ and for μ_i^r are similar to those derived for the uniform distribution.

The case of independent parameters is obtained by substituting

$$\Delta W(\underset{\sim}{i}) = \prod_{j=1}^{k} \Delta W_j(i_j) \tag{4.89}$$

in (4.83), (4.84) and (4.86).

4.12   Example

In order to illustrate the calculation of the weighted hyper-volume, consider the two-dimensional example shown in Table 4.3. The weighted volume is given by

$$V = \left(\frac{1}{2} \times 12 \times 3 \right) \left(\sum_{i_1=1}^{4} \sum_{i_2=1}^{3} \Delta W(i_1, i_2) \, (\delta(i_1, i_2))^2 \right)$$

$$= 1813/3600 \; .$$

The same example can be considered as if the parameters are independent as shown in Table 4.4 and Table 4.5. Here, the weighted volume is given by

$$V = \left(\frac{1}{2} \times 12 \times 3 \right) \left(\sum_{i_1=1}^{4} \Delta W(i_1) \sum_{i_2=1}^{3} \Delta W(i_2) \, (\delta(i_1, i_2))^k \right) \; ,$$

where the δ are as given in Table 4.3. Hence,

$$V = 1813/3600 \; .$$

Assuming that the sizes of the orthocells are fixed, the sensitivities of the weighted hypervolume with respect to the nominal parameter vector ϕ^0 can be evaluated. The location of ϕ^0 itself is not important. It is the relative location of the constraint with respect to the orthotope that matters. The constraint can be considered as

TABLE 4.3

EXAMPLE TO ILLUSTRATE CALCULATION OF WEIGHTED
HYPERVOLUME BY THE GENERAL FORMULA

Orthocell	i_1	0	1	2	3	4
dimensions	ε_{1,i_1}	0	3.0	3.0	2.0	-

i_2	ε_{2,i_2}		0	1	2	3	4
0	0	w,W	0	0	0	0	0
1	2.0	w	0	18/100	12/100	3/10	0
		W	0	3/100	1/50	3/40	0
		ΔW	-	3/100	- 1/100	11/200	-3/40
		δ	-	1	3/4	1/2	1/3
2	3.0	w	0	12/100	8/100	2/10	0
		W	0	1/75	2/225	1/30	0
		ΔW	-	- 1/60	1/180	-11/360	1/24
		δ	-	1/3	1/12	0	0
3	-	w,W	0	0	0	0	0
		ΔW	-	- 1/75	1/225	-11/450	1/30
		δ	-	0	0	0	0

Reference vertex ϕ^r given by $\mu_1^r = -1$, $\mu_2^r = 1$

Intersections of the linear constraint are $\alpha_1 = 12$, $\alpha_2 = 3$

Weighted volume $V = 1813/3600$

TABLE 4.4

LENGTHS AND WEIGHTS OF FIRST PARAMETER INTERVALS

i_1	ε_{1,i_1}	$w(i_1)$	$W(i_1)$	$\Delta W(i_1)$
0	0.0	0	0	-
1	3.0	3/10	1/10	1/10
2	3.0	2/10	1/15	-1/30
3	2.0	5/10	1/4	11/60
4	-	0	0	-1/4

TABLE 4.5

LENGTHS AND WEIGHTS OF SECOND PARAMETER INTERVALS

i_2	ε_{2,i_2}	$w(i_2)$	$W(i_2)$	$\Delta W(i_2)$
0	0.0	0	0	-
1	2.0	6/10	3/10	3/10
2	3.0	4/10	2/15	-1/6
3	-	0	0	-2/15

$$\phi_1/12 - \phi_2/3 \geq 0 .$$

According to (4.45) we have

$$\frac{\partial \alpha_1}{\partial \phi_1^0} = -1 ,$$

$$\frac{\partial \alpha_1}{\partial \phi_2^0} = (-1) (-1/3)/(1/12) = 4 ,$$

$$\frac{\partial \alpha_2}{\partial \phi_1^0} = (1) (1/12)/(-1/3) = -1/4 ,$$

and

$$\frac{\partial \alpha_2}{\partial \phi_2^0} = 1 .$$

Using (4.87), the values of $\partial \delta^{\ell}(i)/\partial \phi_i^0$ are given in Table 4.6 and Table 4.7. Substituting in (4.83) we get

$$\frac{\partial V}{\partial \phi_1^0} = -43/720 ,$$

$$\frac{\partial V}{\partial \phi_2^0} = 43/180 .$$

These sensitivities were verified using the central difference approach with $\Delta \phi_i^0 = 10^{-3}$, $i = 1, 2$. An agreement of 6 digits was obtained.

TABLE 4.6

VALUES OF $\partial \delta^{\ell}(i_1, i_2)/\partial \phi_1^0$

i_2 \ i_1	1	2	3	4
1	0	-1/48	-1/24	-1/18
2	-1/18	-11/144	0	0
3	0	0	0	0

TABLE 4.7

VALUES OF $\partial \delta^{\ell}(i_1, i_2)/\partial \phi_2^0$

i_2 \ i_1	1	2	3	4
1	0	1/12	1/6	2/9
2	2/9	11/36	0	0
3	0	0	0	0

4.13 Conclusions

The approach presented for yield estimation provides an inexpensive yield determination without the need for the multitude of circuit simulations required in the Monte Carlo technique. The method approximates the integration of the PDF over the feasible region. The freedom in discretizing the PDF and hence the sizes of the orthocells allows the use of any previous information about the problem. This is an advantage, particularly if a worst-case solution is already known. In addition, the availability of yield sensitivities permit the use of gradient optimization techniques.

The better the description of the boundary of the constraint region by linear cuts the more accurate is the yield estimate. It is possible to describe a constraint defining the boundary by a different cut at each orthocell, however, the computational effort will increase. In Chapter 6 an algorithm is described which provides updated approximations to the constraints. The sequence of approximations is directed to give better locations of the boundary of the constraint region.

CHAPTER 5

THE MULTIDIMENSIONAL APPROXIMATION

5.1 Introduction

A new procedure for multidimensional approximation integrated with the tolerance problem is described in this chapter. Approximation by interpolation is employed in order to save computation of the exact function. Complicated functions, typically constraints or functions for which gradient information is not available, are approximated. The approximations are to be used in the optimization. Hence, gradient optimization techniques can be employed.

It is shown how points where the approximation coincides with the exact function can be chosen to permit efficient construction of the quadratic approximation. These points are termed base points. Theorems dealing with preserving one-dimensional convexity and parameter symmetry in the approximation are stated and proved. One-dimensional convexity is an important property to preserve, as indicated in Chapter 2, and parameter symmetry may be exploited to computational advantage.

An efficient algorithm for evaluating the quadratic approximation as well as its sensitivities is presented. Since small interpolation regions may be required to obtain accurate approximations, the algorithm is designed to deal with different approximations in different interpolation regions (Bandler and Abdel-Malek 1977a).

5.2   Interpolation by Multidimensional Polynomials

An approximate representation of a function $f(\underset{\sim}{\phi})$ by using its values at a finite set of points is possible (Thacher and Milne 1960 and Sobolev 1961b). These points are called <u>nodes</u> or <u>base points</u>, and denoted by

$$\underset{\sim}{\phi}^n \; , \; n = 1, \; 2, \; \ldots, \; N_b \; ,$$

where N_b is the number of base points.

Interpolation can be done by means of a linear combination of the set of all possible <u>monomials</u>. Hence,

$$f(\underset{\sim}{\phi}) \simeq \sum_{j=1}^{N} a_j \; \Phi_j(\underset{\sim}{\phi}) \tag{5.1}$$

where a_j, $j = 1, \; 2, \; \ldots, \; N$, are unknown coefficients,

$$\Phi_j \triangleq (\phi_1 - \overline{\phi}_1)^{\alpha_1} (\phi_2 - \overline{\phi}_2)^{\alpha_2} \ldots (\phi_k - \overline{\phi}_k)^{\alpha_k} \; , \; \sum_{i=1}^{k} \alpha_i \leq m \; , \tag{5.2}$$

or

$$\Phi_j \triangleq \phi_1^{\alpha_1} \phi_2^{\alpha_2} \ldots \phi_k^{\alpha_k} \; , \; \sum_{i=1}^{k} \alpha_i \leq m \; , \tag{5.3}$$

m is the degree of the interpolating polynomial, k the number of independent variables, i.e., number of components of $\underset{\sim}{\phi}$, α_i, $i = 1, \; 2, \; \ldots, \; k$, are nonnegative integers and $\overline{\underset{\sim}{\phi}}$ may be any reference point. The number of such monomials is given by

$$N = \frac{(m+k)!}{m! k!} \; . \tag{5.4}$$

If the number of base points N_b is such that

$$N_b = N \; , \tag{5.5}$$

exact evaluation of the coefficients a_j, $j = 1, 2, \ldots, N$, to force the approximation to coincide with the actual function at the base points, i.e.,

$$P(\underset{\sim}{\phi}^n) = f(\underset{\sim}{\phi}^n) \; , \; n = 1, 2, \ldots, N \; , \tag{5.6}$$

where

$$P(\underset{\sim}{\phi}) = \sum_{j=1}^{n} b_j \; \Phi_j(\underset{\sim}{\phi}) \tag{5.7}$$

is possible.

The following system of simultaneous linear equations results.

$$\begin{bmatrix} \Phi_1(\underset{\sim}{\phi}^1) & \Phi_2(\underset{\sim}{\phi}^1) & \cdots & \Phi_N(\underset{\sim}{\phi}^1) \\ \Phi_1(\underset{\sim}{\phi}^2) & \Phi_2(\underset{\sim}{\phi}^2) & \cdots & \Phi_N(\underset{\sim}{\phi}^2) \\ \vdots & & & \\ \Phi_1(\underset{\sim}{\phi}^N) & \Phi_2(\underset{\sim}{\phi}^N) & \cdots & \Phi_N(\underset{\sim}{\phi}^N) \end{bmatrix} \begin{bmatrix} b_1 \\ b_2 \\ \vdots \\ b_N \end{bmatrix} = \begin{bmatrix} f(\underset{\sim}{\phi}^1) \\ f(\underset{\sim}{\phi}^2) \\ \vdots \\ f(\underset{\sim}{\phi}^N) \end{bmatrix} \; . \tag{5.8}$$

The solution of (5.8) exists if the system of equations is linearly independent. This is satisfied if the set of base points is degree-m independent (Thacher 1959).

5.3   Interpolation by Quadratic Polynomials

Nikol'skii (1969) proved that, unlike the one-dimensional case, a high-order multidimensional approximation does not guarantee a higher

accuracy for the approximation. For interpolation, in particular, higher accuracy for high-order polynomial interpolation is not guaranteed even in the one-dimensional case. An illustrative example is shown in Fig. 5.1. A smaller interpolation region, however, makes the approximation more accurate. For an error bound on interpolation, see Sobolev (1961a, 1961b). A quadratic polynomial is the simplest polynomial which can have the curvature to bound a maximum, minimum or vertex.

In order to minimize the computational effort to obtain the quadratic polynomial approximation, the number of base points required will be chosen to be equal to the number of unknown coefficients, i.e., interpolation will be adopted. Replacing m by 2 in (5.4) the number of base points is

$$N = (k+1)(k+2)/2 \ . \tag{5.9}$$

Let R_i be the <u>interpolation region</u> defined by

$$R_i \overset{\Delta}{=} \{ \underset{\sim}{\phi} \mid \delta_i \geq \mid \phi_i - \overline{\phi}_i \mid , \ i = 1, 2, \ldots, k\} \ , \tag{5.10}$$

where $\overline{\underset{\sim}{\phi}}$ is the center of the interpolation region and δ_i, $i = 1, 2, \ldots,$ k, are parameters defining the size of the interpolation region. The quadratic polynomial approximation can be expressed in terms of the monomials (5.2) or (5.3) as

$$P(\underset{\sim}{\phi}) = a_0 + \underset{\sim}{a}^T(\underset{\sim}{\phi}-\overline{\underset{\sim}{\phi}}) + \frac{1}{2}(\underset{\sim}{\phi}-\overline{\underset{\sim}{\phi}})^T H(\underset{\sim}{\phi}-\overline{\underset{\sim}{\phi}}) \tag{5.11}$$
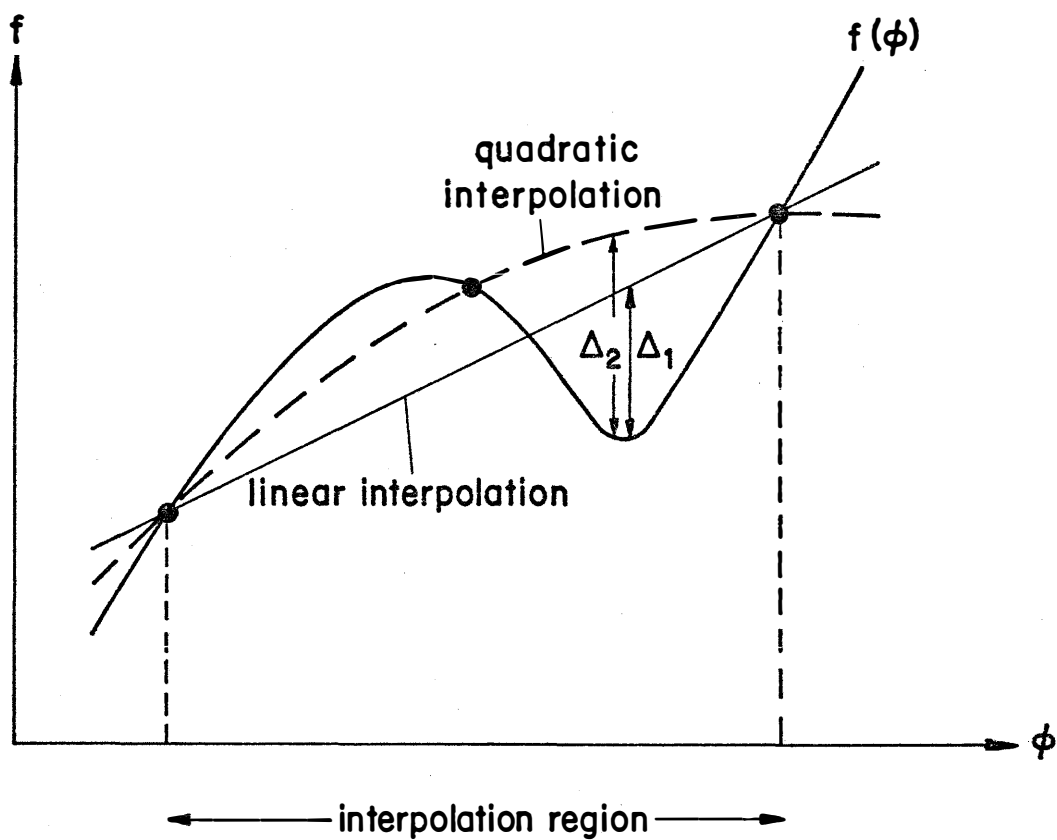
Fig. 5.1 Interpolation by first and second order polynomials.
The errors within the interpolation region are Δ_1
and Δ_2.

or

$$P(\underset{\sim}{\phi}) = b_1 \; \phi_1^2 + b_2 \; \phi_2^2 + \ldots + b_k \; \phi_k^2 + b_{k+1} \; \phi_1 \phi_2$$

$$+ \; b_{k+2} \; \phi_1 \; \phi_3 + \ldots + b_{N-k-1} \; \phi_{k-1} \; \phi_k$$

$$+ \; b_{N-k} \; \phi_1 + b_{N-k+1} \; \phi_2 + \ldots + b_{N-1} \; \phi_k + b_N , \qquad (5.12)$$

where $\underset{\sim}{H}$ is the Hessian matrix of the quadratic approximation and is given by

$$\underset{\sim}{H} = \underset{\sim}{\nabla} \; \underset{\sim}{\nabla}^T \; P(\underset{\sim}{\phi}) , \qquad (5.13)$$

$$\underset{\sim}{\nabla} = \begin{bmatrix} \dfrac{\partial}{\partial \phi_1} \\[2mm] \dfrac{\partial}{\partial \phi_2} \\[2mm] \cdot \\ \cdot \\ \dfrac{\partial}{\partial \phi_k} \end{bmatrix} . \qquad (5.14)$$

The relations between the coefficients in (5.11) and (5.12) are given by

$$b_i = h_{ii}/2 , \quad i = 1, 2, \ldots, k , \qquad (5.15)$$

$$b_\ell = h_{ij}, \quad \ell = j - i + \sum_{p=1}^{i} (k-p+1), \quad i < j , \qquad (5.16)$$

$$b_{N-k-1+i} = a_i - \sum_{j=1}^{k} h_{ij} \, \bar{\phi}_j , \quad i = 1, 2, \ldots, k , \qquad (5.17)$$

$$b_N = a_0 - \sum_{i=1}^{k} a_i \bar{\phi}_i + \frac{1}{2} \sum_{i=1}^{k} \sum_{j=1}^{k} h_{ij} \, \bar{\phi}_i \, \bar{\phi}_j , \qquad (5.18)$$

where N is given by (5.9).

5.4   Sparsity and Choice of Base Points

If we have freedom in choosing the base points, we can save computational effort, particularly if the number of variables k is large. In general, the matrix of monomials in (5.8) is full, however it is possible to make it _sparse_ by using the following choice of base points. Let

$$[\underset{\sim}{\phi}^1 \; \underset{\sim}{\phi}^2 \; \ldots \; \underset{\sim}{\phi}^N] = \underset{\sim}{D} \; [\underset{\sim k}{1} \; -\underset{\sim k}{1} \; \underset{\sim}{B} \; \underset{\sim k}{0}] + [\overline{\underset{\sim}{\phi}} \; \overline{\underset{\sim}{\phi}} \; \ldots \; \overline{\underset{\sim}{\phi}}] \;, \qquad (5.19)$$

where

$\underset{\sim}{D}$ is a k x k diagonal matrix with diagonal elements δ_i,

$\underset{\sim k}{1}$ is a k-dimensional identity matrix,

$\underset{\sim k}{0}$ is a zero vector of dimension k,

$\underset{\sim}{B}$ is a k x L matrix having the structure

$$\underset{\sim}{B} = \begin{bmatrix} \underset{\sim k-1}{u^T} & \underset{\sim k-2}{0^T} & \underset{\sim k-3}{0^T} & & \\ & \underset{\sim k-2}{u^T} & \underset{\sim k-3}{0^T} & & \\ & & \underset{\sim k-3}{u^T} & & \underset{\sim k-2}{0} \\ & & & \ldots & \\ \underset{\sim k-1}{T} & & & & \\ & \underset{\sim k-2}{T} & & & \\ & & \underset{\sim k-3}{T} & & \underset{\sim 1}{u} \\ & & & & \underset{\sim 1}{T} \end{bmatrix} \;, \qquad (5.20)$$

where $\underset{\sim}{u}_j$ is a column vector of dimension j and having components u_{ij} such that

$$0 < |u_{ij}| \leq 1, \quad i = 1, 2, \ldots, j \;, \tag{5.21}$$

$\underset{\sim}{T}_j$ is a diagonal matrix of dimension j with diagonal elements T_{ij} satisfying

$$0 < |T_{ij}| \leq 1, \quad i = 1, 2, \ldots, j \;, \tag{5.22}$$

and

$$L = k(k-1)/2 \;. \tag{5.23}$$

According to this choice of base points it is clear that

$$a_0 = f(\underset{\sim}{\phi}^N) \;. \tag{5.24}$$

The system of simultaneous linear equations is now the sparse system given in (5.25), shown on next page, where

$$\zeta_i^j = u_{j-i,k-i}\,\delta_i \;, \quad \zeta_j^i = T_{j-i,k-i}\,\delta_j \;, \quad i < j \;. \tag{5.26}$$

Hence, solving (5.25) reduces to the following

$$h_{ii} = [f(\underset{\sim}{\phi}^i) + f(\underset{\sim}{\phi}^{N-k-1+i}) - 2f(\underset{\sim}{\phi}^N)]/\delta_i^2 \;, \tag{5.27}$$

$$a_i = [f(\underset{\sim}{\phi}^i) - f(\underset{\sim}{\phi}^{N-k-1+i})]/2\delta_i \;, \quad i = 1, 2, \ldots, k \;, \tag{5.28}$$

$$
\begin{bmatrix}
& \underset{\sim}{D}\ \underset{\sim}{D} & & & 0 & & & \underset{\sim}{D} & \\[2ex]
\hline
& \underset{\sim}{D}\ \underset{\sim}{D} & & & 0 & & & -\underset{\sim}{D} & \\[2ex]
\hline
(\zeta_1^2)^2 & (\zeta_2^1)^2 & 0 & \cdots & 0 & \zeta_1^2\zeta_2^1 & \zeta_1^2 & \zeta_2^1 & 0 & \cdots & 0 \\
(\zeta_1^3)^2 & 0 & (\zeta_3^1)^2 & \cdots & 0 & \zeta_1^3\zeta_3^1 & \zeta_1^3 & 0 & \zeta_3^1 & \cdots & 0 \\
\vdots & & & & & & & & & & \\
(\zeta_1^k)^2 & 0 & 0 & \cdots & (\zeta_k^1)^2 & \zeta_1^k\zeta_k^1 & \zeta_1^k & 0 & 0 & \cdots & \zeta_k^1 \\
0 & (\zeta_2^3)^2 & (\zeta_3^2)^2 & \cdots & 0 & \zeta_2^3\zeta_3^2 & 0 & \zeta_2^3 & \zeta_3^2 & \cdots & 0 \\
\vdots & & & & & & & & & & \\
0 & 0 & \cdots & (\zeta_{k-1}^k)^2 & (\zeta_k^{k-1})^2 & \zeta_{k-1}^k\zeta_k^{k-1} & 0 & 0 & \cdots & \zeta_{k-1}^k & \zeta_k^{k-1}
\end{bmatrix}
\begin{bmatrix}
h_{11}/2 \\ h_{22}/2 \\ \vdots \\ h_{kk}/2 \\ \hline h_{12} \\ h_{13} \\ \vdots \\ h_{k-1,k} \\ \hline a_1 \\ a_2 \\ \vdots \\ a_k
\end{bmatrix}
=
\begin{bmatrix}
f(\underset{\sim}{\phi}^1)-f(\underset{\sim}{\phi}^N) \\
f(\underset{\sim}{\phi}^2)-f(\underset{\sim}{\phi}^N) \\
\vdots \\
\\
\\
\\
\\
\\
f(\underset{\sim}{\phi}^{N-1})-f(\underset{\sim}{\phi}^N)
\end{bmatrix}
\tag{5.25}
$$

77

$$h_{ij} = h_{ji} = [f(\underset{\sim}{\phi}^{\ell}) - f(\underset{\sim}{\phi}^{N}) - (\zeta_i^j)^2 \frac{h_{ii}}{2} - (\zeta_j^i)^2 \frac{h_{jj}}{2}$$

$$- \zeta_i^j a_i - \zeta_j^i a_j]/\zeta_i^j \zeta_j^i \, , \qquad (5.29)$$

where

$$\ell = j - i + \sum_{p=1}^{i} (k - p + 1) \, , \, j > i \, . \qquad (5.30)$$

Subsequently, the number of multiplications/divisions required to obtain the approximation is reduced to $5k^2 - 2k$ instead of $(N^3 + 3N^2 - N)/3$ for Gauss elimination, where N is defined in (5.9).

Fig. 5.2 shows the choice of base points in two dimensions and three dimensions.

If we are not completely free in choosing the base points, for example, if the function evaluation is expensive and some evaluations for parameter values inside the interpolation region are known, the matrix of monomials can appropriately be arranged. Assuming that the resulting matrix of monomials will not be singular, we replace the bottom rows of the matrix of monomials by the monomials of these known, n say, base points. No singularity will result, for example, if the rows introduced are independent and full. This arrangement in the matrix of monomials is shown in Fig. 5.3. In solving the resulting system of simultaneous equations, we proceed with finding the polynomial coefficients using (5.27), (5.28) and (5.29) until we come to the full part of the matrix, i.e., the last n equations. The unknown coefficients beyond this point should be found by solving n simultaneous
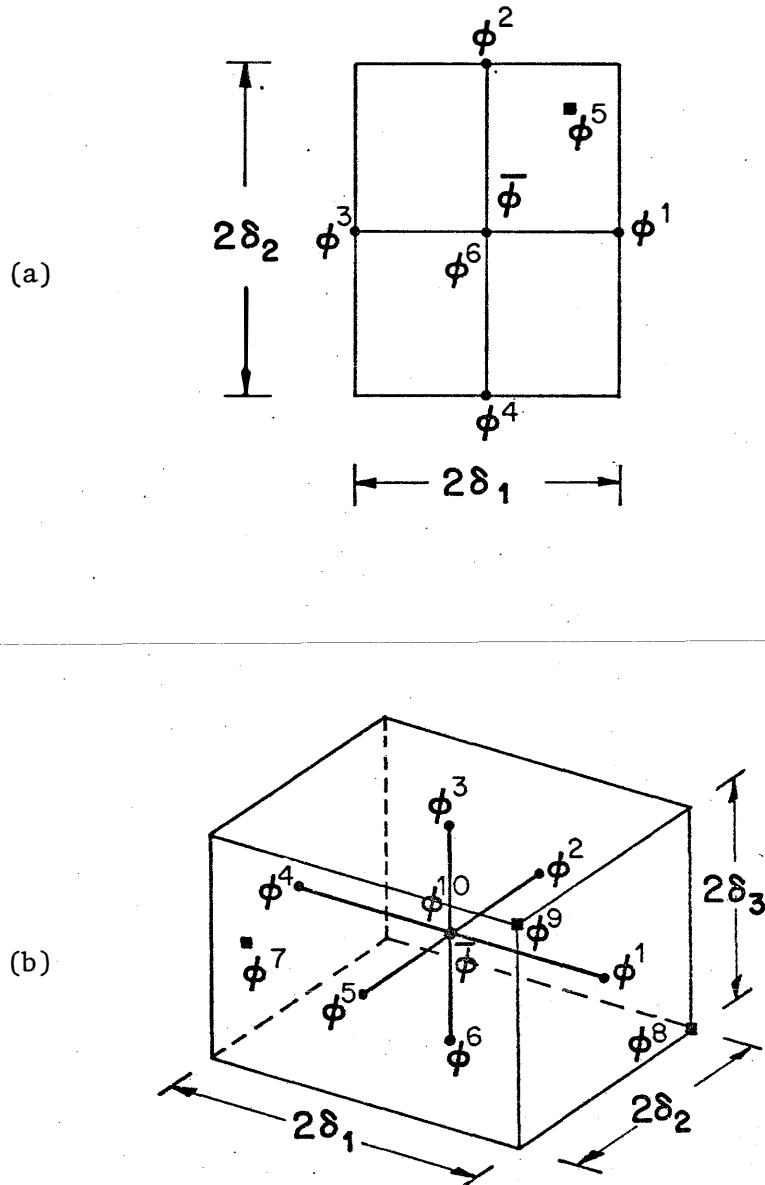
Fig. 5.2   Arrangement of the base points w.r.t. the centers

of interpolation regions in (a) two dimensions and

(b) three dimensions.

$$
\begin{bmatrix}
x & & & & & & & & x & & & \\
 & x & & & & & & & & x & & \\
 & & \cdot & & & & & & & & \cdot & \\
 & & & \cdot & & & & & & & & \cdot \\
 & & & & x & & & & & & & x \\
\hline
x & & & & & & & & x & & & \\
 & x & & & & & & & & x & & \\
 & & \cdot & & & & & & & & \cdot & \\
 & & & \cdot & & & & & & & & \cdot \\
 & & & & x & & & & & & & x \\
\hline
x & x & & & & x & & & & & & \\
x & & x & & & & x & & & & & \\
\cdot & & & \cdot & & & \cdot & & & & & \\
\cdot & & & & \cdot & & & \cdot & & & & \\
\hline
x & x & \cdot & \cdot & x & x & x & \cdot & \cdot & x & x & x & \cdot & \cdot & x \\
x & x & \cdot & \cdot & x & x & x & \cdot & \cdot & x & x & x & \cdot & \cdot & x \\
\cdot & & & & & \cdot & & & & & \cdot & & & & \\
\cdot & & & & & \cdot & & & & & \cdot & & & & \\
x & x & \cdot & \cdot & x & x & x & \cdot & \cdot & x & x & x & \cdot & \cdot & x
\end{bmatrix}
$$

Fig. 5.3   The arrangement of the matrix of monomials for

a restricted selection of base points.

linear equations, for example, by Gauss elimination.

5.4.1 Example

Consider the approximation of the function

$$f(\phi) = \phi_3^2 + 5 \, \phi_2 \, \phi_3 + \phi_1 + 2 \, \phi_2 + \phi_3 + 3 \, ,$$

where

$$\phi = \begin{bmatrix} \phi_1 \\ \phi_2 \\ \phi_3 \\ \phi_4 \end{bmatrix} .$$

The execution time using a CDC 6400 computer to evaluate the approximation using equations (5.27), (5.28) and (5.29) is 0.005 s compared with 0.066 s using Gauss elimination. Using equal step size δ for the interpolation region, the Euclidean norm of the errors in the coefficients of the approximating polynomial is plotted against δ in Fig. 5.4.

5.5 Preservation of Parameter Symmetry

If symmetry exists in the original problem it is preferable to keep it in the approximation. Generally, there is no guarantee that the approximation will be symmetric if the actual function is so unless the base points are specially chosen.

A function $f(\phi)$ is said to be _symmetrical_ with respect to a matrix S if

$$f(S\phi) = f(\phi) \, , \tag{5.31}$$
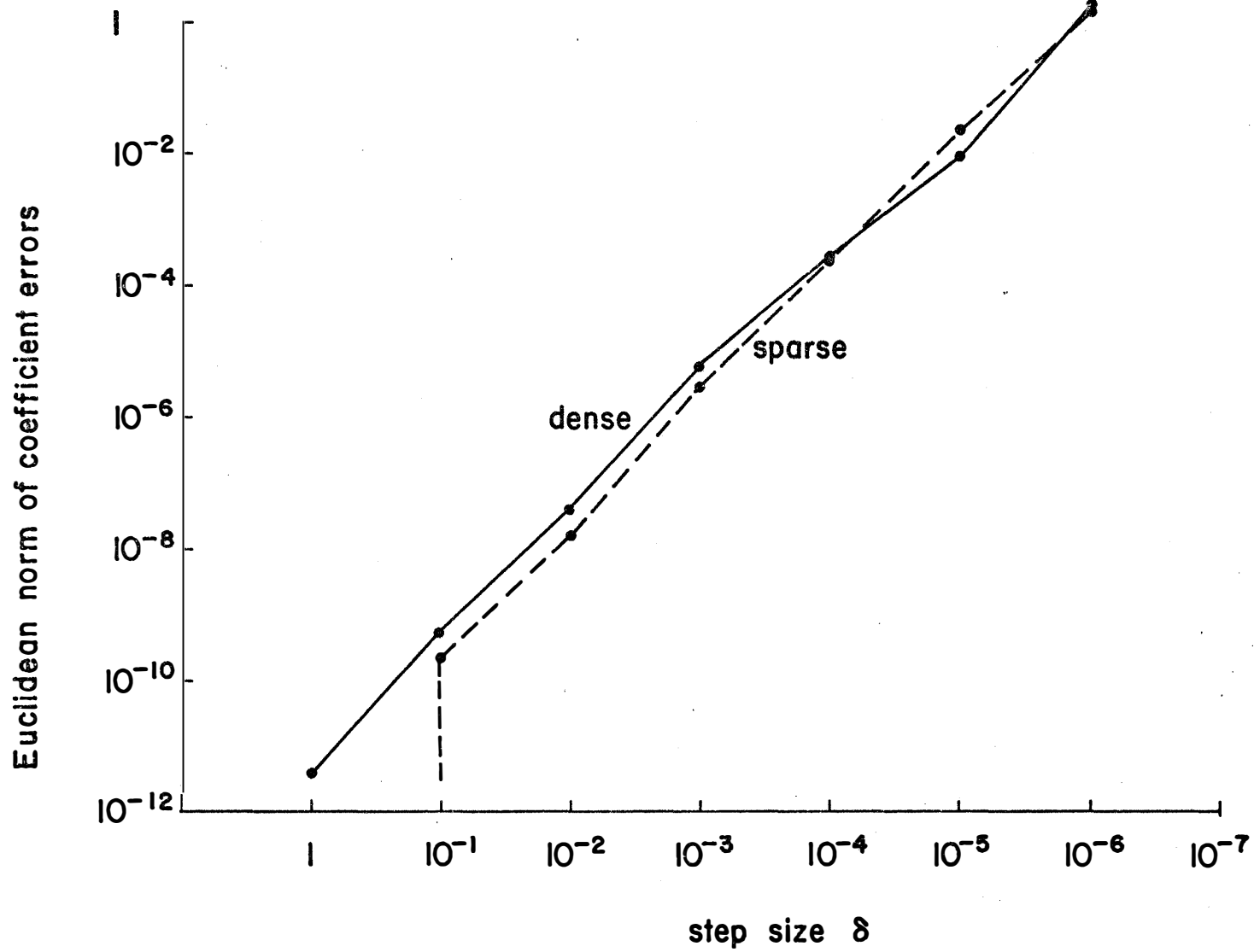
Fig. 5.4   Errors in computing the coefficients of the quadratic approximation

using dense and sparse matrix approaches.

where $\underset{\sim}{S}$ is a kxk permutation matrix obtained by interchaning suitable rows of a unit matrix. It has exactly one entry of 1 in each row and in each column, all other entries being 0.

5.5.1 Lemma 5.1

The transformation $\underset{\sim}{S}$ is a <u>one to one mapping</u>, i.e.,

(i)   if $\underset{\sim}{\phi}^a = \underset{\sim}{S} \underset{\sim}{\phi}^c$ and $\underset{\sim}{\phi}^b = \underset{\sim}{S} \underset{\sim}{\phi}^c$ then $\underset{\sim}{\phi}^a = \underset{\sim}{\phi}^b$,

(ii)   if $\underset{\sim}{\phi}^c = \underset{\sim}{S} \underset{\sim}{\phi}^a$ and $\underset{\sim}{\phi}^c = \underset{\sim}{S} \underset{\sim}{\phi}^b$ then $\underset{\sim}{\phi}^a = \underset{\sim}{\phi}^b$.

<u>Proof</u>

The proof of (i) follows directly from theory of linear algebra. To prove (ii) we have

$$\underset{\sim}{S} \underset{\sim}{\phi}^a = \underset{\sim}{S} \underset{\sim}{\phi}^b . \tag{5.32}$$

The inverse of $\underset{\sim}{S}$ exists, since $|\det(\underset{\sim}{S})| = 1$ and is given by the transpose of $\underset{\sim}{S}$. Thus,

$$\underset{\sim}{S}^T \underset{\sim}{S} \underset{\sim}{\phi}^a = \underset{\sim}{S}^T \underset{\sim}{S} \underset{\sim}{\phi}^b , \tag{5.33}$$

and

$$\underset{\sim}{\phi}^a = \underset{\sim}{\phi}^b . \tag{5.34}$$

Q.E.D.

5.5.2 Corollary 5.1

Let $\underset{\sim}{\phi}^n$, n = 1, 2, ..., N, be N distinct vectors then $\underset{\sim}{S} \underset{\sim}{\phi}^n$, n = 1, 2, ..., N, are N distinct vectors also. The proof is obvious since $\underset{\sim}{S}$

is a one to one transformation.

5.5.3 Theorem 5.1

If ϕ^n, $n = 1, 2, \ldots, N$, are N degree-2 independent base points and if for each base point ϕ^n, $S\,\phi^n$ is a base point also, then $P(\phi)$ will be symmetric with respect to S if $f(\phi)$ is so.

Proof.

Consider the system of simultaneous linear equations given by

$$f(\phi^n) = a_0 + a^T \phi^n + \frac{1}{2} (\phi^n)^T H(\phi^n), \quad n = 1,2,\ldots,N. \qquad (5.35)$$

Knowing that H is symmetric and since the N base points are degree-2 independent, this system will have a unique solution a_0, a and H.

Replace ϕ^n by $S\,\phi^n$ in (5.35) and using the previous corollary, we will have the following system of N simultaneous linear equations in a_0', a' and H'.

$$f(S\phi^n) = a_0' + a'^T \phi^n + \frac{1}{2} (\phi^n)^T H'(\phi^n), \quad n=1,2,\ldots,N, \qquad (5.36)$$

where

$$a_0' = a_0 \cdot \qquad (5.37)$$

$$a' = S^T a \,, \qquad (5.38)$$

and

$$H' = S^T H S \,. \qquad (5.39)$$

Comparing (5.35) and (5.36) and knowing that

$$f(\underset{\sim}{S}\ \underset{\sim}{\phi}^n) = f(\underset{\sim}{\phi}^n)\ ,\tag{5.40}$$

the two systems should have a unique solution satisfying

$$\overline{\underset{\sim}{a}} = \underset{\sim}{S}^T\ \overline{\underset{\sim}{a}}\tag{5.41}$$

and

$$\overline{\underset{\sim}{H}} = \underset{\sim}{S}^T\ \overline{\underset{\sim}{H}}\ \underset{\sim}{S}\ .\tag{5.42}$$

Therefore, the value of the interpolating polynomial $P(\underset{\sim}{\phi})$ at any point $\underset{\sim}{\phi}$ is given by

$$P(\underset{\sim}{\phi}) = \overline{a}_0 + \overline{\underset{\sim}{a}}^T\ \underset{\sim}{\phi} + \frac{1}{2}\ \underset{\sim}{\phi}^T\ \overline{\underset{\sim}{H}}\ \underset{\sim}{\phi}\ .\tag{5.43}$$

Now,

$$P(\underset{\sim}{S}\underset{\sim}{\phi}) = \overline{a}_0 + \overline{\underset{\sim}{a}}^T\ \underset{\sim}{S}\ \underset{\sim}{\phi} + \frac{1}{2}\ \underset{\sim}{\phi}^T\underset{\sim}{S}^T\ \overline{\underset{\sim}{H}}\ \underset{\sim}{S}\ \underset{\sim}{\phi}\ .\tag{5.44}$$

Using (5.41) and (5.42) we obtain

$$P(\underset{\sim}{S}\underset{\sim}{\phi}) = P(\underset{\sim}{\phi})\tag{5.45}$$

for any point $\underset{\sim}{\phi}$, i.e., $P(\underset{\sim}{\phi})$ is symmetric with respect to $\underset{\sim}{S}$.

$$Q.E.D.$$

The requirements for the previous theorem are satisfied, for example, if in (5.19) we have

$$\underset{\sim}{S}\,\overline{\underset{\sim}{\phi}} = \overline{\underset{\sim}{\phi}} , \tag{5.46}$$

$$\underset{\sim}{S}\,\underset{\sim}{D}\,\underset{\sim}{S}^T = \underset{\sim}{D} , \tag{5.47}$$

and

$$\underset{\sim}{S}\,\underset{\sim}{B}_i = \underset{\sim}{B}_j , \tag{5.48}$$

where $\underset{\sim}{B}_i$ and $\underset{\sim}{B}_j$ are not necessarily distinct columns of $\underset{\sim}{B}$. Accordingly, from (5.19) we have

$$\underset{\sim}{S}[\underset{\sim}{\phi}^1\ \underset{\sim}{\phi}^2\ \cdots\ \underset{\sim}{\phi}^N] = \underset{\sim}{S}\,\underset{\sim}{D}[\underset{\sim}{1}_k\ -\underset{\sim}{1}_k\ \underset{\sim}{B}\ \underset{\sim}{0}_k] + \underset{\sim}{S}[\overline{\underset{\sim}{\phi}}\ \overline{\underset{\sim}{\phi}}\ \cdots\ \overline{\underset{\sim}{\phi}}]$$

$$= \underset{\sim}{S}\,\underset{\sim}{D}\,\underset{\sim}{S}^T\,\underset{\sim}{S}[\underset{\sim}{1}_k\ -\underset{\sim}{1}_k\ \underset{\sim}{B}\ \underset{\sim}{0}_k] + [\overline{\underset{\sim}{\phi}}\ \overline{\underset{\sim}{\phi}}\ \cdots\ \overline{\underset{\sim}{\phi}}]$$

$$= \underset{\sim}{D}\,\underset{\sim}{S}[\underset{\sim}{1}_k\ -\underset{\sim}{1}_k\ \underset{\sim}{B}\ \underset{\sim}{0}_k] + [\overline{\underset{\sim}{\phi}}\ \overline{\underset{\sim}{\phi}}\ \cdots\ \overline{\underset{\sim}{\phi}}]$$

$$= [\underset{\sim}{\phi}^{i_1}\ \underset{\sim}{\phi}^{i_2}\ \cdots\ \underset{\sim}{\phi}^{i_N}] , \tag{5.49}$$

where i_1, i_2, ..., i_N, are the corresponding permutations of 1, 2, ... N.

5.6   Preservation of One-dimensional Convexity

As described in Chapter 2, one-dimensional convexity is the property which makes the vertices candidates for the worst case. Hence, it is essential to preserve this property in the approximating polynomial $P(\phi)$ if it already exists in the exact function $f(\phi)$.

The following theorem indicates how to choose the base points in order to preserve one-dimensional convexity.

5.6.1   Theorem 5.2

If there exist three distinct base points ϕ^1, ϕ^2 and ϕ^3 in the ith direction, i.e.,

$$\phi^j = \phi^1 + c_j \, e_i \, , \qquad\qquad (5.50)$$

where c_j, $j = 2, 3$, are scalars and e_i is the unit vector in the ith direction, then the interpolating polynomial $P(\phi)$ is one-dimensionally convex/concave in the ith variable if the interpolated function $f(\phi)$ is so.

Proof

Assume that $P(\phi)$ is not one-dimensionally convex/concave, i.e.,

88

$$P(\lambda \underset{\sim}{\phi}^a + (1-\lambda)\underset{\sim}{\phi}^b) \gtrless \lambda\, P(\underset{\sim}{\phi}^a) + (1-\lambda)\, P(\underset{\sim}{\phi}^b)\ ,\ 0 < \lambda < 1\ , \tag{5.51}$$

where

$$\underset{\sim}{\phi}^b = \underset{\sim}{\phi}^a + c\, \underset{\sim i}{e} \tag{5.52}$$

and where c is a scalar.

Hence,

$$P(\underset{\sim}{\phi}^a + (1-\lambda)c\underset{\sim i}{e}) \gtrless \lambda\, P(\underset{\sim}{\phi}^a) + (1-\lambda)\, P(\underset{\sim}{\phi}^a + c\underset{\sim i}{e})\ . \tag{5.53}$$

Expanding $P(\underset{\sim}{\phi}^a + (1-\lambda)c\underset{\sim i}{e})$ and $P(\underset{\sim}{\phi}^a + c\underset{\sim i}{e})$ in Taylor series and knowing that $P(\underset{\sim}{\phi})$ is a quadratic polynomial, we have

$$P(\underset{\sim}{\phi}^a) + (1-\lambda)\, c\, \underset{\sim i}{e}^T \nabla P(\underset{\sim}{\phi}^a) + \frac{1}{2}(1-\lambda)^2 c^2\, \underset{\sim i}{e}^T H \underset{\sim i}{e}$$

$$\gtrless P(\underset{\sim}{\phi}^a) + (1-\lambda)c\, \underset{\sim i}{e}^T \nabla P(\underset{\sim}{\phi}^a) + \frac{1}{2}(1-\lambda)c^2\, \underset{\sim i}{e}^T H \underset{\sim}{e}\ . \tag{5.54}$$

Thus,

$$(1-\lambda)^2\, \underset{\sim i}{e}^T H \underset{\sim i}{e} \gtrless (1-\lambda)\, \underset{\sim i}{e}^T H \underset{\sim i}{e}\ , \tag{5.55}$$

but since $0 < (1-\lambda) < 1$, hence,

$$\underset{\sim i}{e}^T H \underset{\sim i}{e} \gtrless 0\ . \tag{5.56}$$

Without any loss of generality we can number the three base points such that

$$\phi^3 = \gamma \, \phi^1 + (1-\gamma) \, \phi^2 \, , \, 0 < \gamma < 1 \, . \tag{5.57}$$

and

$$\phi^2 = \phi^1 + \beta \, e_i \, , \tag{5.58}$$

where β is a scalar.

Then,

$$P(\phi^3) = P(\gamma \, \phi^1 + (1-\gamma)\phi^2) \, ,$$

$$= P(\phi^1 + (1-\gamma)\beta \, e_i) \, ,$$

$$= P(\phi^1) + (1-\gamma)\beta \, e_i^T \, \nabla \, P(\phi^1) + \frac{1}{2} \, (1-\gamma)^2\beta^2 \, e_i^T \, H \, e_i \, ,$$

$$= \gamma P(\phi^1) + (1-\gamma) \, [P(\phi^1) + \beta \, e_i^T \, \nabla \, P(\phi^1) + \frac{1}{2} \, \beta^2 \, e_i^T \, H \, e_i]$$

$$- \frac{1}{2}(1-\gamma)\beta^2 e_i^T \, H \, e_i + \frac{1}{2} \, (1-\gamma)^2\beta^2 \, e_i^T \, H \, e_i \, ,$$

$$= \gamma P(\phi^1) + (1-\gamma) \, P(\phi^2) - \frac{1}{2} \, \gamma(1-\gamma)\beta^2 \, e_i^T \, H \, e_i \, .$$

But, using (5.56),

$$P(\phi^3) \gtrless \gamma\, P(\phi^1) + (1-\gamma)\, P(\phi^2) \qquad (5.59)$$

and since f = P at the base points, then

$$f(\phi^3) \gtrless \gamma\, f(\phi^1) + (1-\gamma)\, f(\phi^2)\ , \qquad (5.60)$$

which contradicts the fact that $f(\phi)$ is one-dimensionally convex/concave in the ith variable. Hence, the assumption (5.51) is never true.

Q.E.D.

5.6.2 Corollary 5.2

A quadratic polynomial is one-dimensionally convex/concave if and only if all of the diagonal elements of its Hessian matrix are nonnegative/nonpositive.

The proof follows since inequality (5.56) is never true.

The previous corollary allows an easy check on one-dimensional convexity of any quadratic function. In addition, the choice of base points as given in (5.19) satisfies the requirement of locating three base points in each direction.

5.7   Efficient Calculation of Polynomial and Gradients at Vertices

5.7.1 Theory

During optimization the values of the polynomial approximations of the different constraints and their gradients are required. Hence, an efficient technique for these calculations is essential.

The method used for computing the polynomial and its gradients at the vertices exploits simple properties of a quadratic approximation. Consider the following two equations relating the polynomial values and gradients at a vertex ϕ^r to the values at another vertex ϕ^s,

$$P(\phi^r) = P(\phi^s) + (\phi^r - \phi^s)^T \nabla P(\phi^s) + \frac{1}{2}(\phi^r - \phi^s)^T H(\phi^r - \phi^s) \qquad (5.61)$$

and

$$\nabla P(\phi^r) = \nabla P(\phi^s) + H(\phi^r - \phi^s) \ , \qquad (5.62)$$

where H is the Hessian matrix for the quadratic approximation and ∇ is the vector of partial derivatives with respect to the components of ϕ as defined in (5.13) and (5.14), respectively.

Let ϕ^r and ϕ^s be related as follows

$$\phi^r = \phi^s + 2\varepsilon_i \ e_i \ , \qquad (5.63)$$

where e_i is the unit vector in the ith direction and ε_i is the tolerance in the ith variable.

Hence, we have

$$r = s + 2^{i-1} \tag{5.64}$$

according to the following vertex enumeration scheme:

$$r = 1 + \sum_{i=1}^{k} \frac{(\mu_i^r + 1)}{2} 2^{i-1}, \quad \mu_i^r \in \{-1, 1\}, \tag{5.65}$$

where

$$\underset{\sim}{\phi}^r = \underset{\sim}{\phi}^0 + \underset{\sim}{E} \underset{\sim}{\mu}^r \tag{5.66}$$

and where $\underset{\sim}{\phi}^0$ is the nominal parameter vector and $\underset{\sim}{E}$ is a kxk diagonal matrix with diagonal elements set to ε_i, $i = 1, 2, \ldots, k$.

Then (5.61) and (5.62) reduce to

$$P(\underset{\sim}{\phi}^r) = P(\underset{\sim}{\phi}^s) + 2\varepsilon_i \nabla_i P(\underset{\sim}{\phi}^s) + 2 \varepsilon_i^2 H_{ii} \tag{5.67}$$

$$\underset{\sim}{\nabla}P(\underset{\sim}{\phi}^r) = \underset{\sim}{\nabla}P(\underset{\sim}{\phi}^s) + 2\varepsilon_i \underset{\sim}{H}_i, \tag{5.68}$$

where ∇_i is the ith component of $\underset{\sim}{\nabla}$, H_{ii} is the ith diagonal element of $\underset{\sim}{H}$ and $\underset{\sim}{H}_i$ is the ith column of $\underset{\sim}{H}$.

If ϕ^r and ϕ^s fall into different interpolation regions, which is the case if $\varepsilon_i > \delta_i$ (see Fig. 5.5), (5.67) and (5.68) are no longer applicable because of the different polynomials.

Let N_{in} denotes the number of interpolation regions and H^ℓ, $\ell = 1$, 2, ..., N_{in} denote the Hessian matrices of the quadratic approximation at the different interpolation regions.

Define the set I as

$$I \overset{\Delta}{=} \{i \mid \varepsilon_i \leq \delta_i, \ i \in \{1, 2, \ldots, k\} \} \ . \tag{5.69}$$

It is clear that if n_i is the number of elements of I, then

$$N_{in} = 2^{k-n_i} \ . \tag{5.70}$$

5.7.2 Algorithm

The efficient algorithm is described by the following steps.

Step 1 Compute $P^\ell(\phi^s)$ and $\nabla P^\ell(\phi^s)$ for all $s \in S$, where

$$S = \{s \mid s = 1 + \sum_{i=1}^{k} \frac{\mu_i^s + 1}{2} 2^{i-1}, \ \mu_i^s = -1 \text{ if } i \in I \ ,$$

$$\mu_i^s = \{-1, 1\} \text{ if } i \notin I \} \ . \tag{5.71}$$

$$\ell = 1 + \sum_{i=1}^{k} \frac{\mu_i^s + 1}{2} 2^{\sum_{j=1}^{i} p_j - 1} \ , \tag{5.72}$$
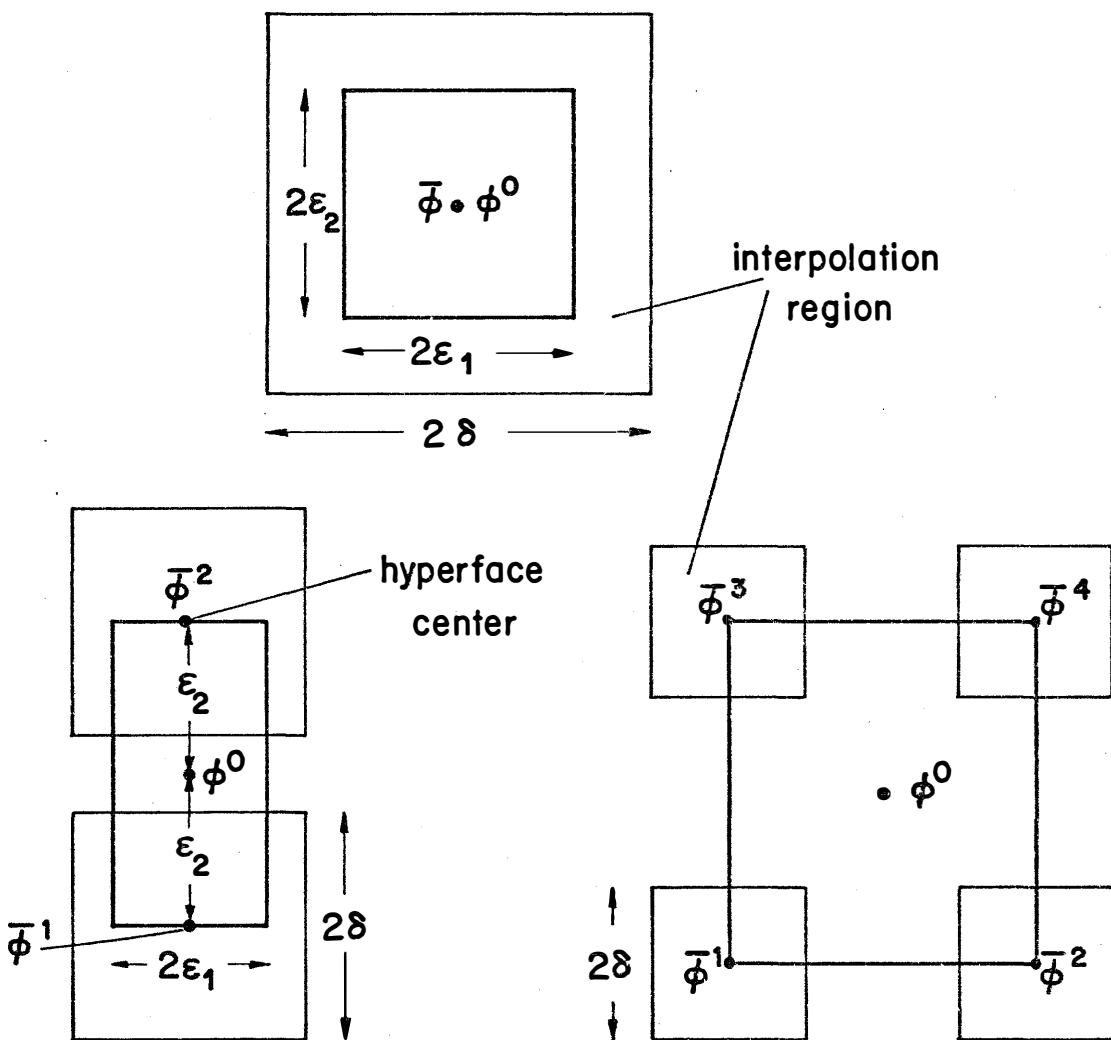
Fig. 5.5   Three situations created by certain step sizes $\delta = \delta_1 = \delta_2$ and tolerances. The different interpolation regions and their centers are indicated.

$$P_j = \begin{cases} 0 & \text{if } j \in I \\ 1 & \text{if } j \notin I \end{cases} \qquad (5.73)$$

and where ℓ identifies an interpolation region.

Set $J \leftarrow I$.

Step 2   If J is empty stop.

Step 3   Set $i \leftarrow i_1$ where $i_1 \in J$ and $i_1 \leq j$ for all $j \in J$.

Step 4   Find $T = \epsilon_i + \epsilon_i$.

Step 5   Find the vector $\underset{\sim}{G}_i^\ell = T \underset{\sim}{H}_i^\ell$ for all ℓ defined by (5.72).

Step 6   For all $s \in S$ and for all ℓ calculate

$$P^\ell(\underset{\sim}{\phi}^r) = P^\ell(\underset{\sim}{\phi}^s) + T \nabla_i P^\ell(\underset{\sim}{\phi}^s) + \epsilon_i G_{ii}^\ell , \qquad (5.74)$$

$$\underset{\sim}{\nabla} P^\ell(\underset{\sim}{\phi}^r) = \underset{\sim}{\nabla} P^\ell(\underset{\sim}{\phi}^s) + \underset{\sim}{G}_i^\ell , \qquad (5.75)$$

where G_{ii}^ℓ is the ith element of $\underset{\sim}{G}_i^\ell$ and r is defined by (5.64).

Step 7   Set $S \leftarrow S \cup \{r \mid r = S + 2^{i-1}, s \in S\} , \qquad (5.76)$

$$J \leftarrow J - \{1, 2, \ldots, i\} \qquad (5.77)$$

and go to Step 2.

This scheme is illustrated for different cases in Fig. 5.6. The computational effort required for considering all vertices compared to that required for one vertex only is shown in Table 5.1.
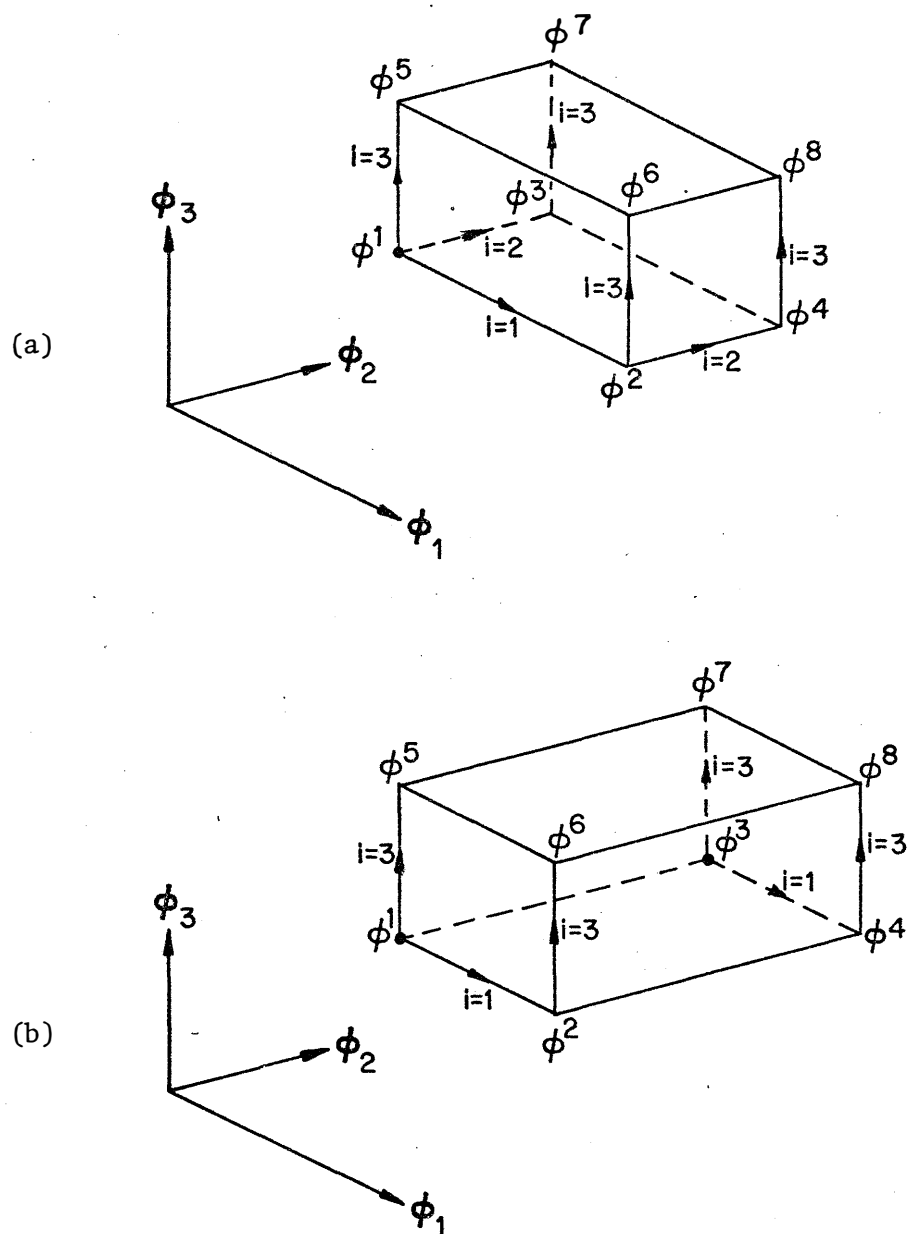
Fig. 5.6   Illustration of the efficient technique for evaluation

of the approximations and their derivatives.

(a) $n_i = 3$, $N_{in} = 1$ and initially $S = \{1\}$.

(b) $n_i = 2$, $N_{in} = 2$ and initially $S = \{1, 3\}$.

TABLE 5.1

COMPUTATIONAL EFFORT FOR EVALUATION OF THE QUADRATIC POLYNOMIAL

AND ITS DERIVATIVES

Description	Number of additions	Number of multiplications
At one vertex only	$\frac{1}{2} k(3k + 5)$	$\frac{3}{2} k(k + 1)$
At all the vertices using original formula	$2^{k-1} k(3k + 5)$	$3 \times 2^{k-1} k(k + 1)$
At all the vertices using the efficient scheme	$2^{k-n_i}[\frac{1}{2}k(3k+5)+(k+2)(2^{n_i}-1)]+n_i$	$2^{k-n_i}[\frac{3}{2}k(k+1)+n_i(k+1)+2^{n_i}-1]$
At all the vertices using the efficient scheme when $n_i = k$	$\frac{1}{2}k(3k+7)+(k+2)(2^k-1)$	$\frac{5}{2}k(k+1)+2^k-1$

5.8   Conclusions

The approximation procedure described permits exploitation of available analysis programs, whether they are efficiently written or not and whether or not they supply derivative information. Experimental data can also be handled, however, a least squares fit might be better in this case due to experimental errors.

The efficient technique for calculating the approximation and its gradients can be implemented with a suitable large-change sensitivity algorithm, for example, see Leung and Spence (1975).

Although it was shown that one-dimensional convexity can be preserved in the approximation, convex approximation for a convex function is not guaranteed. A sufficient condition is to choose three base points along each of an infinite number of possible directions, which is unreasonable.

CHAPTER 6

DESIGN ALGORITHMS

6.1   Introduction

In this chapter, algorithms for worst-case design and for design
with yield less than 100% are presented. The ideas and techniques of
Chapters 4 and 5 are implemented in the algorithms. The aim of the
worst-case design algorithm is to facilitate rapid and accurate
determination of design solutions through a sequence of updated
multidimensional approximations. The algorithm directs the
approximations to be performed to critical regions where constraint
violations might occur. Hence, approximations not only for accurate
worst-case design but also for reliable yield analysis are to be
expected.

The algorithm attempts to minimize the number of evaluations of
exact functions by collecting as many critical regions as possible
within each interpolation region. When the yield drops below 100% the
algorithm retains the approximations obtained during the worst-case
design and employs the yield formulas presented in Chapter 4. It is
shown how we can overcome the problem of <u>overlapping nonfeasible</u>
<u>hypervolumes</u> defined by different constraints.

Two-section transmission-line transformer and lowpass filter
examples illustrate the algorithms.

6.2   Worst-case Design Algorithm

Approximation is only done for complicated functions (objective, responses or constraints) or functions for which gradient information is not available.

6.2.1   Phase 1: Updated approximations for a single interpolation region.

Step 1   Choose initial values for ϕ^0, $\underset{\sim}{\epsilon}$ and $\underset{\sim}{\delta}$.

Step 2   Until $\delta_i \geq \epsilon_i$, $i = 1, 2, \ldots, k$, set $\delta_i \leftarrow 4\delta_i$.

Step 3   Set $\overline{\underset{\sim}{\phi}}$, the center of the interpolation region, to ϕ^0.

Step 4   Choose base points to satisfy (5.19) and such that $\underset{\sim}{\phi}^n \in R_i$, $n = 1, 2, \ldots, N$, where R_i is defined in (5.10).

Step 5   For each approximated function, interpolation is carried out by solving (5.25).

Step 6   Set $\underset{\sim}{\phi}^0$ and $\underset{\sim}{\epsilon}$ to values obtained by solving the nonlinear programming problem, resulting from worst-case design problem described in Chapter 3, and employing the approximations.

Step 7   If $|\phi_i^0 - \overline{\phi_i}| > 1.5\ \delta_i$ for any i, go to Step 2.

Step 8   Stop if $\underset{\sim}{\delta}$ is sufficiently small.

Step 9   Set $\underset{\sim}{\delta} \leftarrow \underset{\sim}{\delta}/4$. Go to Step 3 if $\delta_i \geq \epsilon_i$ for all i.

Step 10   If $\delta_i < \epsilon_i$ for any i, go to Phase 2.

6.2.2   Phase 2: Updated approximations in more than one interpolation region.

Step 1   Interpolation is carried out by solving (5.25) around the centers of interpolation (see Fig. 5.5) regions given by

$$\bar{\underset{\sim}{\phi}}^{\ell} \in \{\underset{\sim}{\phi} \mid \underset{\sim}{\phi} = \underset{\sim}{\phi}^0 + \underset{\sim}{P} \; \underset{\sim}{E} \; \underset{\sim}{\mu}^s \; , \; \mu_i^s \in \{-1,1\}, \; i = 1,2,\ldots,k\} \; , \quad (6.1)$$

where $\ell = 1, 2, \ldots, N_{in}$ identifies the interpolation region and is given by (5.72), $\underset{\sim}{P}$ is a $k \times k$ diagonal matrix with elements p_j defined by (5.73) and where base points $\underset{\sim}{\phi}^n$ satisfy (5.19) and

$$\underset{\sim}{\phi}^n \in R^{\ell} \triangleq \{\underset{\sim}{\phi} \mid \delta_i \geq \mid \phi_i - \bar{\phi}_i^{\ell} \mid \; , \; i = 1, 2, \ldots, k\} \; . \quad (6.2)$$

Step 2   Set $\underset{\sim}{\phi}^0$ and $\underset{\sim}{\varepsilon}$ to values obtained by worst-case design.

Step 3   Let the set of candidates for active vertices be

$$R_{avc} \triangleq \{\underset{\sim}{\phi}^s \mid P_j^{\ell} (\underset{\sim}{\phi}^s) \leq \delta_{av}\} \; , \quad (6.3)$$

where ℓ is given by (5.72), P_j^{ℓ} is the quadratic approximation of the jth constraint at the ℓth interpolation region and δ_{av} is a small positive number for defining the candidates.

Step 4   If, for any vertex $\underset{\sim}{\phi}^s \in R_{avc}$, $\mid \phi_i^s - \phi_i^{\ell} \mid \; > 2\delta_i$ for any i, where ℓ and s are related through (5.72), go to Step 1.

Step 5   Stop if $\underset{\sim}{\delta}$ is sufficiently small.

Step 6   Set $\underset{\sim}{\delta} \leftarrow \underset{\sim}{\delta}/4$. Go to Step 1.

<u>Comment</u> The procedure can be made more efficient by interpolating a constraint $g_j(\underset{\sim}{\phi})$, say, in the ℓth interpolation region only if there exists a vertex $\underset{\sim}{\phi}^S \in R^\ell$ which has been detected as a candidate for being active w.r.t. that constraint after the previous optimization.

6.3   Introduction of Tuning

The centers of interpolation regions given by (6.1) will not be suitable for accurate location of the boundary of the constraint region R_c when tuning is considered. This boundary is still more important than the boundary of the tunable constraint region R_{ct}. The set of candidates for active vertices is given by

$$R_{avc} = \{\underset{\sim}{\phi}^S \mid \max_{\underset{\sim}{\rho} \in R_\rho} U(P_j^\ell(\underset{\sim}{\phi}^S) , J, \infty, -1) \leq \delta_{av}\} , \qquad (6.4)$$

where U is the least pth function defined by (3.1). P_j^ℓ is the quadratic approximation of the jth constraint at the ℓth interpolation region, δ_{av} is a small positive number for defining the candidates,

$$J \overset{\Delta}{=} \{1, 2, \ldots, m_c\} \qquad (6.5)$$

and m_c is the number of constraints at the vertex $\underset{\sim}{\phi}^S$. The suggested centers of interpolation are

$$\overline{\underset{\sim}{\phi}}^S = \underset{\sim}{\phi}^S + \underset{\sim}{T} \underset{\sim}{\rho}^* , \qquad (6.6)$$

where $\underset{\sim}{\phi}^S \in R_{avc}$ and $\underset{\sim}{\rho}^*$ is the optimum of

$$\max_{\underset{\sim}{\varrho} \in R_\rho} U(P_j^\ell (\underset{\sim}{\phi}^S), J, \infty, -1) . \qquad (6.7)$$

Efficiency in finding the approximations can be improved by collecting more than one of these suggested centers in one interpolation region, for example, let

$$\overline{\phi}_i^\ell = \frac{1}{2} \left[\max_{s \in S^\ell} \overline{\phi}_i^s - \min_{s \in S^\ell} \overline{\phi}_i^s \right] , \quad i = 1, 2, \ldots, k, \qquad (6.8)$$

where the sets S^ℓ, $\ell = 1, 2, \ldots, N_{in}$, are constructed using the following steps.

Step 1   Set $R \leftarrow \emptyset$ and let $N_{in} = 0$.

Step 2   Stop if the set $(R_{avc} - R)$ is empty.

Step 3   For an s, such that $\underset{\sim}{\phi}^S \in (R_{avc} - R)$, if

$$\overline{\underset{\sim}{\phi}}^S \in \{\underset{\sim}{\phi} | 2\delta_i \geq |\phi_i - \overline{\phi}_i^r| , \quad i = 1, 2, \ldots, k, \text{ for all } r \in S^\ell\} , \qquad (6.9)$$

for any $\ell = 1, 2, \ldots, N_{in}$, set $S^\ell \leftarrow S^\ell \cup \{s\}$ and go to Step 5.

Step 4   Set $N_{in} \leftarrow N_{in} + 1$ and $S^{N_{in}} = \{s\}$.

Step 5   Set $R = R \cup \{\underset{\sim}{\phi}^S\}$ and go to Step 2.

Finally, N_{in} will be the number of interpolation regions.   It is

to be observed that this construction of the sets S^{ℓ}, $\ell = 1, 2, \ldots,$ N_{in}, is not unique. It depends upon the numbering of the vertices.

6.4 Design for Yield Less than 100%

If the yield is relaxed to be less than 100% an accurate approximation for the boundary in small interpolation regions may be inappropriate. Preferably, the interpolation regions should cover those parts of the boundary where violations occur. The active vertices for worst-case design identify probable locations where constraints are violated if a high but less than 100% yield is acceptable. The approximations are, therefore, ultimately centered on active vertices. Based upon the expected yield, a rough estimate for the size of the interpolation region is given in the following subsection.

6.4.1 Estimation of the Size of the Interpolation Region

Consider the illustrative two-dimensional example shown in Fig. 6.1. Assuming equal nonfeasible hypervolumes determined by the candidates for active vertices, defined in (6.3), during a worst-case design procedure, we have

$$\frac{1}{N_{av}} (1 - Y_{ex}) \, 2^k \prod_{i=1}^{k} (\varepsilon_i + \delta_i) \simeq \frac{1}{k!} \, 2^k \prod_{i=1}^{k} \delta_i \, , \qquad (6.10)$$

where N_{av} is the number of candidates and Y_{ex} is the expected yield. Hence,

$$\prod_{i=1}^{k} (1 + \frac{\varepsilon_i}{\delta_i}) \simeq \frac{N_{av}}{k!(1-Y_{ex})} \, . \qquad (6.11)$$
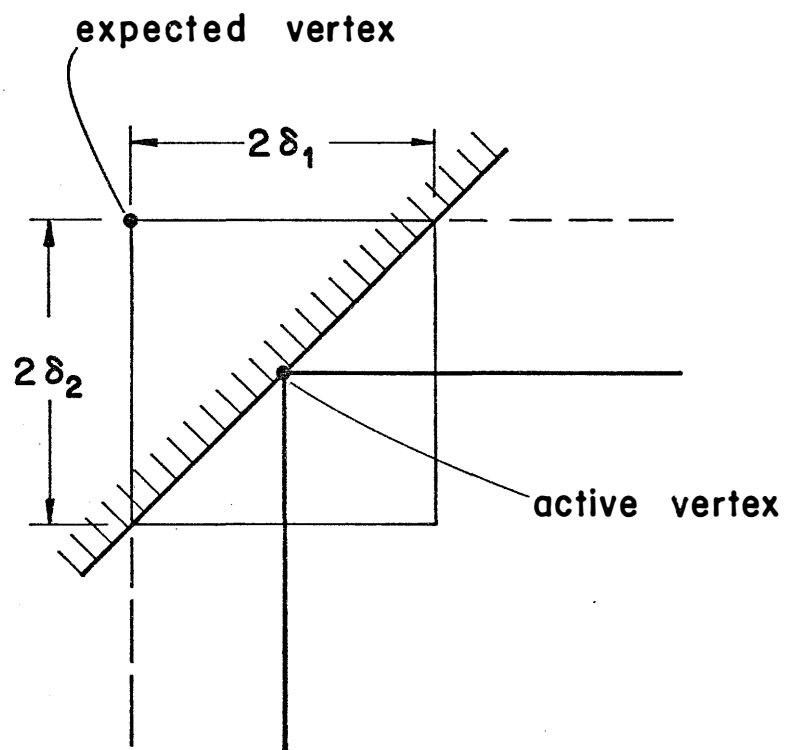
Fig. 6.1   Estimation of a suitable interpolation region

size according to an expected yield.

Assuming a fixed ratio ε_i/δ_i, i = 1, 2, ..., k, then

$$\delta_i \simeq \varepsilon_i / \left\{ [N_{av}/k!(1-Y_{ex})]^{1/k} - 1 \right\} \quad . \tag{6.12}$$

The estimate given in (6.12) is only applicable if the resulting δ_i satisfy

$$0 < \delta_i < \varepsilon_i \ , \ i = 1, \ 2, \ ..., \ k \ . \tag{6.13}$$

Otherwise, we choose

$$\delta_i \geq \varepsilon_i \ , \ i = 1, \ 2, \ ..., \ k \ . \tag{6.14}$$

6.4.2 Algorithm

Step 1   Execute Phase 1 and Phase 2 (if necessary) of the worst-case
          design algorithm using a consistent stopping $\underset{\sim}{\delta}$ as found in
          Subsection 6.4.1.

Step 2   Find the set of candidates for reference vertices given by
$$S_{avc} = \{s \mid P_j^{\ell}(\underset{\sim}{\phi}^s) \leq \delta_{av}\} \quad . \tag{6.15}$$
          See (6.3) for definition of terms.

Comment   The set of reference vertices S_{avc} is the set of candidates for
          worst-case and hence it is available after the worst-case
          design process.

Step 3   For each s ϵ S_{avc} construct the constraint
$$g_s(\underset{\sim}{\phi}) = U(P_j^{\ell}(\underset{\sim}{\phi}), \ J^s, \ p, \ - \ 1) \geq 0 \ , \tag{6.16}$$
          where U is given by (3.1), p > 1 and

$$J^S = \{ j \mid P_j^{\ell}(\underset{\sim}{\phi}^S) \le \delta_{av} \} \ . \tag{6.17}$$

Step 4   Choose factors $\kappa_i > 1$ by which each tolerance is expected to increase, i.e., set $\varepsilon_i \leftarrow \kappa_i \varepsilon_i$, $i = 1, 2, \ldots, k$.

Step 5   Find optimal values for $\underset{\sim}{\phi}^0$ and $\underset{\sim}{\varepsilon}$ using the worst-case nominal and the tolerances obtained in Step 4 as starting values for the optimization process. Yield and yield sensitivities required during optimization are calculated according to the constraints $g_s(\underset{\sim}{\phi}) \ge 0$, $s \in S_{avc}$.

Comment   The yield and its sensitivities are calculated using updated linear cuts as described in Section 4.8. If the method of intersections is used we apply the following steps to avoid problems arising from having less than k intersections.

(a)   Obtain default cuts by linearizing $g_s(\underset{\sim}{\phi})$ at $\underset{\sim}{\phi}^S$, $s \in S_{avc}$ at the worst-case design.

(b)   Update the sth linear cut using the k intersections if they exist, otherwise keep the latest sth linear cut fixed, for all $s \in S_{avc}$.

6.5   Examples

6.5.1   Two-section Transmission-line Transformer

        Consider the two-section 10:1 quarter-wave lossless transmission-line transformer used by Bandler and Macdonald (1969a). The specifications and results of the worst-case tolerance optimization problem of the characteristic impedances Z_1 and Z_2 over 100% bandwidth are shown in Table 6.1 for two different objective functions. The constraint region

TABLE 6.1

WORST-CASE DESIGN OF THE TWO-SECTION 10:1 QUARTER-WAVE TRANSFORMER

Cost Function	Z_1^0	Z_2^0	ϵ_1/Z_1^0 (%)	ϵ_2/Z_2^0 (%)	δ	N.O.F.E.	CDC Time (sec)
C_1	2.5637	5.5048	14.678	9.007	0.4	18	7.213
	2.5234	5.4379	14.988	9.081	0.1	24	9.533
C_2	2.1515	4.7350	12.715	12.697	0.4	12	2.468
	2.1494	4.7305	12.687	12.700	0.1	18	2.959

Starting values $Z_1^0 = 2.2361$, $Z_2^0 = 4.4721$, $\epsilon_1 = 0.2$ and $\epsilon_2 = 0.4$

Frequency points used 0.5, 0.6, ..., 1.5 GHz

Objective cost functions $C_1 = \dfrac{1}{\epsilon_1} + \dfrac{1}{\epsilon_2}$, $C_2 = \dfrac{Z_1^0}{\epsilon_1} + \dfrac{Z_2^0}{\epsilon_2}$

Reflection coefficient specification $|\rho| \leq 0.55$

*N.O.F.E. denotes the number of function evaluations

and the resulting optimum solutions in two cases are shown in Fig. 6.2 and Fig. 6.3. An equal value of δ_1 and δ_2 was used. The figures show the interpolation regions and the resulting approximations for the constraint boundary. The results obtained are contrasted with the results obtained by Bandler, Liu and Chen (1975).

Subsequently, the approximations obtained at the two active vertices for the worst-case problem having the objective function C_1, shown in Table 6.1 and Fig. 6.2, were used for yield optimization. This problem is denoted PO. A rough estimate of $\delta = 0.1$ was obtained using (6.12) and was used for solving the following two problems:

$$\text{minimize } 1/\varepsilon_1 + 1/\varepsilon_2 \ ,$$

P1

$$\text{subject to}$$

$$Y \geq 90\% \ ,$$

$$\text{P2} \quad \text{minimize } (1/\varepsilon_1 + 1/\varepsilon_2)/Y$$

assuming a uniform distribution of outcomes between tolerance extremes.

The optimum solutions for P1 and P2 are shown in Table 6.2 and contrasted with the worst-case solution PO in Fig. 6.4. The program FLNLP2 by Chu (1974) was used for solving the resulting nonlinear programming problem. Since a convex constraint region appears in this problem, the values of yield obtained are lower bounds for the true yields.
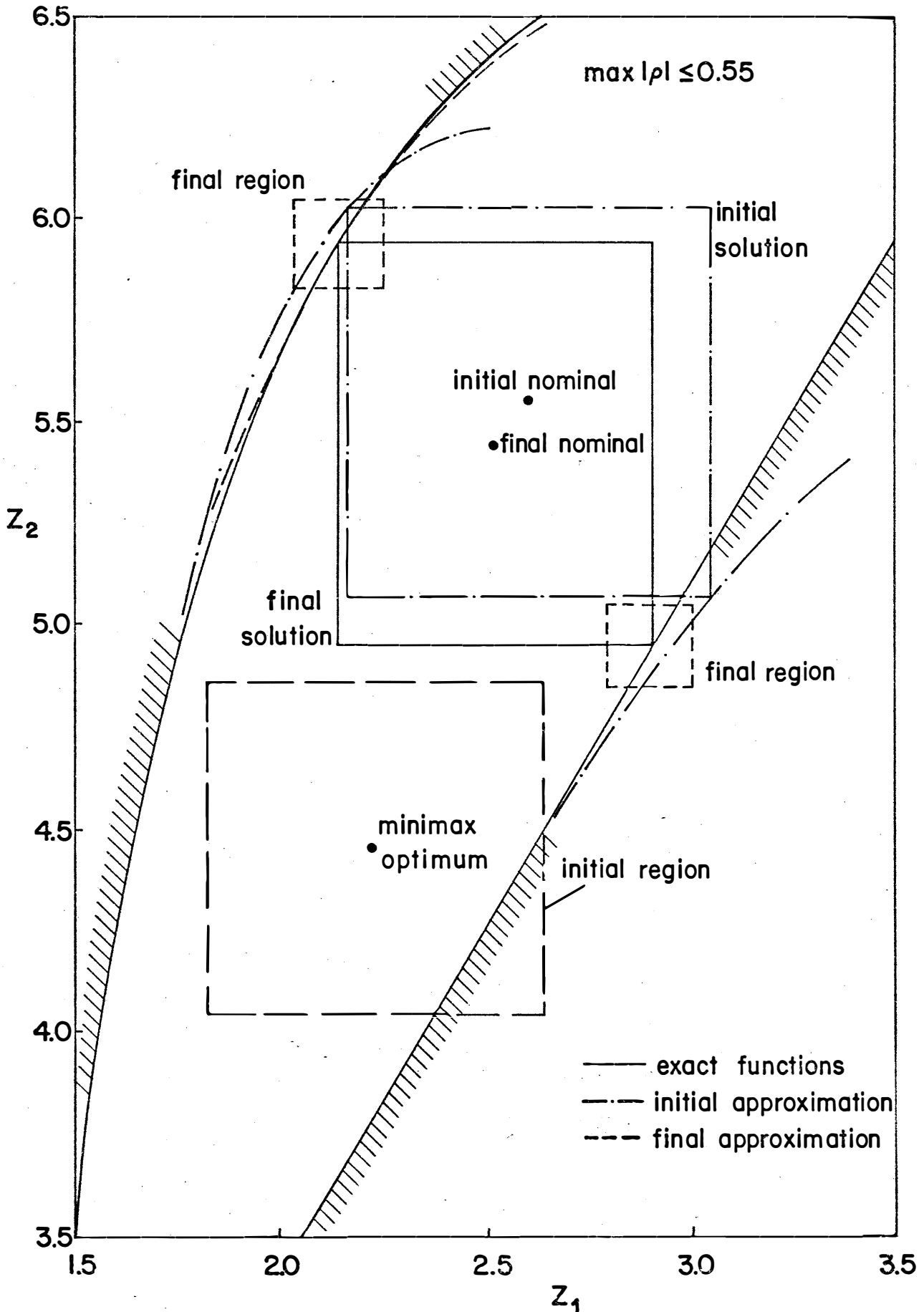
Fig. 6.2   Minimization of $1/\varepsilon_1 + 1/\varepsilon_2$ for the two-section transformer.

max $|\rho| \le 0.55$

final region

initial solution

final solution

initial nominal

final nominal

minimax optimum

initial region

final region

exact functions

initial approximation

final approximation

Z_2

Z_1
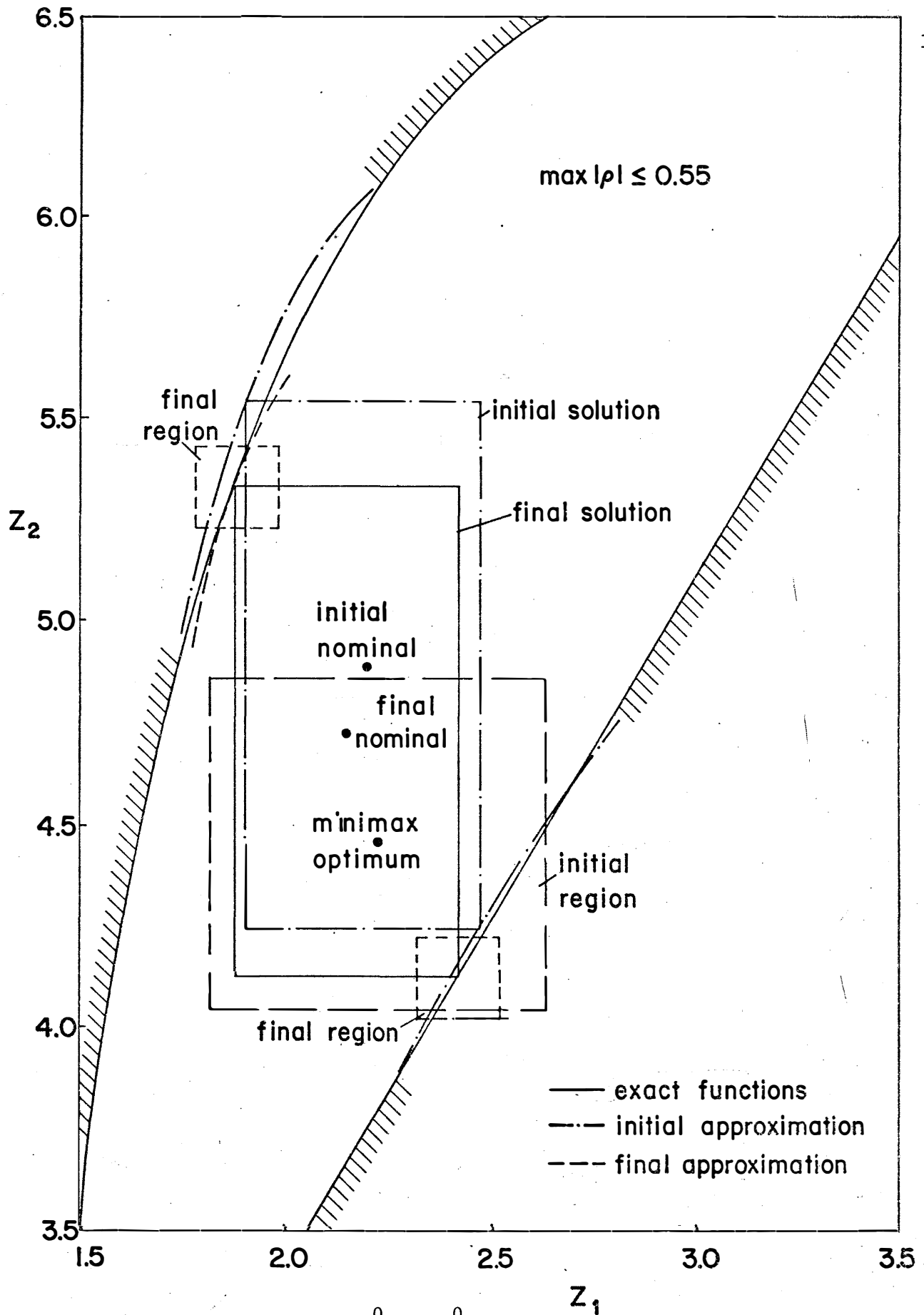
Fig. 6.3 Minimization of $Z_1^0/\epsilon_1 + Z_2^0/\epsilon_2$ for the two-section transformer.

TABLE 6.2

YIELD DETERMINATION AND OPTIMIZATION OF THE TWO-SECTION
10:1 QUARTER-WAVE TRANSFORMER

Problem	Z_1^0	Z_2^0	ε_1/Z_1^0 (%)	ε_2/Z_2^0 (%)	Objective	Yield (%)
P1*	2.5273	5.3998	21.09	13.51	3.2465	90.0
P2**	2.5290	5.1513	31.44	22.13	3.2597	65.5

*   Minimize $1/\varepsilon_1 + 1/\varepsilon_2$ subject to yield $\geq$ 90%

**   Minimize $(1/\varepsilon_1+1/\varepsilon_2)/Y$
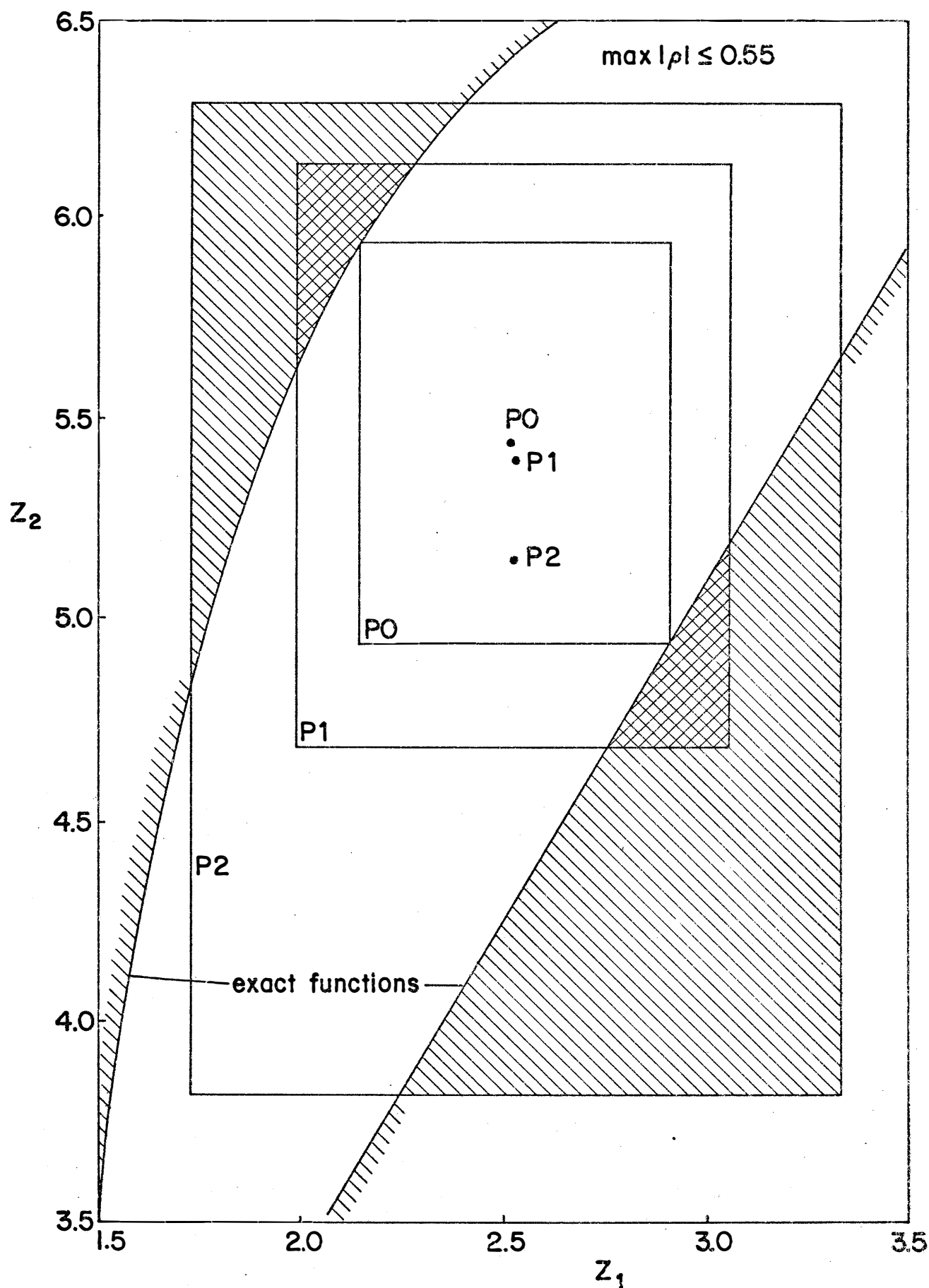
Fig. 6.4   The optimum tolerance regions and nominal values for the
worst-case, 90% yield and optimum yield designs.

6.5.2 Three-component LC Lowpass Filter

A normalized three-component lowpass ladder network, terminated with equal load and source resistances of 1 Ω is shown in Fig. 6.5. The circuit was considered for worst-case design by Bandler, Liu and Chen (1975). Although this filter is symmetric a three-dimensional approximation was required in order to perform the yield technique described before.

Using equal step size δ for all components, a worst-case design was first obtained with final $\delta = 0.01$. The base points used are given by (5.19) with

$$\underset{\sim}{B} = \begin{bmatrix} 0.5 & -0.5 & 1.0 \\ -0.5 & 0.5 & 1.0 \\ 0.8 & 0.8 & 1.0 \end{bmatrix}$$

consistent with the vector of components

$$\underset{\sim}{\phi} = \begin{bmatrix} L_1 \\ L_2 \\ C \end{bmatrix} .$$

This choice of base points should preserve symmetry as indicated in Section 5.5. The specifications and the objective function are given in Table 6.3. The convergence of the quadratic approximation coefficients as the step size δ is reduced is shown in Fig. 6.6 for the insertion loss constraint at the frequency point 2.5 rad/s. The coefficient b_4 is not shown in the figure. Its value is close to zero and hence the
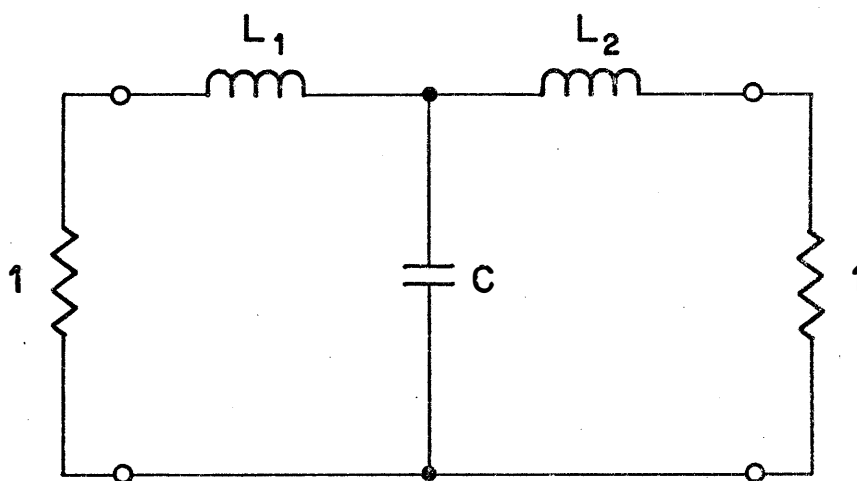
Fig. 6.5   The circuit for the LC lowpass filter example.

TABLE 6.3

WORST-CASE AND YIELD CONSTRAINED RESULTS OF
THE LC LOWPASS FILTER

Yield (%)	L_1^0	L_2^0	C^0	ε_1/L_1^0 (%)	ε_2/L_2^0 (%)	ε_C/C^0 (%)
100	1.999	1.998	0.9058	9.88	9.89	7.60
96	1.997	1.997	0.9033	11.23	11.23	12.46

Frequency points used 0.45, 0.5, 0.55, 1.0 in the passband and 2.5 in the stopband

Objective cost function is $\dfrac{L_1^0}{\varepsilon_1} + \dfrac{L_2^0}{\varepsilon_2} + \dfrac{C^0}{\varepsilon_C}$

Insertion loss specification $\leq$ 1.5 dB in the passband and $\geq$ 25 dB in the stopband

Fig. 6.6   Convergence of the quadratic approximation to the insertion loss constraint at 2.5 rad/s.

normalized value is highly oscillatory. At the worst-case optimum, given in Table 6.3, the active frequency point constraints are 0.55, 1.0 and 2.5 rad/s.

Now, consider the problem given by

$$\text{minimize } L_1^0/\varepsilon_1 + L_2^0/\varepsilon_2 + C^0/\varepsilon_C \; ,$$

subject to

$$Y \geq 96\% \; .$$

The quadratic approximation with $\delta = 0.04$, which was used in this problem, is shown in Table 6.4 after and before averaging symmetric coefficients. The diagonal elements of the Hessian matrix, as defined by the coefficients of the approximating polynomial, suggest a one-dimensionally convex constraint region. Symmetry between L_1 and L_2 was used to reduce computation in finding the values and the gradients of the intersections between the orthotope edges and the quadratic constraints. The results are shown in Table 6.3 and in Fig. 6.7. The tolerance for the capacitor ε_C was approximately doubled, with respect to its value for the worst-case design, by allowing the yield to drop to 96%.

In order to check the results, a uniformly distributed set of 10,000 points was generated inside the tolerance region. The results are shown in Table 6.5. Also shown is the computational time saving when the approximation is used for statistical analysis instead of the exact constraints.

TABLE 6.4

COEFFICIENTS OF THE QUADRATIC APPROXIMATION AROUND ACTIVE VERTICES

Freq. point	State	L_1^2	L_2^2	C^2	L_1L_2	L_1C	L_2C	L_1	L_2	C	-
0.55	before	-0.06847	-0.06847	-0.57056	.33010	0.92247	0.93855	-1.67845	-1.69182	-0.46249	3.83750
	after	-0.06847	-0.06847	-0.57056	.33010	0.93051	0.93051	-1.68513	-1.68513	-0.46249	3.83750
1.00	before	-1.12188	-1.16702	-9.98122	.21439	-8.16357	-8.30295	10.21440	10.51832	44.18607	-33.86206
	after	-1.14445	-1.14445	-9.98122	.21439	-8.23326	-8.23326	10.36637	10.36637	44.18607	-33.86206
2.50	before	-1.38601	-1.42228	-9.90167	.39487	-0.92910	-0.94732	10.19142	10.32736	32.94001	-46.93184
	after	-1.40414	-1.40414	-9.90167	.39487	-0.93821	-0.93821	10.25939	10.25939	32.94001	-46.93184

Coefficients of the quadratic approximations obtained at active vertices with a step $\delta = 0.04$. The table shows the coefficients obtained by the algorithm and the coefficients used for yield determination after averaging symmetric coefficients.
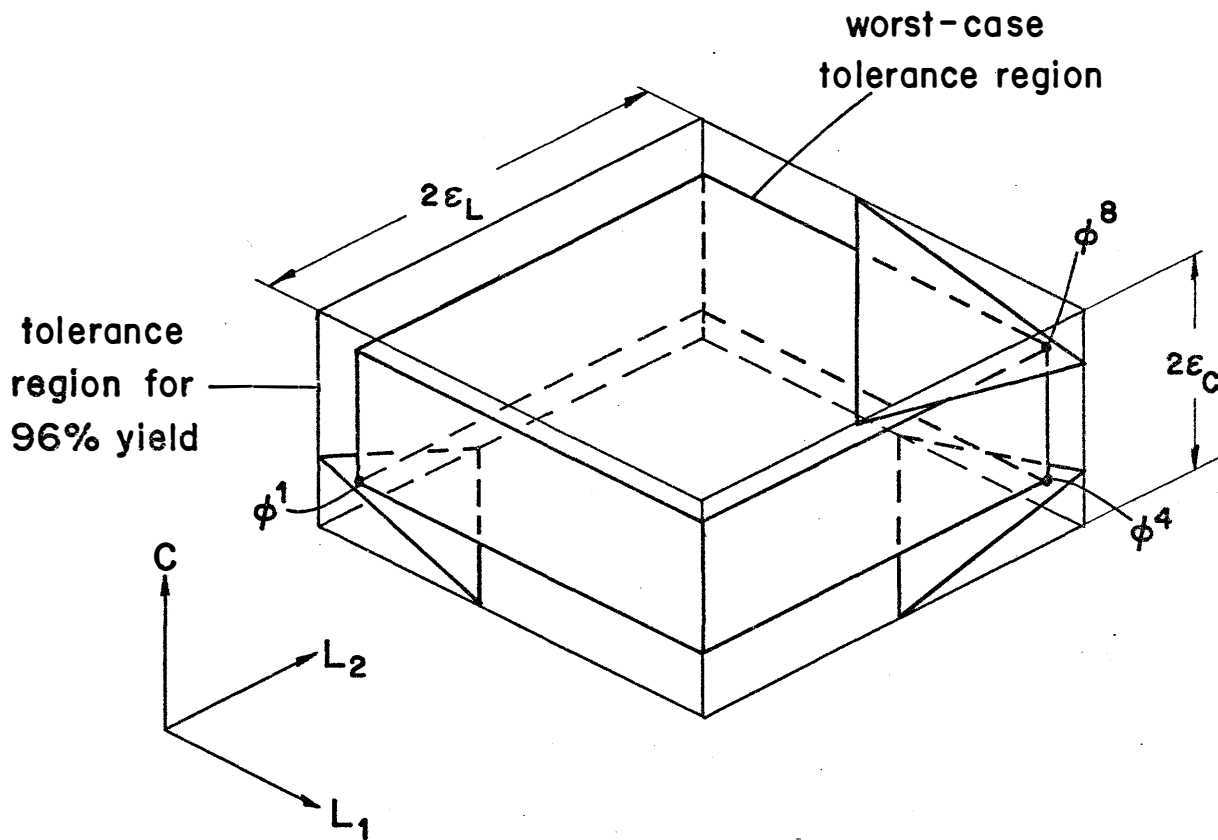
Fig. 6.7 The tolerance regions for the worst-case design and the 96% yield for the LC filter. The linear cuts shown are based on the intersections of the active quadratic constraint approximations with edges of the tolerance orthotope for 96% yield.

TABLE 6.5

COMPARISON OF METHODS OF YIELD ESTIMATION
FOR THE LC LOWPASS FILTER

Description	Yield (%)	CDC Time (sec)
Exact constraints	96.59	20.98
Approximate constraints	96.58	10.43

Yield estimation using a set of 10,000 uniformly distributed points inside the tolerance region for the case of 96% yield according to the linear cut. All of the five frequency points were used.

6.6   Conclusions

The algorithm for worst-case design provides reliable approximations at critical regions where constraint violations might occur. For low yield, however, violation by unexpected constraints might occur. The relevant approximations may require updating if the original approximations were carried out far from the respective boundaries of these constraints.

Finally, an inexpensive estimate of production yield might be checked at a proposed solution by performing the Monte Carlo analysis in conjunction with the final approximations.

CHAPTER 7

PRACTICAL EXAMPLES

7.1   Introduction

Techniques and algorithms presented in Chapters 4, 5 and 6 are now applied to realistic design problems.

The first circuit is the Karafin (1971) bandpass filter, which is subjected to a statistical analysis. Yield is estimated assuming different probability distribution functions of production outcomes, namely, the uniform distribution, the bimodal distribution and the normal distribution. The results obtained are contrasted with the Monte Carlo method.

Nonlinear programming is used to obtain worst-case designs for two-section and three-section inhomogeneous, nonideal waveguide transformers. These structures were previously considered by Bandler (1969), whose analysis program (Bandler and Macdonald 1969b) was used to calculate the required responses.

A current switch emitter follower circuit (Ho 1971) is investigated in some detail. An optimal worst-case design and a design which maximizes production yield for assumed correlations beetween transistor model parameters are obtained.

The examples in this chapter, involving nonlinear programming, are solved by transforming the nonlinear program into an unconstrained minimax problem by the Bandler-Charalambous (1974) technique. The

resulting minimax problem is solved by finding the minimum of the least pth objective (Bandler and Charalambous 1972) using Fletcher's unconstrained optimization method (Fletcher 1972).

PART I

YIELD ANALYSIS

7.2   The Karafin Bandpass Filter

The low-frequency bandpass filter, shown in Fig. 7.1, was used for verification of the yield formula. This filter was studied in various ways by Butler (1971), Karafin (1971, 1974), Pinel and Roberts (1972) and by Bandler and Liu (1974a). The insertion loss specifications are shown in Table 7.1. All filter components were assumed subject to statistical variations, i.e.,

$$\underset{\sim}{\phi} = \begin{bmatrix} L_1 \\ C_2 \\ L_3 \\ C_4 \\ L_5 \\ C_6 \\ L_7 \\ C_8 \end{bmatrix} .$$

The values of the quality factor Q for each inductor are those suggested by Karafin (1974). They are associated with nominal values of corresponding components taken from Bandler and Liu (1974a). (See Table 7.1 for these and the remaining nominal values.) Accordingly, the corresponding resistances are

125
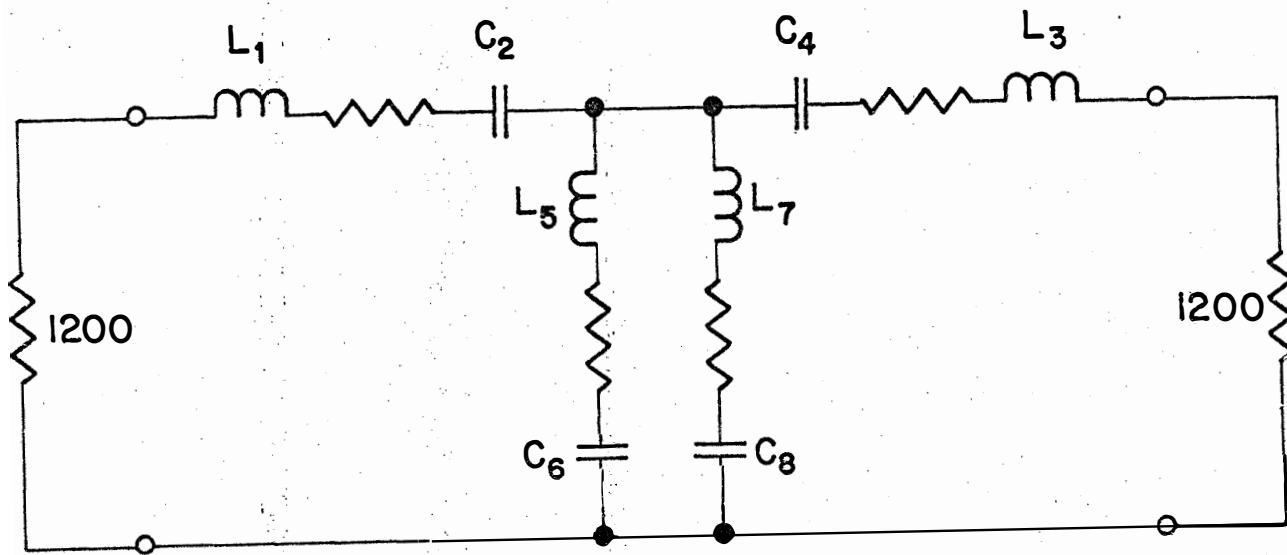
Fig. 7.1   Karafin's bandpass filter.

TABLE 7.1

SPECIFICATIONS FOR THE BANDPASS FILTER

Frequency range (Hz)	Relative insertion loss (dB)	Type
0 - 240	35	lower (stopband)
360 - 490	3	upper (passband)
700 - 1000	35	lower (stopband)

Reference frequency 420 Hz (fixed, therefore, ripples higher than 3 dB are to be expected in the passband)

Nominal values $L_1^0=3.0142$, $C_2^0=4.975 \times 10^{-8}$, $L_3^0=2.902$, $C_4^0=5.0729 \times 10^{-8}$, $L_5^0=0.82836$, $C_6^0=5.5531 \times 10^{-7}$, $L_7^0=0.30319$ and $C_8^0=1.6377 \times 10^{-7}$

$$R_{L_1} = 474.27 \ \Omega \ ,$$

$$R_{L_3} = 127.98 \ \Omega \ ,$$

$$R_{L_5} = 47.47 \ \Omega \ ,$$

and

$$R_{L_7} = 456.62 \ \Omega \ .$$

7.3   Yield Estimation for the Karafin Filter

The adjoint network technique of Director and Rohrer (1969) was used for evaluating first-order sensitivities and, hence, linearizing the constraints at each frequency point in order to obtain the linear cuts. The results produced by Bandler and Liu, as acknowledged by them, violate the specifications at certain unconsidered frequency points. The linearization, taking note of this fact, was done for each constraint at the worst violating vertex, i.e., the vertex which gives the most negative value for the particular constraint. All linearizations were carried out at worst-case design vertices proposed by Bandler and Liu (1974a), for which

$$100 \ \varepsilon_1/\phi_1^0 = 6.99 \ ,$$

$$100 \ \varepsilon_2/\phi_2^0 = 6.52 \ ,$$

$$100 \ \varepsilon_3/\phi_3^0 = 6.97 \ ,$$

$$100 \ \varepsilon_4/\phi_4^0 = 6.55 \ ,$$

$$100 \ \varepsilon_5/\phi_5^0 = 4.36 \ ,$$

$$100 \ \varepsilon_6/\phi_6^0 = 5.69 \ ,$$

$$100 \ \varepsilon_7/\phi_7^0 = 6.80 \ ,$$

$$100 \ \varepsilon_8/\phi_8^0 = 5.25 \ .$$

7.3.1 The Uniform Distribution

A uniform distribution of outcomes inside the tolerance orthotope was assumed. The yields obtained by the approach presented in Chapter 4 and applying the Monte Carlo method with the nonlinear constraints are shown in Table 7.2 for different values of parameter tolerances. Also shown are the execution times using a CDC 6400 computer for the approach of Section 4.7 and the Monte Carlo method. The linearization time is included in the execution time for calculating the yield. More frequency points were considered for larger tolerances. These additional points provide new linear cuts which do not overlap.

7.3.2 The Bimodal Distribution

The parameters were assumed independent with uniform distributions, but with accurate components removed. Such a distribution was observed by Pinel and Roberts (1972) and used by Pinel and Singhal (1977). According to the approach presented in Chapter 4, the following weights for each parameter will result in

$$w_i(1) = 0.5 \ ,$$

$$w_i(2) = 0.0 \ ,$$

$$w_i(3) = 0.5 \ .$$

TABLE 7.2

COMPARISON WITH THE MONTE CARLO ANALYSIS FOR UNIFORM
DISTRIBUTION BETWEEN TOLERANCE EXTREMES

ε_1/L_1^0	ε_2/C_2^0	ε_3/L_3^0	ε_4/C_4^0	ε_5/L_5^0	ε_6/C_6^0	ε_7/L_7^0	ε_8/C_8^0	Sample points (Hz)	Yield (%) Approx.	M.C.	CDC Time (sec) Approx.*	M.C.**
6.99	6.52	6.97	6.55	4.36	5.69	6.80	5.25	188, 700, 876	100.00	99.75	0.67	24.0
7.00	7.00	7.00	7.00	5.00	6.00	7.00	6.00	188, 700, 876	100.00	99.65	0.66	24.2
								188, 700, 876	99.99	99.60	0.67	24.4
8.00	8.00	8.00	8.00	6.00	7.00	8.00	7.00	190, 240, 360, 480, 490, 700, 860	99.94	99.35	1.56	52.4
10.00	10.00	10.00	10.00	10.00	10.00	10.00	10.00	190, 240, 360, 480, 490, 700, 860	92.62	93.00	1.67	51.4

Column header spanning "Tolerances (%)" covers ε_1/L_1^0 through ε_8/C_8^0.

CDC time for selecting frequency points = 7.65 sec

*   This time includes the linearization time

** 2000 points were used in Monte Carlo (M.C.) analyses with the nonlinear constraints

The problem is equivalent to 2^8 disjoint orthotopes. The results are shown in Table 7.3 and are contrasted with the Monte Carlo method.

7.3.3 The Normal Distribution

The joint probability distribution function of a normal distribution is (Neuts 1973)

$$F(\underset{\sim}{\phi}) = \frac{1}{(2\pi)^{k/2}} \frac{1}{\sqrt{|\text{COV}|}} \exp\left[-\frac{1}{2} (\underset{\sim}{\phi}-\underset{\sim}{\phi}^0)^T (\text{COV})^{-1} (\underset{\sim}{\phi}-\underset{\sim}{\phi}^0)\right] \ ,$$

where k is the number of parameters, $\underset{\sim}{\phi}^0$ is the vector of mean values of the parameter vector $\underset{\sim}{\phi}$ and $\underset{\sim}{\text{COV}}$ is the covariance matrix.

If the parameters are uncorrelated, $\underset{\sim}{\text{COV}}$ is a diagonal matrix given by

$$\underset{\sim}{\text{COV}} = \begin{bmatrix} \sigma_1^2 & & & & \\ & \sigma_2^2 & & & \\ & & \ddots & & \\ & & & \ddots & \\ & & & & \sigma_k^2 \end{bmatrix} \ ,$$

where σ_i is the standard deviation of the ith parameter. Hence,

TABLE 7.3

COMPARISON WITH THE MONTE CARLO ANALYSIS FOR
BIMODAL DISTRIBUTION

$\dfrac{\phi_i - \phi_i^0}{\phi_i^0}$ (%)	Yield (%)		CDC Time (sec)	
	Approx.	M.C.	Approx.	M.C.
[-10,-5], [5,10]	68.9	71.0	4.9	.45.6

Frequency points used are 190, 240, 360, 480, 490, 700 and 860 Hz

$$F(\underset{\sim}{\phi}) = \frac{1}{(2\pi)^{k/2}} \frac{1}{\prod\limits_{i=1}^{k} \sigma_i} \exp\left(-\sum_{i=1}^{k} (\phi_i - \phi_i^0)^2 / 2\sigma_i^2\right).$$

The distribution was discretized in the interval $(\phi_i^0 - 2\sigma_i, \phi_i^0 + 2\sigma_i)$ for each parameter into three equal subintervals. The weights were obtained in the following manner. Let (Abramowitz and Stegun 1965)

$$I_1 = \frac{1}{2\pi\sigma_i} \int_{\phi_i^0 - 2\sigma_i}^{\phi_i^0 - 2\sigma_i/3} \exp\left(-(\phi_i - \phi_i^0)^2 / 2\sigma_i^2\right) d\phi_i = 0.2298,$$

$$I_2 = \frac{1}{2\pi\sigma_i} \int_{\phi_i^0 - 2\sigma_i/3}^{\phi_i^0 + 2\sigma_i/3} \exp\left(-(\phi_i - \phi_i^0)^2 / 2\sigma_i^2\right) d\phi_i = 0.4950,$$

$$I_3 = \frac{1}{2\pi\sigma_i} \int_{\phi_i^0 + 2\sigma_i/3}^{\phi_i^0 + 2\sigma_i} \exp\left(-(\phi_i - \phi_i^0)^2 / 2\sigma_i^2\right) d\phi_i = 0.2298.$$

Considering a probability of unity for finding ϕ_i in the interval $(\phi_i^0 - 2\sigma_i, \phi_i^0 + 2\sigma_i)$, i.e., a truncated distribution, the weights for each interval are given by

$$w_i(1) = 0.2298/(I_1 + I_2 + I_3) = 0.2407,$$

$$w_i(2) = 0.4950/(I_1 + I_2 + I_3) = 0.5186,$$

$$w_i(3) = 0.2298/(I_1 + I_2 + I_3) = 0.2407.$$

Fig. 7.2 shows the truncated and the discretized normal distributions.

The yields obtained are shown in Table 7.4. Equal standard deviations for the eight parameters and for two values, namely, 5% and 6% of the nominal values were considered.

Table 7.5 shows the execution times and the resulting yields for different numbers of Monte Carlo analyses applied to the linearized constraints. As expected, the yield is affected by changing the number of Monte Carlo analyses.

7.4   Discussion

Excellent agreement with the Monte Carlo method validates the yield estimates obtained. Thus, a rough solution to a worst-case centering and tolerance assignment problem which provides critical regions for approximating the boundary of the constraint region can be recommended. This allows only essential constraints to be considered and justifies a worst-case solution even if less than 100% yield is subsequently contemplated.
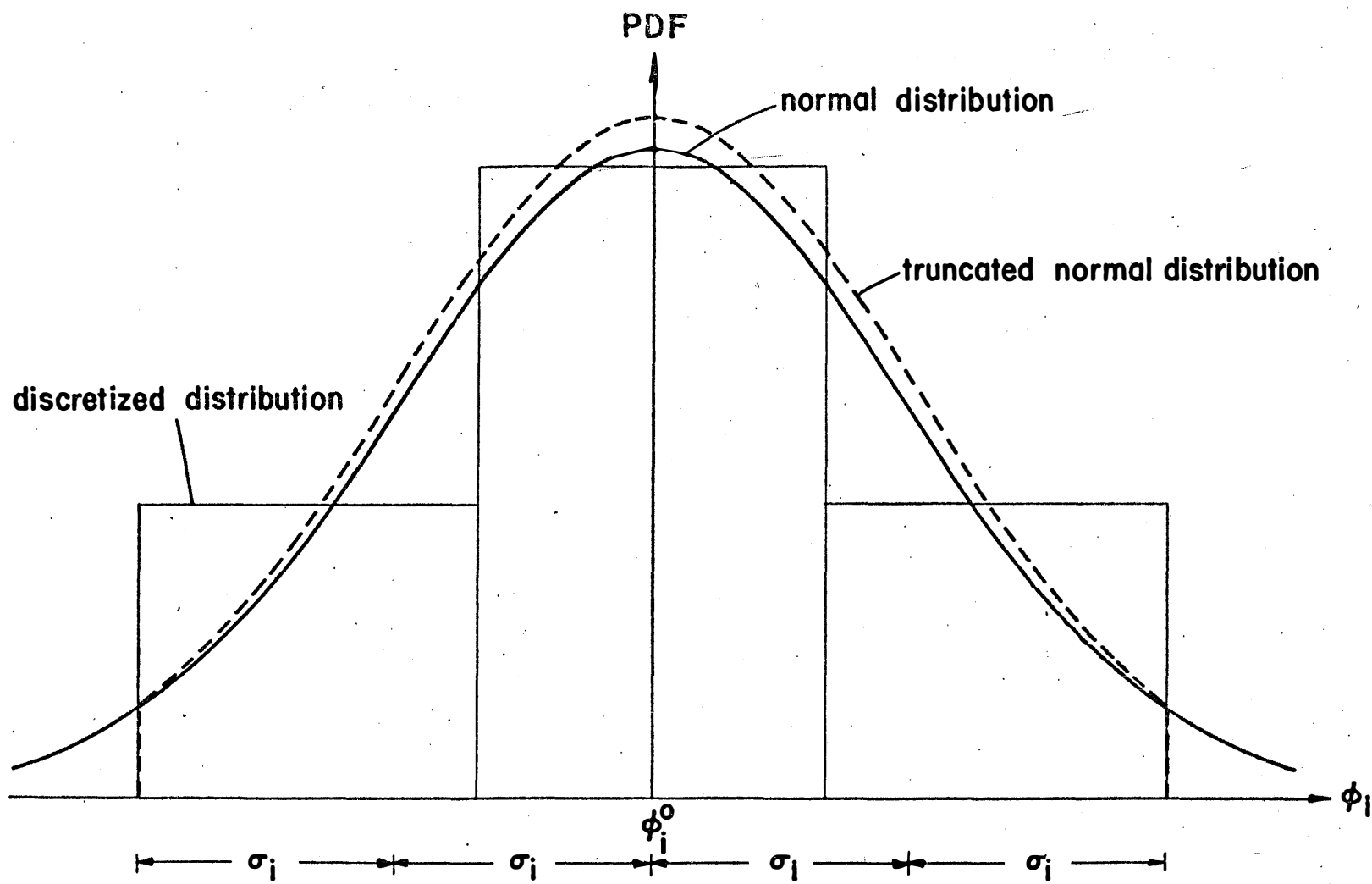
Fig. 7.2   Normal distribution, truncated normal distribution and discretized normal distribution.

TABLE 7.4

COMPARISON WITH MONTE CARLO ANALYSIS FOR
NORMALLY DISTRIBUTED COMPONENTS

$\dfrac{\sigma_i}{\phi_i^0}$ (%)	Yield (%)		CDC Time (sec)	
	Approx.	M.C.	Approx.	M.C.
5.0	96.5	95.1	4.9	69.2
6.0	88.4	87.0	7.4	68.0

TABLE 7.5

EFFECT OF NUMBER OF MONTE CARLO ANALYSES ON THE YIELD
BASED UPON THE LINEARIZED CONSTRAINTS

$\dfrac{\sigma_i}{\phi_i^0}$ (%)	N.O.M.P.*	Yield (%)	CDC Time (sec)
5.0	2000	94.4	24.6
	500	94.2	7.0
	200	91.5	2.8
6.0	2000	86.6	24.3
	500	85.2	6.9
	200	84.0	2.8

* N.O.M.P. denotes the number of Monte Carlo points used

PART II

WORST-CASE DESIGN

7.5   Two-section Waveguide Transformer

The two-section waveguide transformer, investigated for a minimax (equal-ripple) response by Bandler (1969), was selected to perform a tolerance assignment. The general configuration of such a structure is illustrated in Fig. 7.3. A design specification of a reflection coefficient of 0.05 over 500 MHz bandwidth centered at 6.175 GHz was chosen. Table 7.6 shows the dimensions of the input and output waveguides and the widths of the two sections.

The program developed by Bandler and Macdonald (1969b) is used to obtain the reflection coefficient. No sensitivities are provided by this program. An equal absolute tolerance ε is assumed for the heights and the lengths of the two sections. The assumption seems reasonable if they are machined in the same manner.

The objective is to maximize the absolute tolerance ε. The optimum nominal point and associated tolerance, given in Table 7.7, were obtained by the worst-case design algorithm presented in Section 6.2. The program FLOPT4 (Bandler and Sinha 1977) was used for solving the nonlinear program:

$$\text{maximize } \varepsilon$$

subject to

$$R_v \subseteq R_c \ .$$

137
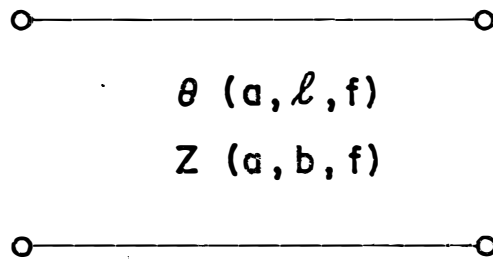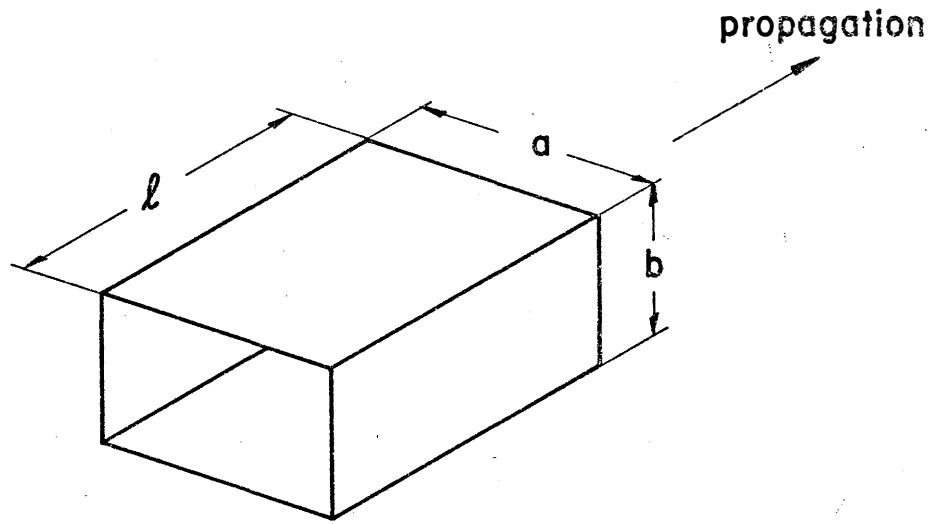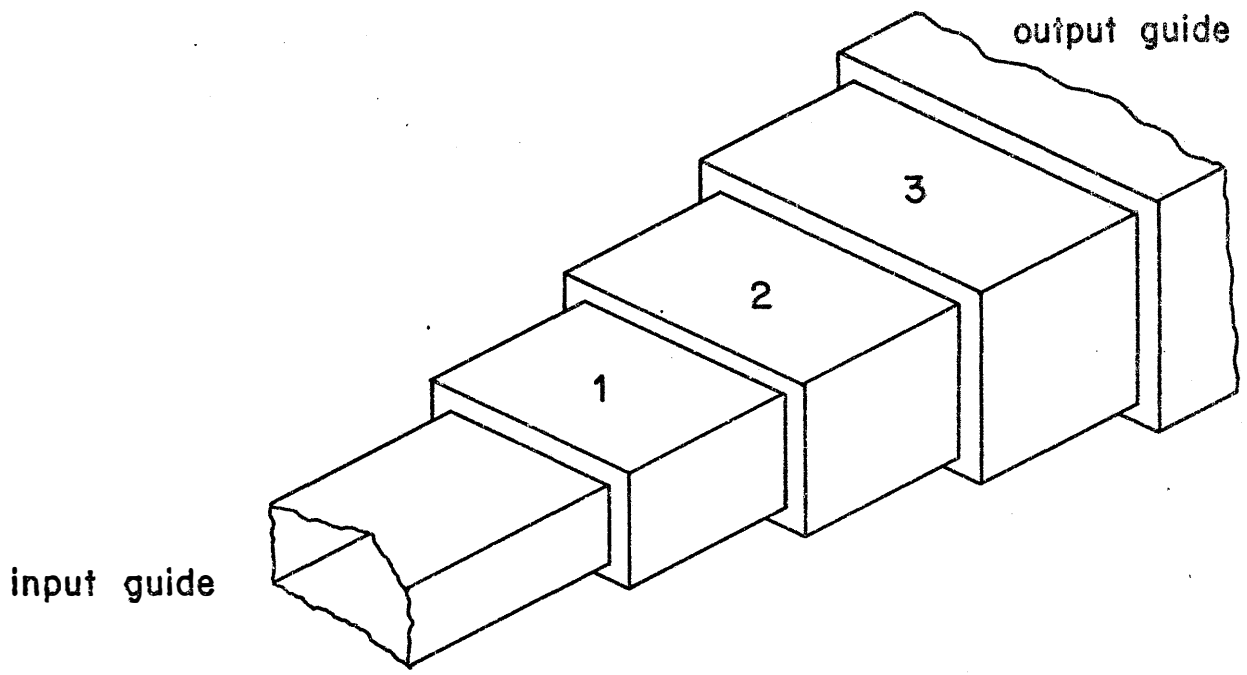
Fig. 7.3   Illustrations of an inhomogeneous waveguide transformer.

TABLE 7.6

FIXED PARAMETERS AND SPECIFICATIONS FOR THE
TWO-SECTION WAVEGUIDE TRANSFORMER

Description	Width (cm)	Height (cm)	Length (cm)
Input guide	3.48488	0.508	∞
First section	3.6	variable	variable
Second section	3.8	variable	variable
Output guide	4.0386	2.0193	∞

Frequency points used 5.925, 6.175, 6.425 GHz

Reflection coefficient specification $|\rho| \leq 0.05$

Minimax solution (no tolerances) $|\rho| = 0.00443$

TABLE 7.7

RESULTS CONTRASTING THE TOLERANCED SOLUTION AND
THE MINIMAX SOLUTION WITH NO TOLERANCES FOR THE
TWO-SECTION WAVEGUIDE TRANSFORMER

Description	b_1 (cm)	b_2 (cm)	ℓ_1 (cm)	ℓ_2 (cm)
Toleranced optimum	0.72812	1.42432	1.55409	1.51153
Minimax optimum	0.71315	1.39661	1.56044	1.51621

Equal absolute value of tolerance = 0.02013 cm

Number of complete response evaluations = 45

CDC time (approximation and optimization) = 33 s

Due to ill conditioning, early results (Bandler and Abdel-Malek 1977a) were not the best possible. Shifting by a constant value the level of all functions involved in the minimax formulation, a tolerance of 0.02013 cm was obtained. The number of actual response evaluations to reach the optimum starting from the minimax optimum (no tolerances) is shown in Table 7.7. The execution time shown includes both approximation and optimization times.

The minimax, nominal and the upper envelope of worst-case responses are shown in Fig. 7.4. The numbering scheme of the vertices is that given by (2.9) with the parameter vector

$$\phi = \begin{bmatrix} b_1 \\ b_2 \\ \ell_1 \\ \ell_2 \end{bmatrix}.$$

Vertices which fall within the worst-case upper envelope are not indicated in Fig. 7.4. It was observed, however, that vertices 2, 6, 10 and 14 are either active or almost active w.r.t. the reflection coefficient constraint at band center. Furthermore, vertices 3, 7, 11 and 15 are either active or almost active near the band extremes. Hence, when b_1 is at its positive extreme while b_2 at its negative extreme, the frequency point at the center of the band is more likely to be violated. The edges of the band are critical frequency points when b_1 is at its negative extreme while b_2 is at its positive extreme.

Retaining the approximations obtained by the worst-case design
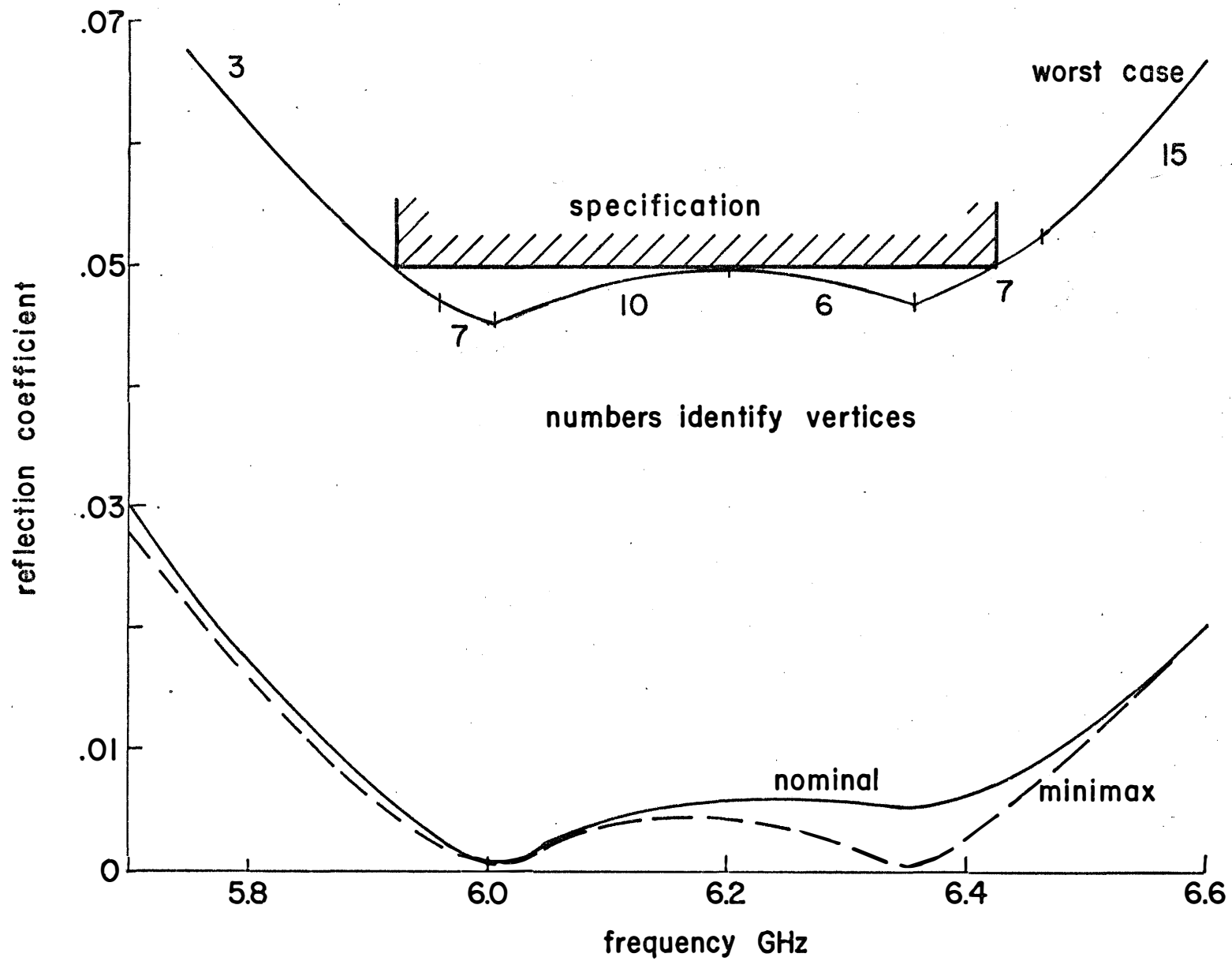
Fig. 7.4   Nominal, minimax and upper envelope of worst-case

responses for the two-section waveguide transformer.

procedure subsequently facilitates inexpensive Monte Carlo analyses. Hence, different statistical distributions of outcomes may be assumed and estimates of corresponding yields obtained. Assuming ε = 0.03 cm, for example, while keeping the worst-case nominal obtained, 500 uniformly distributed Monte Carlo analyses were conducted with the approximation and with the actual functions. The approximation yields excellent results 12 times faster as shown in Table 7.8.

7.6   Three-section Waveguide Transformer

The three-section transformer with ideal junctions for which a minimax optimum was obtained by Bandler (1969) is considered for tolerance assignment. Specifications and dimensions of input and output waveguides are given in Table 7.9.

Nonideal junctions were assumed and the widths of the three sections were fixed for convenience, so that the step changes are equal from one section to the next. An equal tolerance in the heights and lengths of the three sections was maximized for the reason given in Section 7.5.

Starting at the minimax optimum with equal steps of 0.02 for the interpolation region the results shown in Table 7.10 were obtained. The program FLOPT4 (Bandler and Sinha 1977) was used for solving the nonlinear programming problem formulated for the worst-case design. Fig. 7.5 shows the upper envelope of worst-case responses as well as the nominal design response. Although the envelope shows one vertex which is active at the lower frequency edge of the band, several other adjacent vertices, which restricted the increase in tolerance, are

TABLE 7.8

COMPARISON OF METHODS OF YIELD ESTIMATION FOR THE
TWO-SECTION WAVEGUIDE TRANSFORMER

Number of points	Tolerance ε	Yield(%)		CDC Time (sec)	
		Approx.	Actual	Approx.	Actual
500	0.03	87.6	88.6	0.4	5

TABLE 7.9

FIXED PARAMETERS AND SPECIFICATIONS FOR THE
THREE-SECTION WAVEGUIDE TRANSFORMER

Description	Width (cm)	Height (cm)	Length (cm)
Input guide	3.48488	0.762	∞
First section	3.30581	variable	variable
Second section	3.12674	variable	variable
Third section	2.94767	variable	variable
Output guide	2.76860	1.60325	∞

Frequency points used 5.7, 6.1, 6.45, 6.8, 7.2 GHz

Reflection coefficient specification $|\rho| \leq 0.050$ (nonideal junctions)

Minimax solution (no tolerances) $|\rho| = 0.017$ (ideal junctions)

TABLE 7.10

RESULTS CONTRASTING THE TOLERANCED SOLUTION AND THE MINIMAX SOLUTION
WITH NO TOLERANCES FOR THE THREE-SECTION WAVEGUIDE TRANSFORMER

Description	b_1 (cm)	b_2 (cm)	b_3 (cm)	ℓ_1 (cm)	ℓ_2 (cm)	ℓ_3 (cm)
Toleranced optimum	0.91034	1.36526	1.70189	1.45242	1.53875	1.63253
Minimax optimum	0.90318	1.37093	1.73609	1.54879	1.58375	1.64590

Equal absolute value of tolerance = 0.01383 cm

Number of complete response evaluations = 56

CDC time (approximation and optimization) = 167 s
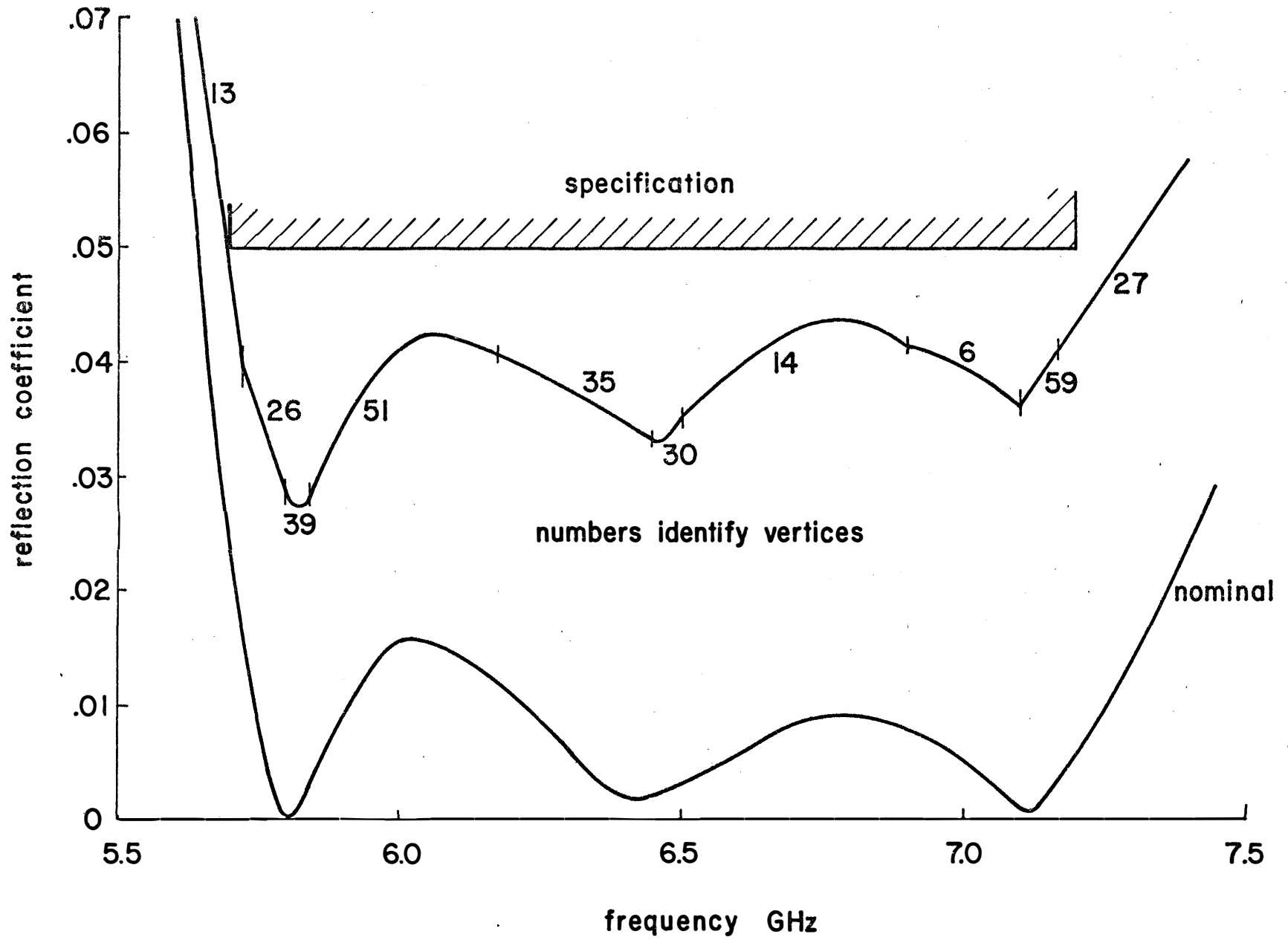
Fig. 7.5   Nominal and upper envelope of worst-case responses

for the three-section waveguide transformer.

almost active. This appears to explain the fact that the envelope is substantially lower than the specification at other frequencies.

In order to show the benefits of retaining the approximations developed by the worst-case design algorithm, a Monte Carlo analysis was conducted with the actual functions and with the approximations. An equal tolerance of 0.02 cm was assumed around the worst-case nominal design and 500 uniformly distributed points were generated. The resulting yields and execution times are contrasted in Table 7.11.

7.7 Discussion

Optimal assignment of tolerances on the physical dimensions of multisection inhomogeneous waveguide transformers has been successfully investigated. It is evident how the design centering scheme provides reliable approximations facilitating subsequent inexpensive statistical analyses.

A check on the goodness of an approximation at each frequency point considered was done by comparing it with the final actual worst-case response. An agreement of at least three significant figures was obtained in these transformer examples, which is well suited to current fabrication and measurement capabilities for these waveguide structures.

TABLE 7.11

COMPARISON OF METHODS OF YIELD ESTIMATION FOR
THE THREE-SECTION WAVEGUIDE TRANSFORMER

Number of points	Tolerance ε	Yield (%)		CDC Time (sec)	
		Approx.	Actual	Approx.	Actual
500	0.02	96.4	96.0	1	11.5

PART III

YIELD OPTIMIZATION

7.8   Optimal Design of a Nonlinear Switching Circuit

Statistical design is applied to a current switch emitter follower (CSEF) circuit which was previously investigated by Ho (1971) in the context of sensitivity calculations.

The circuit is shown in Fig. 7.6.   The decoupled equivalent circuit of the transmission line is used (Calahan 1972).   Considering a lossless transmission line and the charge-control model of the transistors as well as the diode the circuit is shown in Fig. 7.7.   The following two equations are used for the transmission line model.

$$u_i(t) = [e_0(t-\tau) + Z_0 \, i_0(t-\tau)] \, U(t-\tau) + \Phi_i(t),$$

$$u_r(t) = [e_\ell(t-\tau) + Z_0 \, i_\ell(t-\tau)] \, U(t-\tau) + \Phi_r(t),$$

where Z_0 and τ are the characteristic impedance and the delay time of the transmission line, respectively, U is the step function given by

$$U(t-\tau) = \begin{cases} 0 & t < \tau, \\ 1 & t \geq \tau. \end{cases}$$

The parameter Φ represents the initial voltage distribution stored on the transmission line.   Thus, we take

$$\Phi_i(t) = \Phi_r(t) = 0 \quad \text{for } t \geq \tau.$$

150
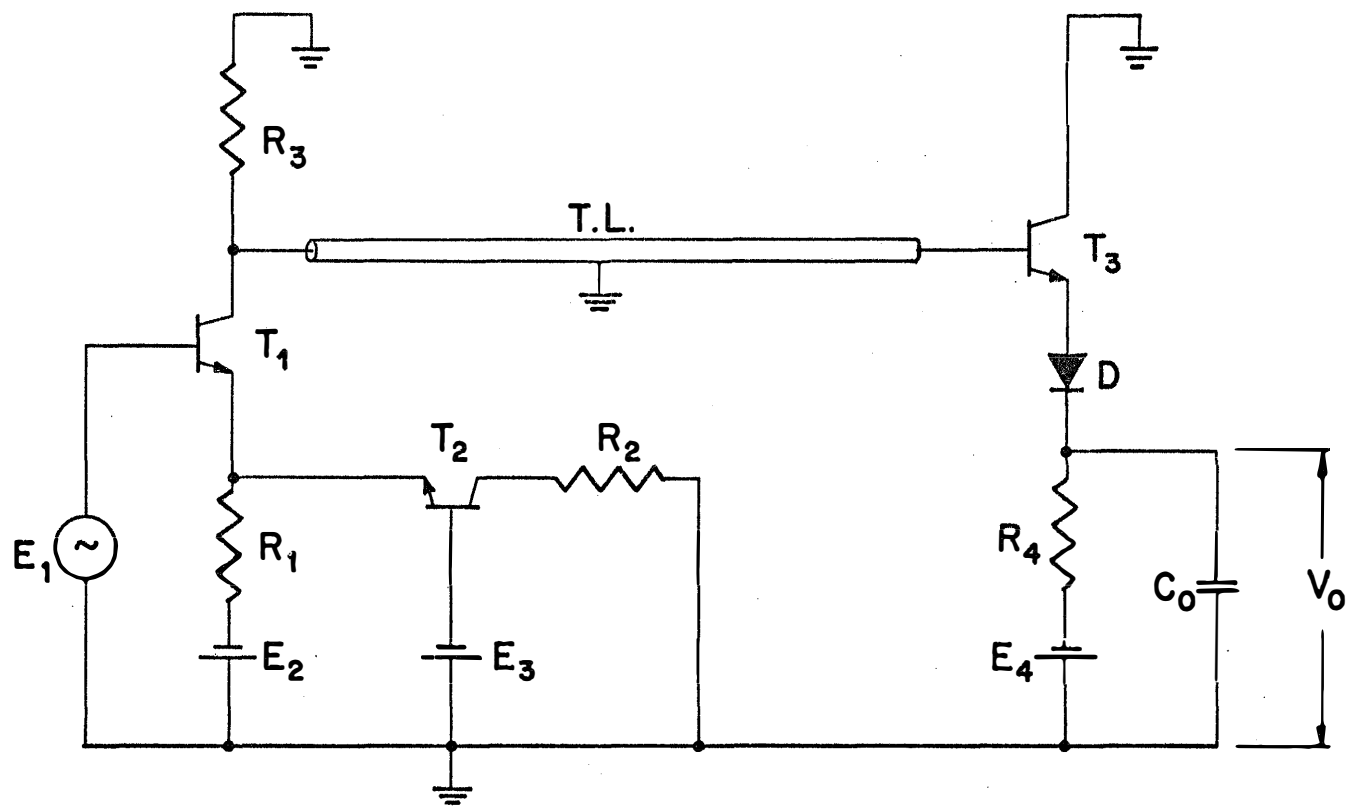
Fig. 7.6   The CSEF circuit (Ho 1971).
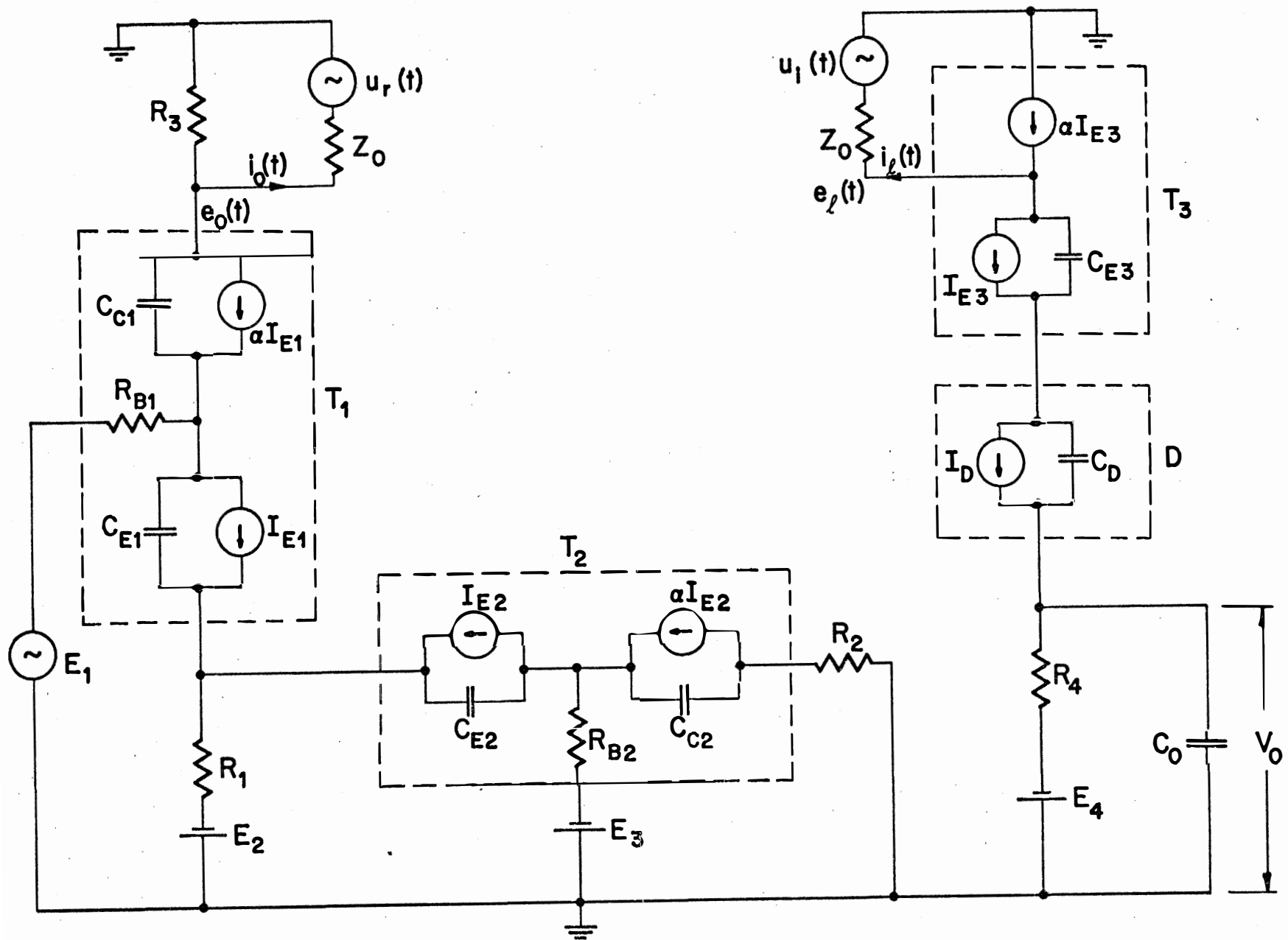
Fig. 7.7   The CSEF equivalent circuit used, indicating transmission-line, transistor and diode models.

The original circuit parameters and model parameters are given in Table 7.12. The state equations are formulated as described in Appendix A.

The Subroutine DVOGER (IMSL Library 1975), based on Gear's integration algorithm (Gear 1971a), was used. The algorithm has a variable step and hence interpolation was used to find the values of $u_i(t)$ and $u_r(t)$ if $t - \tau$ falls between time steps. Alternatively, τ/n, where n is an integer can be used as a fixed step, however, integration will be expensive.

7.9 Worst-case Design of the CSEF

The parameter vector considered for a worst-case design (see Fig. 7.7) is

$$\underline{\phi} = \begin{bmatrix} E_4 \\ Z_0 \\ R_4 \\ C_0 \end{bmatrix}.$$

The corresponding tolerances are denoted by ε_1, ε_2, ε_3 and ε_4. Fig. 7.8 shows the input voltage E_1 and the time point constraints used. The response obtained with the parameter values in Table 7.12 are also shown. The circuit is initially at equilibrium with $E_1 = -0.776$ V.

The optimal worst-case nominal parameters and tolerances are shown in Table 7.13. Two approximations according to Phase 1 of the worst-case design algorithm (Subsection 6.2.1) were required and hence 30 response evaluations. The nominal design response as well as the

TABLE 7.12(a)

CIRCUIT PARAMETER VALUES

R_1	281.33 Ω
R_2	75.00 Ω
R_3	78.24 Ω
R_4	50.00 Ω
E_2	4.03 V
E_3	1.13 V
E_4	1.70 V
C_0	1.50 pF

TABLE 7.12(b)

DIODE MODEL PARAMETERS

I_{SD}	diode saturation current	0.6×10^{-9} A
C_{JD}	depletion layer capacitance	0.12 pF
TT_D	transit time	0.01 ns
θ	inverse of thermal potential	38.668 V^{-1}

$$I_D = I_{SD}(\exp(\theta V_D)-1)$$

$$C_D = C_{JD} + TT_D \frac{dI_D}{dV_D}$$

TABLE 7.12(c)

TRANSISTOR MODEL PARAMETERS

I_S	saturation current	0.6×10^{-9} A
α	common base current gain	0.99
R_B	base resistance	50.0 Ω
C_C	collector junction capacitance	0.5 pF
C_{JE}	emitter junction depletion layer capacitance	0.12 pF
TT	base transit time	0.01 ns
θ	inverse of thermal potential	38.668 V^{-1}

$$I_E = I_S \ (\exp(\theta V_{BE}) - 1)$$

$$I_C = \alpha \ I_E$$

$$C_E = C_{JE} + TT \ \frac{dI_E}{dV_{BE}}$$

R_B and C_C are assumed zero for transistor T_3

TABLE 7.12(d)

TRANSMISSION LINE PARAMETERS

Z_0	characteristic impedance	50 Ω
τ	delay time	0.25 ns
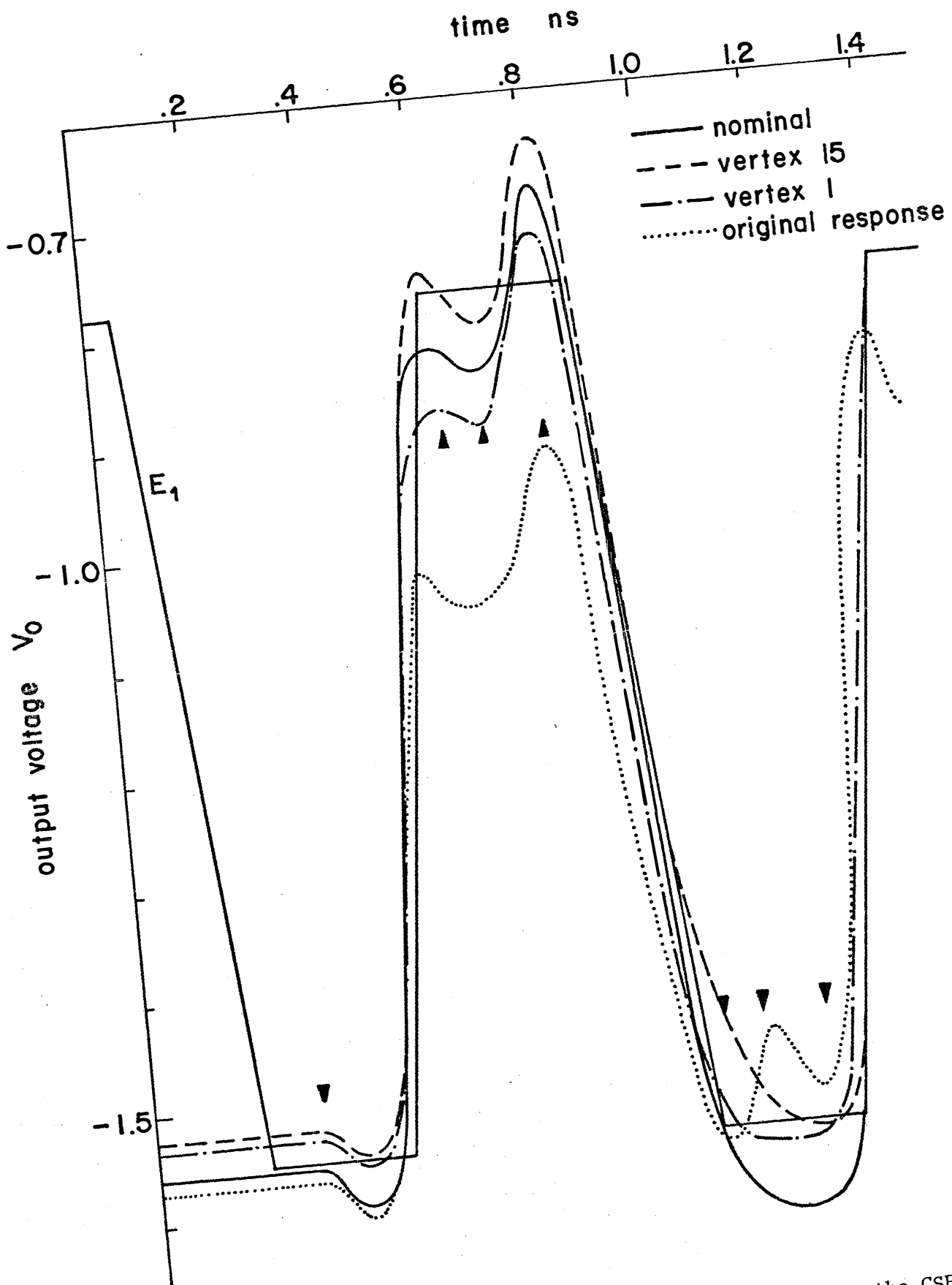
Fig. 7.8   Original, nominal and worst-case responses for the CSEF.

TABLE 7.13

WORST-CASE DESIGN FOR THE CSEF CIRCUIT

E_4^0 (V)	Z_0^0 (Ω)	R_4^0 (Ω)	C_0^0 (pF)	ε_1/E_4^0 (%)	ε_2/Z_0^0 (%)	ε_3/R_4^0 (%)	ε_4/C_0^0 (%)
1.655	92.004	45.533	1.248	4.46	8.29	13.77	14.00

Objective cost function $\displaystyle\sum_{i=1}^{4} \phi_i^0/\varepsilon_i$

Number of complete response evaluations = 30

CDC modeling time = 48 s

CDC time (approximation and optimization) = 103 s

responses for the active vertices are also shown in Fig. 7.8. The output capacitor C_0 was constrained such that

$$C_0^0 - \varepsilon_4 \geq 1.0 \text{ pF.}$$

This constraint was designed to prevent an unrealistic nominal value.

7.10   Statistical Design of the CSEF

The output section of the CSEF circuit was optimally designed to provide maximum yield. The statistical distributions of the circuit parameters and the transistor model parameters were assumed to be fixed. The nominal values of the output circuit parameters were optimized in order to obtain maximum yield.

The statistical distributions of the transistor T_3 model parameters are based upon results published by Butler (1974) and by Balaban and Golembeski (1975). The transistor current gain β was assumed to have a triangular probability distribution function with a peak at $\beta = 60$ and $40 \leq \beta \leq 100$. Correlation between transistor model parameters (see Table 7.12(c)) was established according to the following equations

$$I_S = 0.0061 \, \beta \, (1 + 0.3516 \, X_{r1}) \times 10^{-9} \text{ A },$$
$$C_{JE} = (0.144 - 0.242 \times 10^{-3}\beta) \, (1 + 0.2 \, X_{r2}) \text{ pF },$$
$$TT = 0.01 \, (1 + 0.2 \, X_{r3}) \text{ ns,}$$

where X_{ri} are independent uniformly distributed random numbers over the

range

$$-1 \leq X_{ri} \leq 1, \quad i = 1, 2, 3.$$

The numerical coefficients in each of these equations were obtained by preserving the ratios of the corresponding coefficients of Balaban and Golembeski (1975) and, at the same time, ensuring that they lead to the same nominal values we have. According to these distributions the weights and intervals for the discretized distribution were determined and are shown in Table 7.14.

The circuit parameters were assumed to have the distributions

$$E_4 = E_4^0 + 0.1632 \, X_{r4} \, ,$$
$$Z_0 = Z_0^0 + 9.5 \, X_{r5} \, ,$$
$$R_4 = R_4^0 + 4.4 \, X_{r6} \, ,$$
$$C_0 = C_0^0 + 0.27 \, X_{r7} \, ,$$

where, again,

$$-1 \leq X_{ri} \leq 1 \, , \quad i = 4, 5, 6, 7 \, .$$

The yield was maximized and constraints on the output capacitance C_0 as well as on the transmission line characteristic impedance were introduced. These constraints are

$$C_0^0 \geq 1.27 \text{ pF} \, ,$$

TABLE 7.14

RESULTING WEIGHTS DUE TO CORRELATION BETWEEN β, I_S AND C_{JE}

β		α*		I_S $\varepsilon_{I_S,i}^{**} = 0.221 \times 10^{-9}$A			C_{JE} $\varepsilon_{C_{JE},i}^{**} = 0.0218$ pF		
$\varepsilon_{\beta,i_\beta}$	w	$\varepsilon_{\alpha,i_\alpha}$	w	w_1	w_2	w_3	w_1	w_2	w_3
20.0	0.3333	0.0080	0.3333	0.8320	0.1680	0.0000	0.2345	0.4084	0.3571
20.0	0.5000	0.0041	0.5000	0.3599	0.6113	0.0288	0.3174	0.4258	0.2568
20.0	0.1667	0.0024	0.1667	0.0744	0.5731	0.3525	0.4059	0.4472	0.1469

* $\alpha = \beta/(\beta+1)$

**   Equal intervals for I_S and C_{JE} are considered

Lower extremes of the parameters are $\beta = 40.0$, $\alpha = 0.9756$, $I_S = 0.1582 \times 10^{-9}$A

and $C_{JE} = 0.0958$ pF

$$Z_0^0 \leq Z_{0u} \ ,$$

where Z_{0u} is an upper bound on the characteristic impedance of the transmission line. The specifications considered are

$$V_0(t) \leq -1.45 \text{ V}, \quad t = 0.3 \text{ ns},$$

$$V_0(t) \geq -0.85 \text{ V}, \quad t = 0.62, 0.69, 0.8 \text{ ns },$$

$$V_0(t) \leq -1.40 \text{ V}, \quad t = 1.02, 1.09, 1.2 \text{ ns }.$$

According to these specifications and the assumed statistical distributions the yield was maximized allowing the nominal parameter vector

$$\phi_{\sim} = \begin{bmatrix} E_4^0 \\ Z_0^0 \\ R_4^0 \\ C_0^0 \end{bmatrix}$$

to vary. The yield and yield sensitivities were obtained using linear cuts obtained from the quadratic approximations as described in Subsection 4.8.2. The interpolation region size and center are shown in Table 7.15.

The results obtained for two different upper bounds on the characteristic impedance Z_0 are shown in Table 7.16. In order to check the results, 1000 Monte Carlo points were generated according to the assumed statistical distribution in conjunction with the quadratic approximations. The resulting yields are also tabulated in Table 7.16.

TABLE 7.15

INTERPOLATION REGION SIZE AND CENTER

FOR THE CSEF EXAMPLE

	E_4 (V)	Z_0 (Ω)	R_4 (Ω)	C_0 (pF)	α_3	I_{S3} (10^{-9}A)	C_{JE3} (pF)	TT_3 (ns)
$\overline{\phi}$	1.632	95.0	44.0	1.35	0.98285	0.49135	0.1285	0.0100
$\underset{\sim}{\delta}$	0.170	15.0	10.0	0.45	0.00786	0.34400	0.0380	0.0025

TABLE 7.16

RESULTS FOR THE MAXIMIZATION OF YIELD

FOR THE CSEF CIRCUIT

Description	E_4^0 (V)	Z_0^0 (Ω)	R_4^0 (Ω)	C_0^0 (pF)	Optimization time (sec)	Yield (%)	
						Linear cut	M.C.
Starting values	1.632	95.00	44.00	1.35	-	25.7	39.4
Optimum for $Z_{0u} = 100$ Ω	1.595	100.00	51.15	1.27	67.8	58.6	68.9
Optimum for $Z_{0u} = 105$ Ω	1.638	105.00	53.07	1.27	40.6	85.6	89.1

CDC modeling time = 74 s

CDC time required for M.C. employing approximation ≃ 5 s

7.11   Discussion

It has been indicated that constraints may be required to bound the nominal parameter values.   Otherwise, unrealistic parameter values can be obtained, for example, zero output capacitance.

For the worst-case design obtained the power dissipated in the output circuit is 0.1854 mW at the nominal solution.   It is 0.365 mW for the original design at equilibrium when $E_1 = -0.776$.   This saves power and limits fluctuations in chip temperature.

Other integration techniques, different from Gear's method, were tried for simulating the circuit response.   It seems that the state equations we have are stiff differential equations and hence the Runge-Kutta and Adams methods were not successful (Gear 1971b, Chua and Lin 1975).

A single interpolation region was found to be satisfactory.   The difference between the predicted responses at vertices according to the approximations and the actual responses subsequently checked by integration was, over the sample points used, less than 2%.   A Monte Carlo analysis was not conducted with the response calculated by integration since each such simulation on a CDC 6400 computer takes about 1.7 execution seconds.

CHAPTER 8

CONCLUSIONS

In this thesis, the problem of design centering, tolerancing and tuning for both restricted and unrestricted production yield have been considered. The equivalent tolerance problem allows us to deal only with the optimal assignment of design tolerances. The concept of a tunable constraint region, resulting from the equivalent tolerance problem, permits the estimation of production yield by calculating weighted hypervolumes even if the design employs tunable parameters.

The analytical approach to calculating production yield facilitates the evaluation of yield sensitivities. As far as the author is aware, the only available method which provides yield sensitivities and hence permits the use of efficient optimization techniques is that presented in Chapter 4. The method is general enough to be applied with any statistical distribution and not necessarily for electrical circuits. The idea of evaluating yield based on linear cuts has been thought of independently by Spence*. In principal, the technique approximates the integration of the PDF over the constraint region or the tunable constraint region.

A multidimensional approximation procedure designed to suit the tolerance problem has been presented. The procedure not only facilitates efficient use of any simulation program but also provides

* R. Spence, Dept. of Electrical Engineering, Imperial College, London, England, private communication, April 1977.

reliable approximations to be used for calculating production yield through linear cuts. The cuts provided by the quadratic approximations are not fixed but dynamic depending upon the location of the tolerance orthotope relative to the approximate constraint boundary.

Alternative methods for evaluating production yield have been indicated. For a fixed nominal point, statistical analysis may be performed based upon fixed linear cuts or Monte Carlo analysis in conjunction with the actual constraints. The former method proved to be less expensive. If a design center is being sought use is recommended of a method which provides reliable approximations. These approximations facilitate subsequent inexpensive statistical analyses. Hence, manufacturing yield may be maximized for a fixed distribution of production outcomes or unit cost may be minimized for unrestricted yield efficiently by employing the approximations.

Promising directions for further research have been revealed by this work.

(1)   Modification of the hypervolume formula in order to obtain the exact hypervolume in the case of overlapping linear cuts inside the tolerance orthotope.

(2)   The evaluation of production yield for circuits having responses which can be expressed as biquadratic functions of the parameter of interest. Since finding the intersections of these responses with the orthotope edges reduce to solving quadratic equations, linear cuts based upon these intersections as described in Subsection 4.8.1 can be obtained.

(3)   An implementation of the efficient technique for evaluating the

quadratic approximation in a discrete problem. Large savings are expected by employing the quadratic approximation in the branch and bound technique (Dakin 1966).

(4) The selection of candidates for worst cases in order to reduce the number of constraints in the nonlinear program is not yet optimally automated. Fast detection of worst cases still requires further investigation (Tromp 1977).

APPENDIX A

TOPOLOGICAL FORMULATION OF THE STATE EQUATIONS

FOR THE CSEF CIRCUIT

The basic steps required in the formulation of the state equations for nonlinear networks are sketched out. For further details see Chua and Lin (1975).

Step 1   Formation and characterization of network branches

This step involves the characterization of linear and nonlinear elements, controlled and independent sources and tree and cotree (link) branches. The choice of the tree branches is based upon

(i)   all independent and controlled voltage sources,

(ii)   as many capacitors as possible,

(iii) as many resistors as possible,

(iv)   as few inductors as possible,

(v)   no independent current sources.

Step 2   Solving the resistive nonlinear subnetwork

We solve for the voltages across the nonlinear resistors in the tree as well as the currents in the nonlinear resistors in the cotree.

Step 3   Solving the loops which include capacitors only and the cutsets which include inductors only

In this step we express the currents in the cotree

capacitors and the voltages across the tree inductors in terms of the derivatives (w.r.t. time) of the tree capacitor voltages and the cotree inductor currents. Also, they may well be functions of the derivatives of voltages of the tree independent voltage sources and derivatives of currents of cotree independent current sources (if these derivatives exist).

Step 4   Collecting relationships derived so far to formulate the state equations.

Regarding the CSEF circuit shown in Fig. 7.7, the input and output circuits can be treated independently.

A.1   Formulation of the State Equations for the Input Circuit

The tree chosen according to the priorities mentioned before is shown in Fig. A.1. According to this tree, the set of independent KCL equations is

$$\underset{\sim}{D}\,\underset{\sim}{i} = \underset{\sim}{0}\ , \tag{A.1}$$

where

$$\underset{\sim}{i} = \begin{bmatrix} \underset{\sim}{I}_{ET} \\ \underset{\sim}{I}_{CT} \\ \underset{\sim}{I}_{RT} \\ \underset{\sim}{I}_{RL} \\ \underset{\sim}{I}_{JL} \end{bmatrix}\ , \tag{A.2}$$
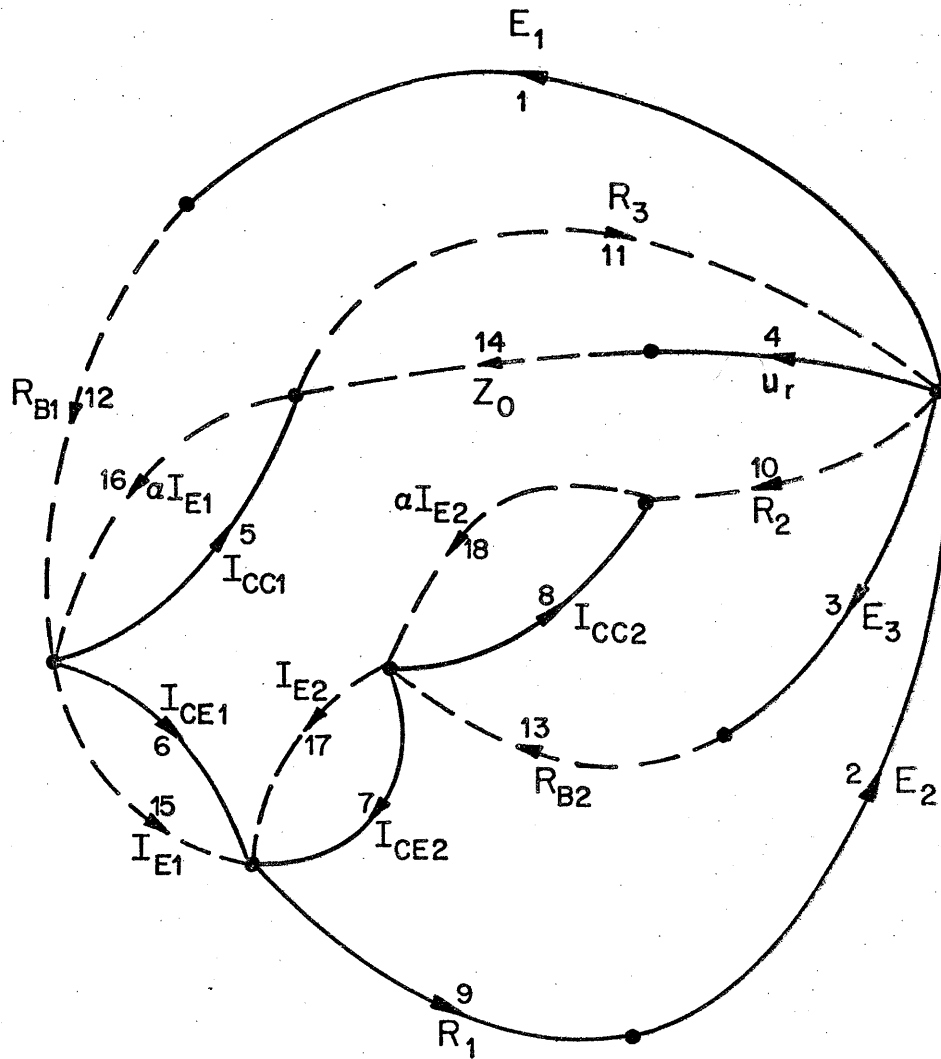
Fig. A.1   Directed graph of the input circuit and branch

numbering.

———— Tree chosen

- - - - Link

$$\underset{\sim}{I}_{ET} \overset{\Delta}{=} \text{Tree voltage source currents} = \begin{bmatrix} I_1 \\ I_2 \\ I_3 \\ I_4 \end{bmatrix} , \qquad \text{(A.3)}$$

$$\underset{\sim}{I}_{CT} \overset{\Delta}{=} \text{Tree capacitor currents} = \begin{bmatrix} I_5 \\ I_6 \\ I_7 \\ I_8 \end{bmatrix} , \qquad \text{(A.4)}$$

$$\underset{\sim}{I}_{RT} \overset{\Delta}{=} \text{Tree resistor currents} = \begin{bmatrix} I_9 \end{bmatrix} , \qquad \text{(A.5)}$$

$$\underset{\sim}{I}_{RL} \overset{\Delta}{=} \text{Link resistor currents} = \begin{bmatrix} I_{10} \\ I_{11} \\ I_{12} \\ I_{13} \\ I_{14} \end{bmatrix} , \qquad \text{(A.6)}$$

$$\underset{\sim}{I}_{JL} \overset{\Delta}{=} \text{Link current sources} = \begin{bmatrix} I_{15} \\ I_{16} \\ I_{17} \\ I_{18} \end{bmatrix} \qquad \text{(A.7)}$$

and where

$$\underset{\sim}{D} = \left[\begin{array}{ccccc|ccccc|ccccc} 1 & & & & & & & -1 & & & & & & & \\ & 1 & & & & -1 & 1 & -1 & -1 & -1 & & & & & \\ & & \cdot & & & & & & -1 & & & & & & \\ & & & \cdot & & & & & & -1 & & & & & \\ \hline & & & & & -1 & & & 1 & & -1 & & & & \\ & & & & & & 1 & -1 & & -1 & & 1 & & & \\ & & & & & -1 & & & -1 & & & & 1 & & \\ & & & & & 1 & & & & & & & & -1 & \\ \hline & & & & 1 & -1 & 1 & -1 & -1 & -1 & & & & & \end{array} \right] . \qquad \text{(A.8)}$$

Hence, we can write (A.1) as

$$
\left[
\begin{array}{c|cc}
 & \underset{\sim}{D}_{11} & \underset{\sim}{D}_{12} \\
\underset{\sim}{\mathbb{1}}_9 & \underset{\sim}{D}_{21} & \underset{\sim}{D}_{22} \\
 & \underset{\sim}{D}_{31} & \underset{\sim}{D}_{32}
\end{array}
\right]
\left[
\begin{array}{c}
\underset{\sim}{I}_{ET} \\
\underset{\sim}{I}_{CT} \\
\underset{\sim}{I}_{RT} \\
\underset{\sim}{I}_{RL} \\
\underset{\sim}{I}_{JL}
\end{array}
\right] = \underset{\sim}{0} \ ,
\tag{A.9}
$$

where

$$
\underset{\sim}{D}_{11} =
\left[
\begin{array}{ccccc}
 & & -1 & & \\
-1 & 1 & -1 & -1 & -1 \\
 & & & -1 & \\
 & & & & -1
\end{array}
\right] ,
\tag{A.10}
$$

$$
\underset{\sim}{D}_{12} = \underset{\sim}{0} \ ,
\tag{A.11}
$$

$$
\underset{\sim}{D}_{21} =
\left[
\begin{array}{ccccc}
 & -1 & & & 1 \\
 & 1 & -1 & & -1 \\
-1 & & & -1 & \\
1 & & & &
\end{array}
\right] ,
\tag{A.12}
$$

$$
\underset{\sim}{D}_{22} =
\left[
\begin{array}{ccc}
 & -1 & \\
1 & & \\
 & 1 & \\
 & & -1
\end{array}
\right] ,
\tag{A.13}
$$

$$
\underset{\sim}{D}_{31} = [-1 \quad 1 \quad -1 \quad -1 \quad -1] \ ,
\tag{A.14}
$$

$$
\underset{\sim}{D}_{32} = \underset{\sim}{0} \ .
\tag{A.15}
$$

and $\underset{\sim}{\mathbb{1}}_9$ is the identity matrix of order 9.

The KVL equations can be written as

$$\begin{bmatrix} \underset{\sim}{D}_{11}^{T} & \underset{\sim}{D}_{21}^{T} & \underset{\sim}{D}_{31}^{T} \\ \underset{\sim}{D}_{12}^{T} & \underset{\sim}{D}_{22}^{T} & \underset{\sim}{D}_{32}^{T} \end{bmatrix} \quad -\underset{\sim}{1}_{9} \quad \end{bmatrix} \begin{bmatrix} \underset{\sim}{V}_{ET} \\ \underset{\sim}{V}_{CT} \\ \underset{\sim}{V}_{RT} \\ \underset{\sim}{V}_{RL} \\ \underset{\sim}{V}_{JL} \end{bmatrix} = \underset{\sim}{0} \; , \qquad (A.16)$$

where superscript T denotes transposition.

It is required to represent the link currents $\underset{\sim}{I}_{RL}$ in terms of $\underset{\sim}{V}_{ET}$ and $\underset{\sim}{V}_{CT}$. We have

$$\underset{\sim}{V}_{RL} = \underset{\sim}{R}_{L} \; \underset{\sim}{I}_{RL}$$

$$= \underset{\sim}{D}_{11}^{T} \; \underset{\sim}{V}_{ET} + \underset{\sim}{D}_{21}^{T} \; \underset{\sim}{V}_{CT} + \underset{\sim}{D}_{31}^{T} \; \underset{\sim}{V}_{RT} \; , \qquad (A.17)$$

where

$$\underset{\sim}{R}_{L} = \begin{bmatrix} R_{2} & & & & \\ & R_{3} & & & \\ & & R_{B1} & & \\ & & & R_{B2} & \\ & & & & Z_{0} \end{bmatrix} . \qquad (A.18)$$

Using (A.9) and (A.15) we can write

$$\underset{\sim}{I}_{RT} = -\underset{\sim}{D}_{31} \; \underset{\sim}{I}_{RL} - \underset{\sim}{D}_{32} \; \underset{\sim}{I}_{JL}$$

$$= -\underset{\sim}{D}_{31} \; \underset{\sim}{I}_{RL} \; . \qquad (A.19)$$

Thus,

$$\underset{\sim}{V}_{RT} = \underset{\sim}{R}_{T} \; \underset{\sim}{I}_{RT} = - \underset{\sim}{R}_{T} \; \underset{\sim}{D}_{31} \; \underset{\sim}{I}_{RL} \; , \qquad (A.20)$$

where

$$\underset{\sim}{R}_T = [R_1] \; .$$ (A.21)

Substituting for $\underset{\sim}{V}_{RT}$ in (A.17) and with some manipulations, we obtain

$$\underset{\sim}{I}_{RL} = \underset{\sim}{R}^{-1} [\underset{\sim}{D}_{11}^T \underset{\sim}{V}_{ET} + \underset{\sim}{D}_{21}^T \underset{\sim}{V}_{CT}] \; ,$$ (A.22)

where

$$\underset{\sim}{R} = \underset{\sim}{R}_L + \underset{\sim}{D}_{31}^T \underset{\sim}{R}_T \underset{\sim}{D}_{31} \; .$$ (A.23)

From (A.5), we have

$$\underset{\sim}{I}_{CT} = -\underset{\sim}{D}_{21} \underset{\sim}{I}_{RL} - \underset{\sim}{D}_{22} \underset{\sim}{I}_{JL} \; .$$ (A.24)

Substituting for $\underset{\sim}{I}_{RL}$ from (A.22), the state equations are

$$\underset{\sim}{I}_{CT} = -\underset{\sim}{D}_{21} \underset{\sim}{R}^{-1} [\underset{\sim}{D}_{11}^T \underset{\sim}{V}_{ET} + \underset{\sim}{D}_{21}^T \underset{\sim}{V}_{CT}] - \underset{\sim}{D}_{22} \underset{\sim}{I}_{JL} \; .$$ (A.25)

More explicitly, they can be written as

$$\begin{bmatrix} C_{C1} \ dV_{C1}/dt \\ C_{E1} \ dV_{BE1}/dt \\ C_{E2} \ dV_{BE2}/dt \\ C_{C2} \ dV_{C2}/dt \end{bmatrix} = -\underset{\sim}{D}_{21} \ \underset{\sim}{R}^{-1} \left[\underset{\sim}{D}_{11}^T \begin{bmatrix} E_1 \\ E_2 \\ E_3 \\ u_r \end{bmatrix} + \underset{\sim}{D}_{21}^T \begin{bmatrix} V_{C1} \\ V_{BE1} \\ V_{BE2} \\ V_{C2} \end{bmatrix} \right] + \begin{bmatrix} I_{16} \\ -I_{15} \\ -I_{17} \\ I_{18} \end{bmatrix} ,$$ (A.26)

where

$$C_{E1} = C_{JE} + TT \ \theta \ I_S \ \exp(\theta \ V_{BE1}) \; ,$$ (A.27)

$$C_{E2} = C_{JE} + TT \ \theta \ I_S \ \exp(\theta \ V_{BE2}) \; ,$$ (A.28)

$$I_{15} = I_S(\exp(\theta\ V_{BE1})-1)\ ,\qquad\qquad (A.29)$$

$$I_{16} = {}^\alpha I_{15}\ ,\qquad\qquad (A.30)$$

$$I_{17} = I_S(\exp(\theta\ V_{BE2})-1)\ ,\qquad\qquad (A.31)$$

$$I_{18} = {}^\alpha I_{17}\ .\qquad\qquad (A.32)$$

A.2   Formulation of the State Equations for the Output Circuit

Figure A.2 shows the chosen tree and branch numbering. The set of independent KCL equations is

$$\underset{\sim}{D}\ \underset{\sim}{i} = \underset{\sim}{0}\ ,\qquad\qquad (A.33)$$

where

$$\underset{\sim}{D} = \begin{bmatrix} 1 & & & & & -1 & & & \\ & 1 & & & & & -1 & & \\ & & 1 & & & 1 & -1 & & -1 \\ & & & 1 & & & -1 & 1 & -1 \\ & & & & 1 & -1 & & -1 & 1 \end{bmatrix}\ ,\qquad (A.34)$$

$$\underset{\sim}{i} = \begin{bmatrix} \underset{\sim}{I}_{ET} \\ \underset{\sim}{I}_{CT} \\ \underset{\sim}{I}_{RL} \\ \underset{\sim}{I}_{JL} \end{bmatrix}\ ,\qquad\qquad (A.35)$$

$$\underset{\sim}{I}_{ET} \overset{\Delta}{=} \text{Tree voltage source currents} = \begin{bmatrix} I_1 \\ I_2 \end{bmatrix}\ ,\qquad (A.36)$$
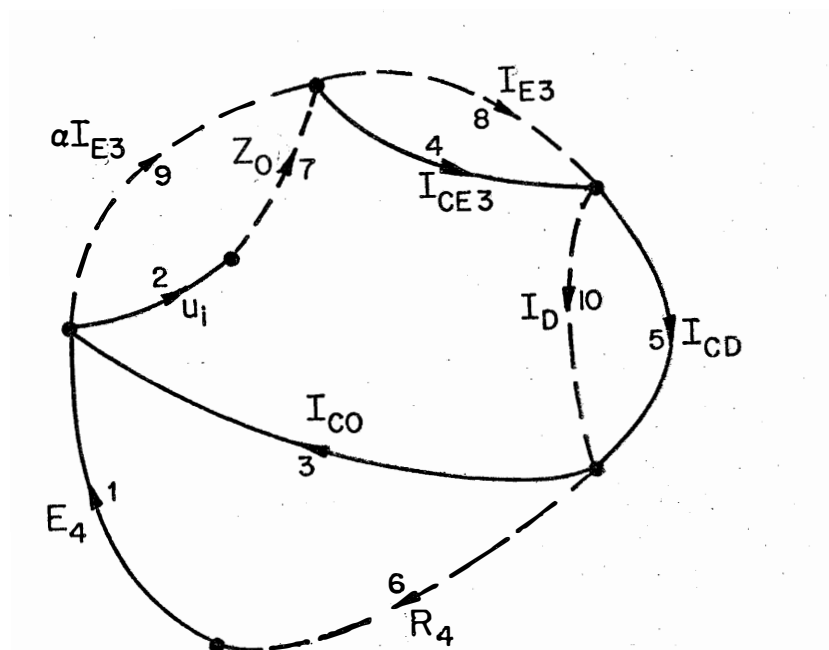
Fig. A.2   Directed graph of the output circuit and branch numbering.

——— Tree chosen

---- Link

$$\underset{\sim}{I}_{CT} \overset{\Delta}{=} \text{Tree capacitor currents} = \begin{bmatrix} \underset{\sim}{I}_3 \\ \underset{\sim}{I}_4 \\ \underset{\sim}{I}_5 \end{bmatrix} , \qquad \text{(A.37)}$$

$$\underset{\sim}{I}_{RL} \overset{\Delta}{=} \text{Link resistor currents} = \begin{bmatrix} \underset{\sim}{I}_6 \\ \underset{\sim}{I}_7 \end{bmatrix} , \qquad \text{(A.38)}$$

$$\underset{\sim}{I}_{JL} \overset{\Delta}{=} \text{Link current sources} = \begin{bmatrix} \underset{\sim}{I}_8 \\ \underset{\sim}{I}_9 \\ \underset{\sim}{I}_{10} \end{bmatrix} . \qquad \text{(A.39)}$$

The KVL equations are

$$\begin{bmatrix} -1 & & 1 & & \vdots & -1 & & & \\ & -1 & -1 & -1 & -1 & \vdots & & -1 & & \\ & & 1 & & \vdots & & & -1 & \\ & -1 & -1 & -1 & \vdots & & & & -1 \\ & & 1 & & \vdots & & & & -1 \end{bmatrix} \begin{bmatrix} \underset{\sim}{V}_{ET} \\ \underset{\sim}{V}_{CT} \\ \underset{\sim}{V}_{RL} \\ \underset{\sim}{V}_{JL} \end{bmatrix} = \underset{\sim}{0} , \qquad \text{(A.40)}$$

Hence,

$$\underset{\sim}{V}_{RL} = \underset{\sim}{R}_L \underset{\sim}{I}_{RL}$$

$$= \underset{\sim}{D}_{11}^T \underset{\sim}{V}_{ET} + \underset{\sim}{D}_{21}^T \underset{\sim}{V}_{CT} , \qquad \text{(A.41)}$$

where

$$\underset{\sim}{R}_L = \begin{bmatrix} R_4 & \\ & Z_0 \end{bmatrix} , \qquad \text{(A.42)}$$

$$\underset{\sim}{D}_{11} = \begin{bmatrix} -1 & \\ & -1 \end{bmatrix} , \qquad \text{(A.43)}$$

$$\underset{\sim}{D}_{21} = \begin{bmatrix} 1 & -1 \\ & -1 \\ & -1 \end{bmatrix} . \qquad (A.44)$$

Thus,

$$\underset{\sim}{I}_{RL} = \underset{\sim}{R}_L^{-1} \, [\underset{\sim}{D}_{11}^T \, \underset{\sim}{V}_{ET} + \underset{\sim}{D}_{21}^T \, \underset{\sim}{V}_{CT}] . \qquad (A.45)$$

From (A.33), we have

$$\underset{\sim}{I}_{ET} = -\underset{\sim}{D}_{11} \, \underset{\sim}{I}_{RL} \qquad (A.46)$$

and

$$\underset{\sim}{I}_{CT} = -\underset{\sim}{D}_{21} \, \underset{\sim}{I}_{RL} - \underset{\sim}{D}_{22} \, \underset{\sim}{I}_{JL} . \qquad (A.47)$$

Substituting for $\underset{\sim}{I}_{RL}$ from (A.45) into (A.47), the state equations are

$$\underset{\sim}{I}_{CT} = -\underset{\sim}{D}_{21} \, \underset{\sim}{R}_L^{-1} \, [\underset{\sim}{D}_{11}^T \, \underset{\sim}{V}_{ET} + \underset{\sim}{D}_{21}^T \, \underset{\sim}{V}_{CT}] - \underset{\sim}{D}_{22} \, \underset{\sim}{I}_{JL} . \qquad (A.48)$$

Or, more explicitly, the state equations are

$$\begin{bmatrix} C_0 \ dV_0/dt \\ C_{E3} \ dV_{BE3}/dt \\ C_D \ dV_D/dt \end{bmatrix} = -\underset{\sim}{D}_{21} \begin{bmatrix} 1/R_4 & \\ & 1/Z_0 \end{bmatrix} [\underset{\sim}{D}_{11}^T \ \underset{\sim}{D}_{21}^T] \begin{bmatrix} E_4 \\ u_i \\ V_0 \\ V_{BE3} \\ V_D \end{bmatrix} + \begin{bmatrix} I_9 \\ I_9 - I_8 \\ I_9 - I_{10} \end{bmatrix} , \qquad (A.49)$$

where

$$C_{E3} = C_{JE} + TT \ \theta \ I_S \ \exp(\theta \, V_{BE3}) , \qquad (A.50)$$

$$C_D = C_{JD} + TT_D \ \theta \ I_{SD} \ \exp(\theta \, V_D) , \qquad (A.51)$$

$$I_8 = I_S \ (\exp(\theta \, V_{BE3}) - 1) , \qquad (A.52)$$

$$I_9 = {}^{\alpha} I_8 , \qquad\qquad (A.53)$$

$$I_{10} = I_{SD} (\exp(\theta V_D)-1) . \qquad\qquad (A.54)$$

If the diode is similar to the transistor base emitter junction, then

$$V_D = V_{BE3} \qquad\qquad (A.55)$$

and

$$I_{10} = I_8 . \qquad\qquad (A.56)$$

Hence, the three state equations (A.49) can be reduced to the following two equations

$$
\begin{bmatrix} C_0 \ dV_0/dt \\ \\ C_{E3} \ dV_{BE3}/dt \end{bmatrix}
=
\begin{bmatrix} -1 & 1 \\ & 1 \end{bmatrix}
\begin{bmatrix} 1/R_4 & \\ & 1/Z_0 \end{bmatrix}
+
\begin{bmatrix} -1 & 1 & \\ & -1 & -1 & -2 \end{bmatrix}
\begin{bmatrix} E_4 \\ u_i \\ V_0 \\ V_{BE3} \end{bmatrix}
+
\begin{bmatrix} I_9 \\ I_9-I_8 \end{bmatrix}
. \qquad (A.57)
$$

REFERENCES

H.L. Abdel-Malek and J.W. Bandler (1977), "Yield estimation for efficient design centering assuming arbitrary statistical distributions", _Proc. Conf. on Computer Aided Design of Electronic and Microwave Circuits and Systems_ (Hull, England), pp. 66-71. Also, in _Int. J. Circuit Theory and Applications,_ accepted for publication.

M. Abramowitz and I. Stegun (1965), _Handbook of Mathematical Functions._ New York: Dover Publications.

P. Balaban and J.J. Golembeski (1975), "Statistical analysis for practical circuit design", _IEEE Trans. Circuits and Systems,_ vol. CAS-22, pp. 100-108.

J.W. Bandler (1969), "Computer optimization of inhomogeneous waveguide transformers", _IEEE Trans. Microwave Theory Tech.,_ vol. MTT-17, pp. 563-571.

J.W. Bandler (1972), "Optimization of design tolerances using nonlinear programming", _Proc. 6th Princeton Conf. Information Sciences and Systems_ (Princeton, N.J.), pp. 655-659. Also in _Computer-Aided Filter Design,_ G. Szentirmai, Ed. New York: IEEE Press, 1973.

J.W. Bandler (1974), "Optimization of design tolerances using nonlinear programming", _J. Optimization Theory and Applications,_ vol. 14, pp. 99-114.

J.W. Bandler and H.L. Abdel-Malek (1977a), "Optimal centering, tolerancing and yield determination using multidimensional approximations", _Proc. IEEE Int. Symp. Circuits and Systems_ (Phoenix, AZ), pp. 219-222.

J.W. Bandler and H.L. Abdel-Malek (1977b), "Modeling and approximation for statistical evaluation and optimization of microwave designs", _Proc. 7th European Microwave Conf._ (Copenhagen, Denmark).

J.W. Bandler, H.L. Abdel-Malek, P.B. Johns and M.R.M. Rizk (1976), "Optimal design via modeling and approximation", _Proc. IEEE Int. Symp. Circuits and Systems_ (Munich), pp. 767-770.

J.W. Bandler and C. Charalambous (1972), "Practical least pth optimization of networks", _IEEE Trans. Microwave Theory Tech.,_ vol. MTT-20, pp. 834-840.

J.W. Bandler and C. Charalambous (1974), "Nonlinear programming using minimax techniques", _J. Optimization Theory and Applications,_ vol.

13, pp. 607-619.

J.W. Bandler and P.C. Liu (1974a), "Automated network design with optimal tolerances", IEEE Trans. Circuits and Systems, vol. CAS-21, pp. 219-222.

J.W. Bandler and P.C. Liu (1974b), "The tolerance-tuning problem: a nonlinear programming approach", Proc. 12th Allerton Conf. Circuit and System Theory (Urbana, Ill.), pp. 922-931.

J.W. Bandler, P.C. Liu and J.H.K. Chen (1975), "Worst case network tolerance optimization", IEEE Trans. Microwave Theory Tech., vol. MTT-23, pp. 630-641.

J.W. Bandler, P.C. Liu and H. Tromp (1976), "A nonlinear programming approach to optimal design centering, tolerancing and tuning", IEEE Trans. Circuits and Systems, vol. CAS-23, pp. 155-165.

J.W. Bandler and P.A. Macdonald (1969a), "Cascaded noncommensurate transmission-line networks as optimization problems", IEEE Trans. Circuit Theory, vol. CT-16, pp. 391-394.

J.W. Bandler and P.A. Macdonald (1969b), "Response program for an inhomogeneous cascade of rectangular waveguides", IEEE Trans. Microwave Theory Tech., vol. MTT-17, pp. 646-649.

J.W. Bandler and D. Sinha (1977), "FLOPT4 - a program for least pth optimization with extrapolation to minimax solutions", Faculty of Engineering, McMaster University, Hamilton, Canada, Report SOC-151.

E.M. Butler (1971), "Realistic design using large-change sensitivities and performance contours", IEEE Trans. Circuit Theory, vol. CT-18, pp. 58-66.

E.M. Butler (1974), "Techniques for statistical DC modeling of bipolar transistors", Proc. IEEE Int. Symp. Circuit Theory (San Francisco), pp. 725-729.

D.A. Calahan (1972), Computer-Aided Network Design (Revised Edition). New York: McGraw Hill.

W.Y. Chu (1974), "Extrapolation in least pth approximation and nonlinear programming", M. Eng. Thesis, McMaster University.

L.O. Chua and P.M. Lin (1975), Computer-Aided Analysis of Electronic Circuits. Englewood Cliffs, NJ: Prentice-Hall.

H.S.M. Coxeter (1963), Regular Polytopes, (2nd Ed.). New York: MacMillan.

R.J. Dakin (1966), "A tree-search algorithm for mixed integer

programming problems", <u>Computer J.</u>, vol. 8, pp. 250-255.

S.W. Director (1977), University of Florida, Gainesville, Florida, private communications, April.

S.W. Director and G.D. Hachtel (1976), "The simplicial approximation approach to design centering and tolerance assignment", <u>Proc. IEEE Int. Symp. Circuits and Systems</u> (Munich), pp. 706-709.

S.W. Director and G.D. Hachtel (1977), "Yield estimation using simplicial approximation", <u>Proc. IEEE Int. Symp. Circuits and Systems</u> (Phoenix, AZ), pp. 579-582.

S.W. Director and R.A. Rohrer (1969), "Generalized adjoint network and network sensitivities", <u>IEEE Trans. Circuit Theory,</u> vol. CT-16, pp. 318-323.

N.J. Elias (1975), "New statistical methods for assigning device tolerances", <u>Proc. IEEE Int. Symp. Circuits and Systems</u> (Newton, MA) pp. 329-332.

R. Fletcher (1972), "FORTRAN subroutines for minimization by quasi-Newton methods", Atomic Energy Research Establishment, Harwell, Berkshire, Englad, Report AERE-R7125.

C.W. Gear (1971a), "The automatic integration of differential equations", <u>Comm. ACM.</u>, vol. 14, pp. 176-179.

C.W. Gear (1971b), <u>Numerical Initial Value Problems in Ordinary Differential Equations</u>. Englewood Cliffs, N.J.: Prentice-Hall.

J.M. Hammersley and D.C. Handscomb (1964), <u>Monte Carlo Methods.</u> New York: J. Wiley.

C.W. Ho (1971), "Time-domain sensitivity computation for networks containing transmission lines", <u>IEEE Trans. Circuit Theory,</u> vol. CT-18, pp. 114-122.

B.J. Karafin (1971), "The optimum assignment of component tolerances for electrical networks", <u>BSTJ,</u> vol. 50, pp. 1225-1242.

B.J. Karafin (1974), "The general component tolerance assignment problem in electrical networks", Ph.D. Thesis, Univ. of Pennsylvania, Philadelphia, PA.

M. Lee and K.L. Su (1977), "An all-tolerance multiparameter sensitivity", <u>Proc. IEEE Int. Symp. Circuits and Systems</u> (Phoenix, AZ), pp. 215-218.

K.H. Leung and R. Spence (1975), "Multiparameter large-change sensitivity analysis and systematic exploration", <u>IEEE Trans.</u>

Circuits and Systems, vol. CAS-22, pp. 796-804.

K.H. Leung and R. Spence (1976), "Efficient frequency-domain statistical circuit analysis", Proc. IEEE Int. Symp. Circuits and Systems (Munich), pp. 197-200.

K.H. Leung and R. Spence (1977), "Idealized statistical models for low-cost linear circuit yield analysis", IEEE Trans. Circuits and Systems, vol. CAS-24, pp. 62-66.

P.C. Liu (1975), "A theory for optimal worst-case design embodying centering, tolerancing and tuning, with circuit applications", Ph.D. Thesis, McMaster University.

O.L. Mangasarian (1969), Nonlinear Programming. New York: McGraw-Hill.

L.W. Nagel (1975), "SPICE2: a computer program to simulate semiconductor circuits", Electronics Research Laboratory, University of California, Berkeley, Memorandum No. ERL-M520.

M.F. Neuts (1973), Probability. Boston, MA: Allyn and Bacon.

S.M. Nikol'skii (1969), "Approximation of functions of several variables by polynomials", Siberian Math. J., vol. 10, pp. 792-799.

J.F. Pinel and K.A. Roberts (1972), "Tolerance assignment in linear networks using nonlinear programming", IEEE Trans. Circuit Theory, vol. CT-19, pp. 475-479.

J.F. Pinel and K. Singhal (1977), "Efficient Monte Carlo computation of circuit yield using importance sampling", Proc. IEEE Int. Symp. Circuits and Systems (Phoenix, AZ), pp. 575-578.

T.R. Scott and T.P. Walker (1976), "Regionalization: a method for generating joint density estimates", IEEE Trans. Circuits and Systems, vol. CAS-23, pp. 229-234.

S.L. Sobolev (1961a), "Formulas for mechanical cubatures in n-dimensional space", (transl.), Sov. Math. Dokl., vol. 2, pp. 317-320.

S.L. Sobolev (1961b), "On the interpolation of functions of n variables", (transl.), Sov. Math. Dokl., vol. 2, pp. 343-346.

M. Styblinski (1977), "Sensitivity minimization with an optimal assignment of network element tolerances", Proc. IEEE Int. Symp. Circuits and Systems (Phoenix, AZ), pp. 223-226.

Subroutine DVOGER (1975), International Mathematical and Statistical Libraries, IMSL Library 3, Edition 5, (FORTRAN) CDC 6000/7000.

H.C. Thacher, Jr. (1959), "Generalization of concepts related to linear dependence", SIAM J., vol. 6, pp. 288-299.

H.C. Thacher, Jr., and W.E. Milne (1960), "Interpolation in several variables", SIAM J., vol. 8, pp. 33-42.

H. Tromp (1977), "The generalized tolerance problem and worst case search", Proc. Conf. on Computer Aided Design of Electronic and Microwave Circuits and Systems (Hull, England), pp. 72-77.

AUTHOR INDEX

185

SUBJECT INDEX

187

SUBJECT INDEX (continued)

SUBJECT INDEX (continued)